The Abdus Salam
International Centre for Theoretical Physics

United Nations
Educational, Scientific and
Cultural Organization

IAEA
International Atomic Energy Agency

2167-6

Advanced School on Direct and Inverse Problems of Seismology

27 September - 9 October, 2010

Polarized plate tectonics

G.F. Panza
University of Trieste/ICTP
Trieste

Polarized plate tectonics

Carlo Doglioni[1] and Giuliano Panza[2]

[1] Dipartimento di Scienze della Terra, Università Sapienza, Roma, Italy
[2] Dipartimento Geoscienze, Università di Trieste, and ICTP, Italy

Abstract

Plate tectonics theory is revisited combing observable features connected with the main morphostructural properties of our planet with the most recent acquisitions about the Earth's internal physical and chemical properties. Kinematic and dynamic models are formulated considering geodetic (mostly GPS) data. Currently accepted engines for plate tectonics do not seem to supply sufficient energy for plate's motion and do not explain the globally observed asymmetries that from the surface reach mantle depths. Additional forces are required. An excellent source of energy, well consistent with the facts (1) that plates move along a westerly polarized flow that forms an angle relative to the equator close to the revolution plane of the Moon, (2) that plate boundaries are asymmetric, being their geographic polarity the first order controlling parameter, (3) that the global seismicity depends on latitude and correlates with the decadal oscillations of the excess length of day (LOD), (4) that the Earth's deceleration supplies energy to plate tectonics comparable to the computed budget dissipated by the deformation processes and (5) that the Gutenberg–Richter law indicates whole lithosphere as a self-organized system in critical state, is supplied by the tidal drag on Earth's rotation.

Introduction

Plate tectonics provides the tectonic framework supporting Wegener's hypothesis of continental drift. Objections to the original formulation of continental drift and plate tectonics have been focused on the driving mechanism (Jeffreys, 1976; Gordon and Jurdy, 1986; Jurdy and Stefanick, 1988; Ricard and Vigny, 1989) and on the evidence that continental lithosphere is subducted in continent-continent collison areas (Panza and Mueller, 1978; Panza et al., 1982; Mueller and Panza, 1986; Suhadolc et al., 1988; Panza and Suhadolc, 1990; Pfiffner et al. 1997; Lippitsch et al., 2003).

In plate tectonics it is assumed that the inertia and acceleration of the individual plates are nonexistent or negligible, and thus the plates

are in dynamic equilibrium (Forsyth and Uyeda, 1975). At present, the solid Earth can be considered in energetic equilibrium: there is no statistically meaningful difference between the total of income and expenditure energy rates (Riguzzi et al. 2010). This circumstance allows for relatively small energy sources to influence global tectonic processes and therefore the tidal despinning can contribute to plate tectonics through the westward lithospheric drift (Bostrom, 1971; Knopoff and Leeds, 1972). Small perturbations in the velocity of rotation trigger the release of a large amount of energy and seismicity (Press and Briggs, 1975).

The role of upper-mantle convection in plate tectonics, originally postulated by Elsasser (1969) remains poorly understood but it is now commonly believed that convective drag on lithospheric plates is not an important driving force in plate tectonics (e.g. Knopoff, 1972; Forsyth and Uyeda, 1975; Turcotte and Scubert, 1982). Gravitational body forces produced at subduction zones (slab pull) and at oceanic ridges (ridge push) are still considered relevant driving forces of the plate-tectonic process. However, it is not clear why slab pull, i.e the action of the portion of the plate that has been subducted, does not operate to the north of the Tonga trench, where the Pacific oceanic crust has the same age and thickness, or why it should operate in a different way in the Mediterranean, where old and thickened oceanic or continental (?) crust is subducting both below southern Italy and in the Hellenic trench with different dips (Doglioni, 1990). On the other hand, in the Red Sea and in the Gulf of Suez, it has been demonstrated that uprising of the mantle post-dates stretching in the lithosphere (Bohannon et al., 1989; Moretti and Chenet, 1987) and consequently the mantle rise seems to be more a passive isostatic phenomenon than the primary driving mechanism (ridge push). The evidence presented by Cruciani et al. (2005) casts some doubt on the effectiveness of the slab pull, as indicated also by the downdip compression occurring in several slabs (Isaks and Molnar, 1971; Frepoli et al., 1996) and the subduction of continental lithosphere is now a quite widely accepted process by the Earth Sciences community (e.g. Panza et al., 2007; Frezzotti et al., 2009).

Geological evidence for a global tectonic polarity.

Insufficient attention has been paid to the general westward drift of the plates (Le Pichon, 1968: Bostrom, 1971) and the possible configuration of upper-mantle convection cells consistent with recent global tomography images of the upper mantle represents a quite strong argument supporting the relevant role played by the westward drift, very likely of astronomical origin (Riguzzi et al., 2010; Panza et al., 2010).

A main controlling factor of plate tectonics are the lateral heterogeneities in the lithosphere and underlying upper mantle. If the decoupling, due to viscosity contrast, between the lithosphere and the astenosphere is more or less the same everywhere within the Earth, the lithospheric shell would behave, in its westward drift, as a single coherent shell with no relative motion among different plates.

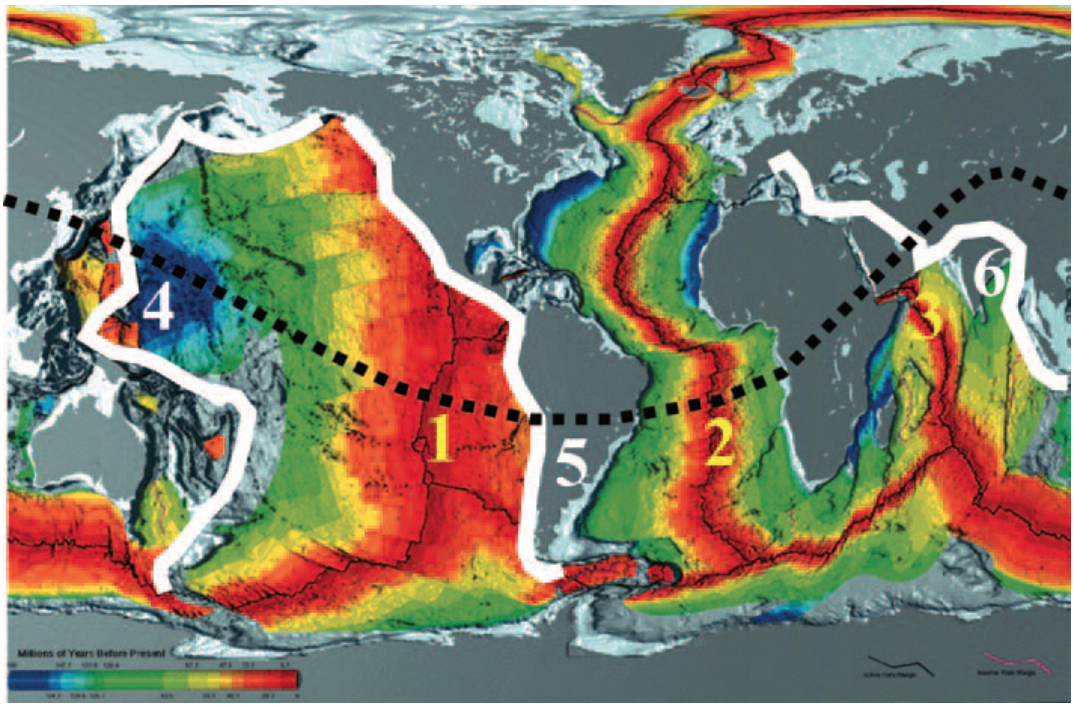

Fig. 1. The Tectonic Equator. Tectonic mainstream, starting from the Pacific motion direction and linking all the other relative motions in a global circuit using first-order tectonic features such as the East Pacific Rise (EPR) (1), the Atlantic rift (2), the Red Sea, the Indian Ocean rift (3) for the rift zones, and the west Pacific subduction (4), the Andean Subduction (AS) (5) and the Zagros-Himalayas Subduction and (6) for convergent margins (after Crespi et al., 2007).

Similarly, plate tectonic could not occur if the lithosphere is formed simply by a layer of constant thickness (say 100-150 km) all of continental or oceanic character, since such a homogenous layer is in equilibrium and does not undergo to compression or stretching.

The density contrast between continental and oceanic lithosphere is at the base of the differential motion of the lithospheric plates. These inhomogeneities in the mantle are consistent with the presence of viscosity contrasts that favor the existence of non-zero differential velocities among plates.

As a rule the subduction of lithosphere is oriented, along the tectonic equator (TE), shown as dashed line in Fig. 1, towards W if the thinner (more dense) plate lies to the E of the collision front, or viceversa towards E, if the thinner (more dense) plate lies to the W of the collision front. Plate tectonics comes true since the different plates move along the

flow lines parallel to the TE, with relative velocities variable in the range 0-18 cm/yr. A "westward" drift of the lithosphere relative to the asthenosphere is indicated by plate motions in the hot-spot reference framework and when using a hot-spot reference framework filtered to exclude shallow hot-spots such a drift is even more evident (Doglioni, 1993a; Doglioni et al., 2005).

Accretionary prisms

The areas where mountain chains are generated, the accretionary prims, can be classified in three main kinds. In an accretionary prims of first kind, with E- (or NE-) oriented subduction that follows the mantle flow, the plate to the E of the collision is the most mobile, therefore it overruns actively the other plate. In other words, both plates move towards W, but the one to the E moves faster. Examples are Dinarides (see Fig. 42), Himalaya, Zagros, Alps, and the whole Cordillera from Land of Fire to Alaska, all mountain belts in which the crystalline basement is largely involved in the tectonic process. Subductions that form an angle with respect to the main mantle flow show a less clear-cut picture.

The second kind of accretionary prism, very different from the first, just described, forms in subduction zones W- (or SW-) oriented, that oppose to the mantle flow. This kind of accretionary prism is always associated with a back-arc basin, has a much lower topography than the prism of first kind and involves mostly relatively shallower and younger rocks. Examples are Barbados, subductions in the W-Pacific (Japan, Aleutians), Carpathians, Apennines (see Fig. 31b), Caribbean and Scotia sea. The coexistence of compression and stretching is consistent with a E-flowing mantle with respect to a lithosphere that has a different degree of coupling E and W of the prism.

The third kind of prism is the less common and can be classified as II order structure, i.e. product of local plate rotations, like in the case of the Pyrenees. The geometries of these accretionary prisms are function of the relevant active tectonic, initial geometry of involved plates and their kind: oceanic, continental or transitional.

Rifts

As in the case of accretionary prisms, within rifts three different kinds can be identified. The linear rift (Atlantic, E-Africa) requires that the lithosphere on the W side is more decoupled from the underlying mantle than its E side counterpart, so that it can move faster towards W. The second kind of rift has a semicircular shape, is called back-arc basin and it is associated with W- (or SW-) directed subductions (Japan , Caribbean and Scotia sea). It can have more irregular shape when

there are large heterogeneities in the lithosphere as, for example, in the Tyrrhenian sea area (Panza et al., 2007b). The third kind of rift, like the Gulf of Biscay, forms in correspondence of the II order structures (Pyrenees). This rift, started by the anticlockwise Cretaceous rotation of Iberia, aborted since its axis is far from being orthogonal to the mantle flow direction and it is almost contemporary with the formation of the Pyrenees. Another example of aborted rift is the Benue basin, in Central-western Africa.

Although not predicted by classic plate tectonics theory, the eastern sides of most of the Earth's rift zones have an average higher elevation of 100–300 m (Fig. 2). This affects not only the oceanic lithosphere, but also the continents to the ''east'', e.g., Africa and Arabia, several hundreds or thousands km away from the rift. The asymmetry could be explained by a shift to the east of the asthenosphere previously depleted along the rift zone, and producing a mass deficit relative to the western counterpart (Doglioni et al, 2003; Panza et al., 2010). Therefore continental uplift can be accounted for not only by vertical mantle motion, but also by horizontal substitution of undepleted, denser mantle with a slightly depleted mantle that causes upward isostatic readjustment. The eastward motion of the mantle in the oceans and beneath Africa represents a further support to a globally persistent relative westward drift of the lithosphere along the sinusoidal flow lines of plate motion (Doglioni et al., 1999a), reconciling the geological and geophysical asymmetries observed both along subduction and rift zones.

From the existing literature it is possible to identify nine main extensional types related to convergent geodynamic settings (Table 1) (Doglioni, 1995). The uplift of deep crustal rocks at the surface is related

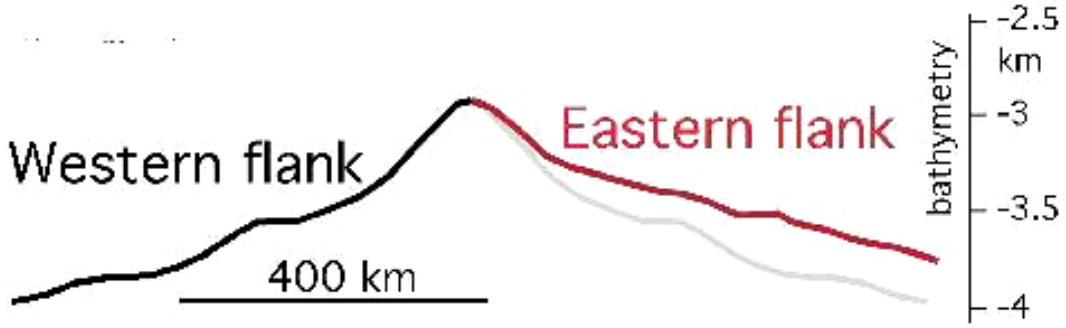

Fig. 2. Average bathymetry of western and eastern flanks of rifts (Panza et al. 2010).

to deep thrust planes that are associated with thrust belts that form with E- and NE-directed subduction zones; later extension of any of the former types may affect such orogens, in particular type 1 (e.g. the Tyrrhenian sea overprinting the Alpine orogen), or type 5 (e.g. Alps, Himalayas), or type 6 (e.g. Aegean rift), or type 7 (e.g. Atlantic and Tethys), or type 8 (e.g. Basin and Range). As a rule, an interplay among the different types

of extensional settings may be expected. Different types of extension can overprint the entire variety of pre-existing tectonic fabrics.

Table 1.

Main extensional types related to convergent geodynamic settings. Other differences like shape, time evolution and rheological parameters vary in each type of setting

Geodynamic setting planes	Subduction polarity	syn- or post-conv.	Generalized subsidence or upliftf	Basal decollement	Extension migration	Number of plates	Opening rates
1 Back-arc basin extension	westward	syn	subsidence 700 m/Ma	lithosphere–asthenosphere	eastward	1 or 2	3–10 cm/yr
2 Asthenospheric wedging-related ext.	westward	syn	uplift 500 m/Ma	crust–asthenosphere	eastward	1 or 2	
3 Subduction hinge extension	westward	syn	subsidence or uplift	upper lithosphere	eastward	1 or 2	
4 Increasing arc length extension	westward	syn	subsidence	lithosphere–asthenosphere	eastward	1 or 2	
5 Morphologic gradient-related ext.	eastward or northeastward	syn	uplift	middle–upper crust		1 or 2	
6 Hanging-wall gradient velocities	eastward or northeastward	syn	subsidence	lithosphere–asthenosphere	southwestward	3	0.1–5 cm/yr
7 Lithospheric roots-related extension	eastward or northeastward	post	subsidence 100 m/Ma	lithosphere–asthenosphere		1 to 2	0.1–1 cm/yr
8 Inversion of velocity gradients	eastward or northeastward	post	subsidence	lithosphere–asthenosphere		3 to 2	1–10 cm/yr
9 Transfer zones-related extension	both west and east	syn	subsidence or uplift	basal thrust plane		1 or 2	

Thrust belts, foredeeps and subduction zones.

It is possible to differentiate between thrust belts that are related to E- (or NE-) directed (along mantle flow) or W- (or SW-) directed (against mantle flow) subduction (Fig. 3). In E- (or NE-) directed subduction the basal decollement, which underlies the eastern plate, reaches the surface and it involves deep crustal rocks while in W- (or SW-) directed subduction the basal decollement of the eastern plate is warped and subducted (Doglioni, 1993b).

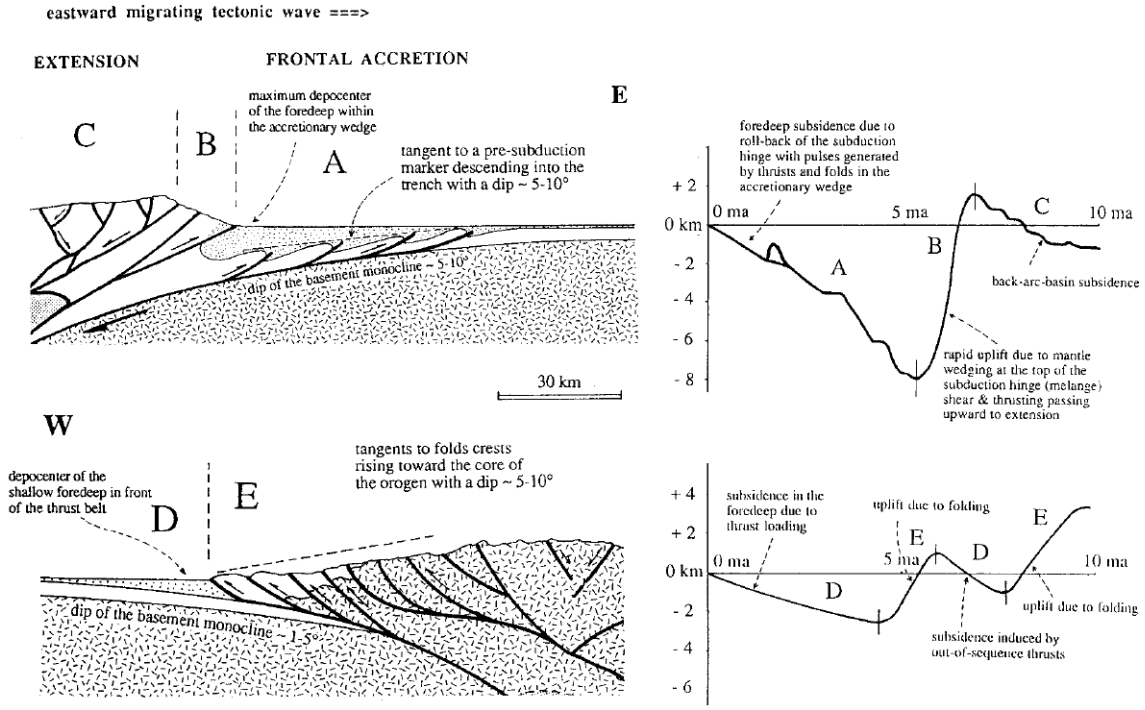

Fig. 3. Main features and structural differences between thrust belts associated to subductions opposing (W- or SW- directed, upper left) or following (E- or NE- directed, lower left) the mantle flow. Thrust belts related to W- (or SW-) directed subductions show low structural and morphological elevation, shallow rocks involved; the tangent to the anticlines of a pre-deformation marker is descending into the trench and the depocenter of the deep foredeep basin is within the accretionary wedge (e.g. Apennines). Thrust belts related to E- (or NE-) directed subductions are characterized by high structural and morphological elevation, deep rocks involved (i.e. America Cordillera) and the tangent to a pre-deformation marker is rising toward the hinterland. The shallow foredeep is mainly located in front of the belt. The two curves on the right represent a possible elevation history of one reference point during the structural evolution of the two different end members. The upper elevation curve refers to a benchmark at the surface crossed by the migration of the three main tectonic fields (A, B, C), associated to a thrust belt produced by a subduction contrasting the mantle flow. The average of subsidence in the foredeep is up to 1600 m/Myr (0.16 cm/y). The lower elevation curve is relative to a benchmark crossed by the migration of the two main tectonic fields (D, E) in a thrust belt due to subduction following the mantle flow. The average of subsidence in the foredeep is about five times smaller: 300 m/Myr (0.03 cm/y). The curves are very different in shape and meaning and confirm the strong physical differences between the accretionary wedges which are related to subductions following or contrasting the mantle flow. The occurrence of subsistence or uplift in the curves is due to different tectonic fields: for instance the initial subsistence in the foredeep related to W (or SW-) directed subduction is controlled by roll-back of the subduction hinge and this occurs during frontal accretion; during E- (or NE-) directed subductions (lower section) the subsistence is generated by thrust loading and the uplift is controlled by the accretion phase (modified after Doglioni, 1992).

Consequently thrust belts related to E- (or NE-) directed subduction show conspicuous structural and morphologic relief, involve deep crustal rocks and are associated with shallow foredeeps. Thrust belts related to W- (or SW-) directed subduction, on the other side, show relatively low structural and morphologic relief, involve only shallow crustal rocks and are associated with deep foredeeps and back-arc stretching. In W- (or SW-) directed subduction the tangent to a predeformation marker descends into the foredeep at an angle in the range 1°-20° (world average about 6°, see Fig. 32) while in E- (or NE-) directed subduction the same marker would dip towards the hinterland

with typical angles of about 1°-10° (Doglioni, 1992) (average about 2.5°, see Fig. 32).

High rates of subsidence up to 1600m/Myr and a ratio lower than 1, between the area of the elevated belt and the area of the basin, characterize the foredeeps associated with W- (or SW-) directed subduction (type I), while low rates of subsidence not exceeding 300 m/Myr and a ratio greater than 1, between the area of the orogen and the area of the basin, characterize the foredeeps associated with E- (or NE-) directed subduction (type II). This naturally explains the slow filling of foredeeps of the first type with respect to the much faster filling of the second type. The foredeep depth in W- (or SW-) directed subduction is mainly controlled by the roll-back of the subduction hinge pushed by the relative eastward mantle flow while foredeep depth in E- (or NE-) directed subduction is instead manly generated by the load of the thrust sheets and by the roll-back of the subduction hinge, due to the advancing upper plate contrasting the upward push of the mantle (Fig. 4).

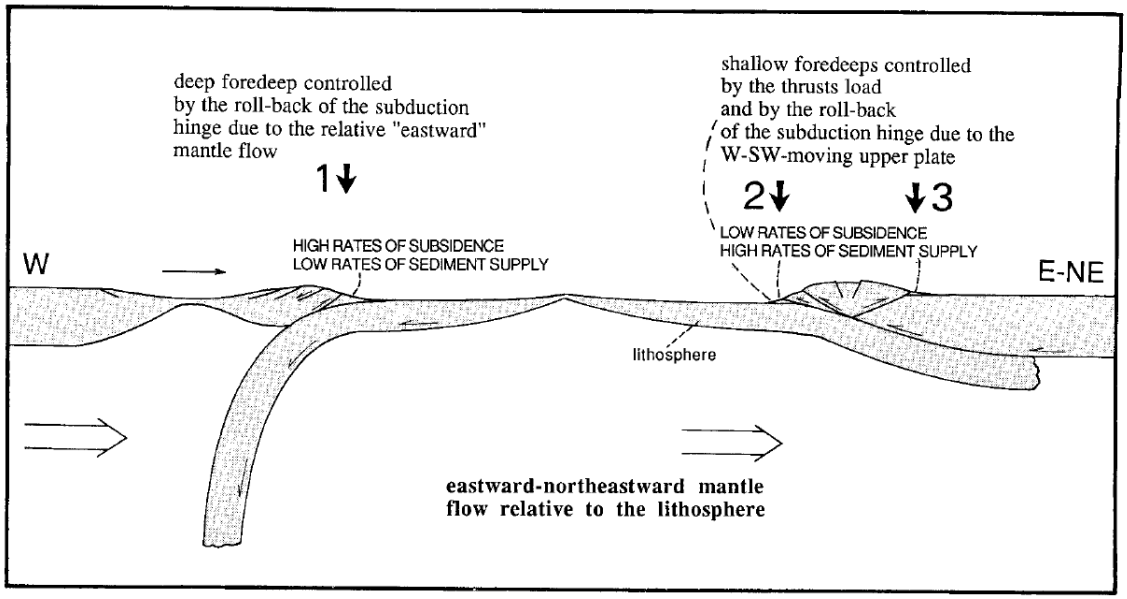

Fig. 4. Foredeeps can be differentiated on the basis of the related subduction, namely W- (or SW-) directed or E- (or NE-) directed. Three main geodynamic settings provide foredeeps (1) at the front of W- (or SW-) directed subduction, (2) at the front of E- (or NE-) directed subduction and (3) at the front of its conjugate back-thrust belt.

The shape of the foredeeps is regularly arcuate in case of W- (or SW-) directed subductions (see also Fig. 10), while it is almost linear or it follows the shape of the inherited continental margin in case of E- (or NE-) directed subduction. Fold development in the two kinds of foredeeps is significantly different: in W- (or SW-) directed subductions the folds are carried down in subduction while they are forming and consequently they are poorly eroded. In the E- (or NE-) directed

subduction folds and thrust sheets are instead uplifted and deeply eroded (Fig. 5 and 6).

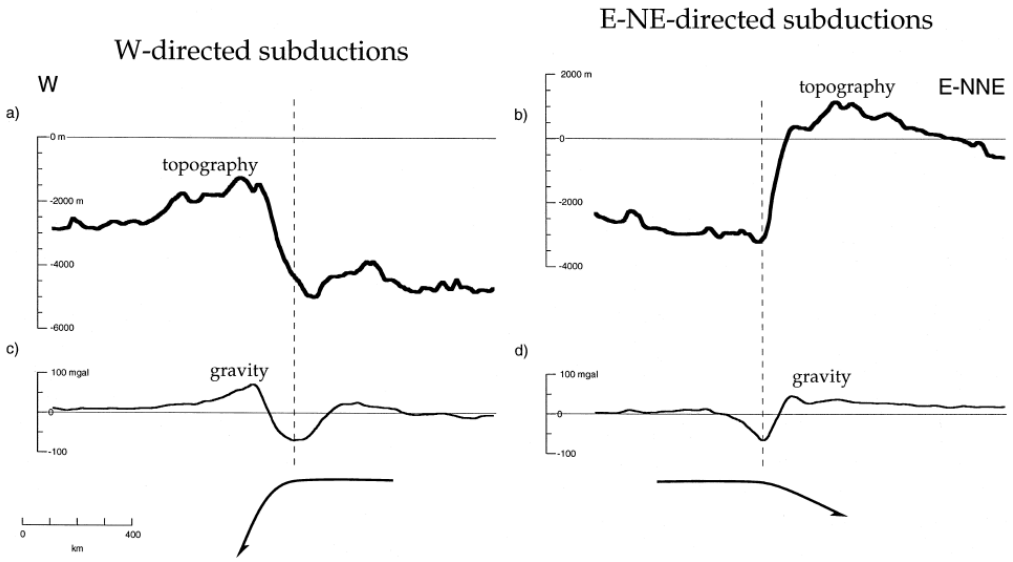

Fig. 5. Average topographic profiles (a), (b), and free-air gravity anomaly profiles (c), (d) across the main subduction zones of the Earth. They confirm the presence of two classes of subduction zones whose differences are related to the geographic polarity of the subduction zone (Harabaglia and Doglioni, 1998).

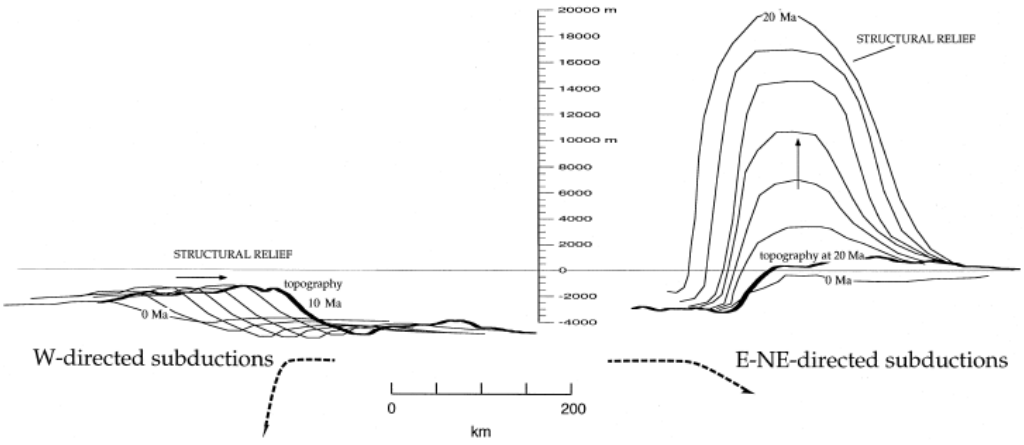

Fig. 6. Different structural evolution along the opposite subduction zones. W-directed subduction zones are characterized by an 'E-ward' migrating structural wave that closely matches topography. The E- or NE-directed subduction zones have a much higher structural elevation. The growth of the waves is constructed assuming conservative values of 2–3 cm/year of eastward migration of W-directed subduction zones and 1 mm/year uplift for the opposite subduction zones. The structural differences among the subduction zones are even more evident than the topographic signatures.

Foredeeps and accretionary wedges can be sorted out on the basis of the direction of the associated subduction. The differentiation holds both for oceanic and continental subductions, like eastern versus western Pacific subductions or east-directed Alpine versus west-directed Apenninic subduction. In the Alps the ratio of the area of the orogen to

the area of the foredeep is about 2:1, while this ratio is about ten times smaller for the Apennines (Doglioni, 1994). These very different ratios explain why feredeeps related to E- (or NE-) directed subductions are quickly filled and are bypassed by clastic rocks, whereas foredeeps related to W- (or SW-) directed subductions maintain a deep-water environment for a much longer time. These differences can be naturally explained by the existence of the eastward asthenospheric flow relative to the westward drift of the lithosphere identified in the hot-spot reference frame.

The same flow explains the fact that subduction zones appear primarily controlled by the polarity of their direction (Fig. 7), i.e. towards W (or SW) or towards E (or NE). The decollement planes behave differently in the two end-members. In the W- (or SW-) directed subduction zones, the decollement of the plate to the east is warped and subducted, whereas in the E- (or NE-) directed subduction zones, it is ramping upward at the surface. There are W- (or SW-) directed subduction zones that work also in absence of active convergence like the Carpathians or the Apennines. W- (or SW-) directed subduction zones have shorter life (30–40 Ma) than E- (or NE-) directed subduction zones (even longer than 100 Ma). The different decollements in the two end-members of subduction should control different PTt paths and, therefore, generate variable metamorphic assemblages in the associated accretionary wedges and orogens. The magmatic pair calc-alkaline and alkaline-tholeiitic volcanic products of the island arc and the back-arc basin characterise the W- (or SW-) directed subduction zones. Magmatic rocks associated with E- (or NE-) directed subduction zones have higher abundances of incompatible elements, and mainly consist of calc-alkaline-shoshonitic suites, with large volumes of batholithic intrusions and porphyry copper ore deposits (Doglioni et al., 1999a).

These asymmetries determine different topographic and structural evolutions that are marked by low topography and a fast ‘eastward’ migrating structural wave along W- (or SW-) directed subduction zones, whereas the topography and the structure are rapidly growing upward and expanding laterally along the opposite, E- (or NE-) directed subduction zones. Differences in subduction styles have been explained as due to variations in convergence velocity, plate thickness and age (e.g., Royden, 1993). However, there are cases where the same plate is subducting with a different style (W- (or SW-) directed or E- (or NE-) directed) and the subduction angle and relative geologic signature depend only on its orientation. One example is the Ionian/Adriatic microplate (Fig. 7). This plate is sinking towards the west almost vertically beneath the Apenninic arc whereas on the east it is sinking at a low angle beneath the Dinarides and Hellenides (Caputo et al., 1970,

1972; Selvaggi and Chiarabba, 1995; Papazachos and Comninakis, 1978; Christova and Nikolova, 1993; Piromallo and Morelli, 1997; Panza et al., 2007 a,b; Pontevivo and Panza, 2006). The same plate determines orogens that fall into the W- (or SW-) class and E- (or NE-) class independently from the nature and age of the downgoing lithosphere.

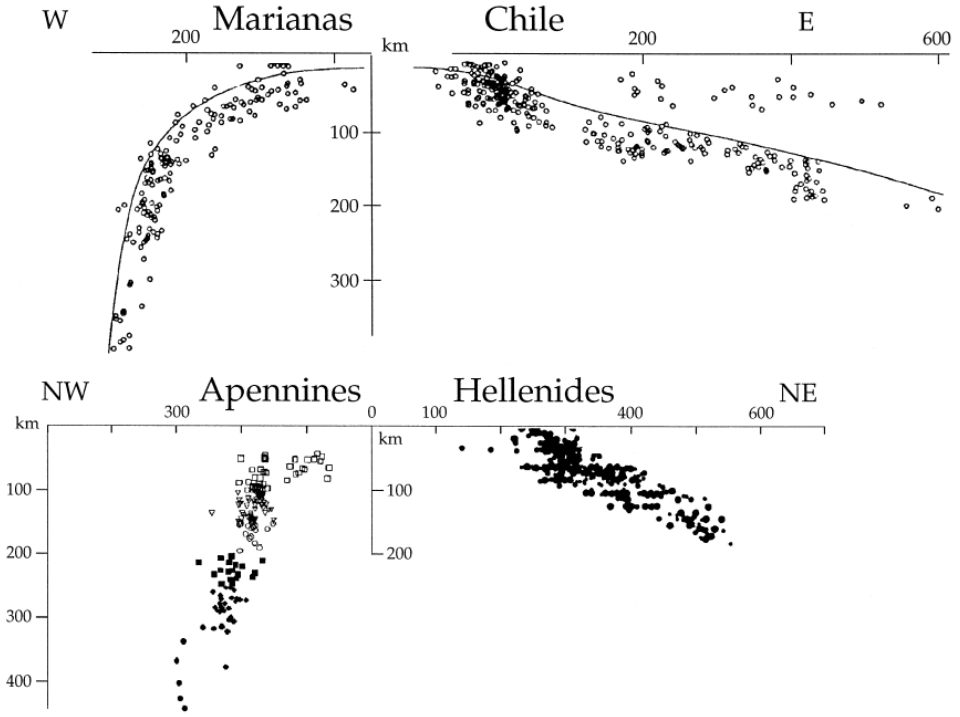

Fig. 7. Hypocenters of the Marianas and Chile subduction zones in the Pacific (Isacks and Barazangi, 1977), compared with the seismicity of the Apennines and Hellenides (Caputo et al., 1970, 1972; Papazachos and Comninakis, 1978; Selvaggi and Chiarabba, 1995). As in the the Pacific, in the central Mediterranean, where the Ionian/Adriatic lithosphere is subducting contemporaneously both underneath the Apennines and the Hellenides (Doglioni, 1999a), subduction zones are asymmetric. Their dip depends upon subduction direction, independently from the nature and age of the downgoing lithosphere.

A detailed geodynamic discussion about the E- (or NE-) class nature of the Hellenic–Aegean system is given by Doglioni (1995) and deals with topography, gravimetry, structure and all the other relevant geological and geophysical parameters, which characterize the two subductions, that fall into the W- (or SW-) class and E- (or NE-) class, respectively (see Fig. 8).

Another example of the fact that the nature and age of the down-going lithosphere is not the primary factor which determines the characteristics of the W- (or SW-) and E- (or NE-) classes is the Kermadec–Macquarie subduction. To the north, the Pacific plate subducts westward at a high angle, with low elevation of the hangingwall plate and a deep trench. To the south along the opposite NE-directed New Zealand subduction zone the slab has a low angle, there is high elevation

of the hanging wall plate and the trenches are shallower, irrespective of the nature of the upper plate: either continental or oceanic. However, in this case, the New Zealand-Macquarie subduction has the Tasmanian sea oceanic lithosphere in the footwall, which is younger than the Pacific lithosphere of the Kermadec subduction, but still all the parameters fall into the W- (or SW-) class for Kermadec and into the E- (or NE-) class for New Zealand subduction zones. On the other hand, along the Sandwich subduction zone the undergoing Atlantic and Antartic oceanic lithospheres show age variations (from 5 to 120 Myr), but the subduction system maintains the characteristics of the W- (or SW-) class.

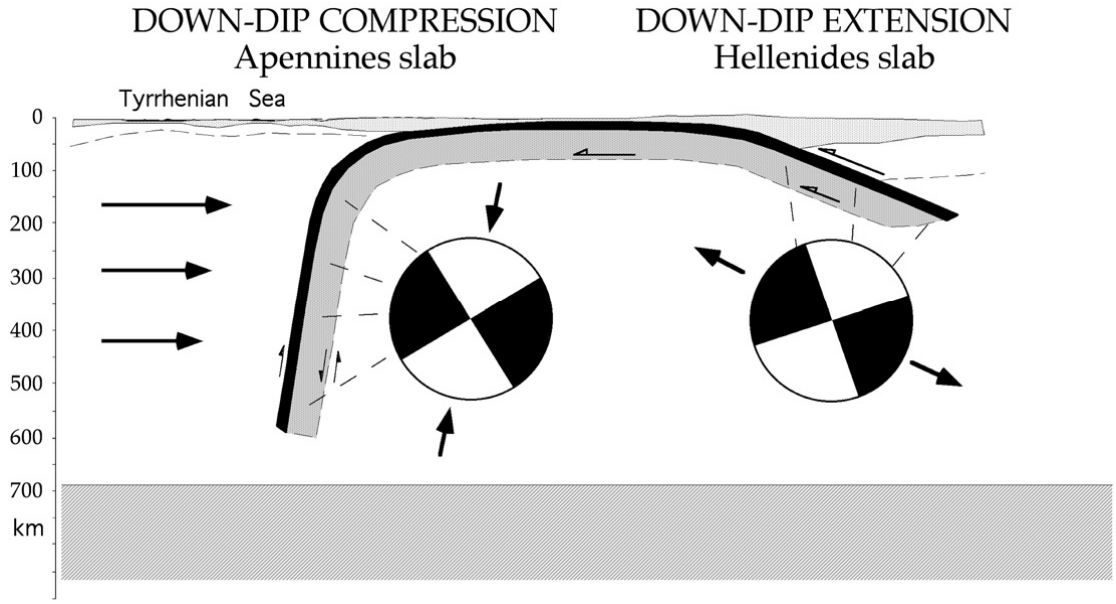

Fig. 8. The deep seismicity along the Apennines and Hellenides slab shows opposite behavior, being steeper and deeper vs. shallower and less inclined respectively (see Fig. 7). Moreover the Apennines slab is undergoing down-dip compression (Frepoli et al., 1996), whereas the Hellenic slab suffers down-dip extension (Papazachos et al., 2005). This behavior is observed when comparing the western and the eastern margins of the Pacific subduction zones, as well, and the asymmetry is consistent with the W-ward drift of the lithosphere relative to the mantle (Doglioni et al., 2007).

This contradiction of one of the paradigm of subduction zones that relates the dip of the slab to the buoyancy of the downgoing lithosphere, with the negative buoyancy proportional to the age of the oceanic lithosphere, is nicely confirmed by Cruciani et al. (2005) who measured the dip of the slab down to depths of 250 km along 164 sections crossing 13 subduction zones and compared it with the age of the subducting oceanic lithosphere both at the trench and at depth. They have shown that the relationship dip-age is far more irregular than previously suggested, and that it is not possible to simply correlate the increase of the slab dip to the increasing age of the down going cooler lithosphere (Fig. 9a and 9b). In contrast with predictions of models considering only

slab pull, younger oceanic lithosphere may show steeper dip than older segments of slabs (e.g., Central America vs. South America). A simple linear relation between slab dip and age of the down going oceanic lithosphere does not exist. Nevertheless the lack of a clear correlation between the observed dip angle of slabs and plate velocity and slab age in modern subduction zones has been explained with the hypothesis that subduction is a time-dependent phenomenon (King, 2001). A combination of slab age and subduction velocity correlates better with slab dip, but the correlation is still poor (correlation coefficient equal to 0.45). Therefore supplemental forces to the negative buoyancy of the slab have to be considered such as thickness and shape of the hanging wall plate, absolute plate velocity, presence of lateral density variations in the hosting upper mantle, effects of accretion/erosion, subduction of oceanic plateaus and slab deformation due to the motion of the mantle relative to the subducting plate.

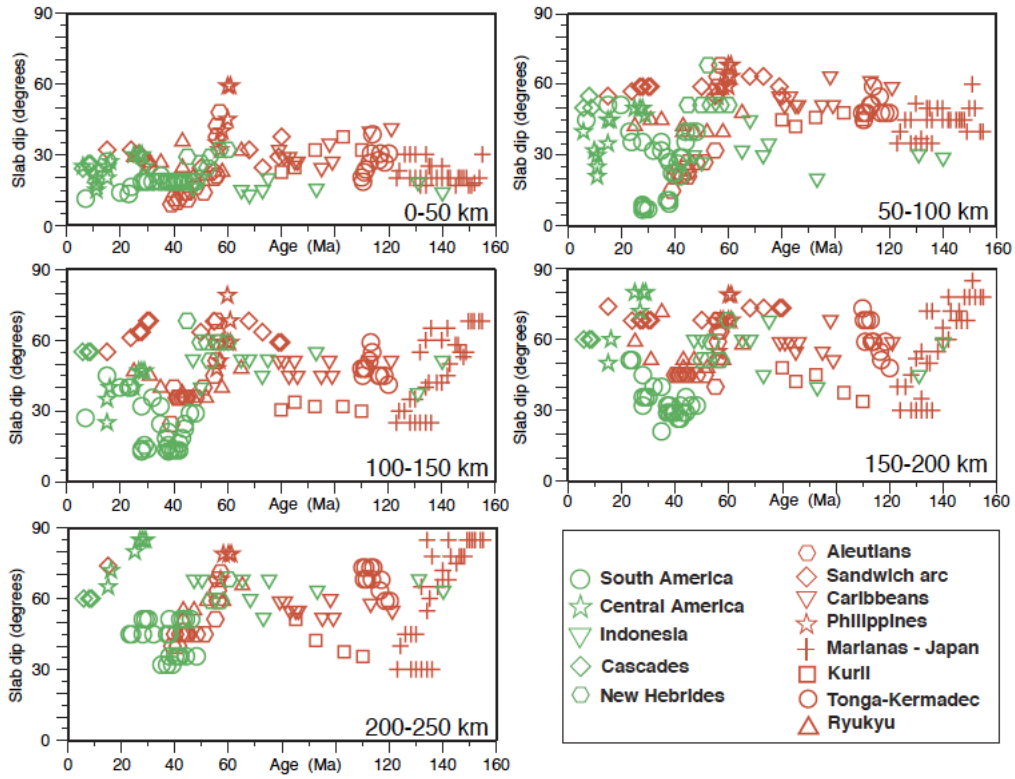

Fig. 9a. Age vs. slab dip plots for 5 different depth ranges, with data measured along sections perpendicular to the trench.

Plate kinematics, i.e. absolute motion of the upper plate (Luyendyk, 1971; Tovish and Schubert, 1978) could play a role, but other aspects have to be taken into account. The first one is the presence of lateral density variations in the hosting upper mantle, allowing different buoyancy contrasts with respect to the down going slab. However, apart from proven lateral heterogeneities in mantle tomography, there is no evidence yet for such large anisotropies in composition that can justify

sufficient density anomalies in the upper mantle. The effect of latent heat released by phase transitions could, moreover, alter the thermal distribution and buoyancy of subducting slabs and control their dips (van Hunen et al., 2001). Another parameter possibly controlling the dip of the first 250 km is the thickness and shape of the hanging wall plate, i.e., the thicker the hanging wall plate, the steeper is the slab. Still at shallow depths, the effects of accretion/erosion (Karig et al., 1976; Lallemand et al., 1992), the thickness of sediments in the trench and the subduction of oceanic plateaus (Cross and Pilger, 1982) could influence the geometry of the descending lithosphere.

Another basic controlling action could be operated by resistance forces induced by the motion of the mantle relative to the subducting plate (Scholz and Campos, 1995; Doglioni et al., 1999b). According to Hager and O'Connell (1978) the dip of the subduction zones is controlled by the return flow of the mantle produced by the plate motion rather than by slab density contrast.

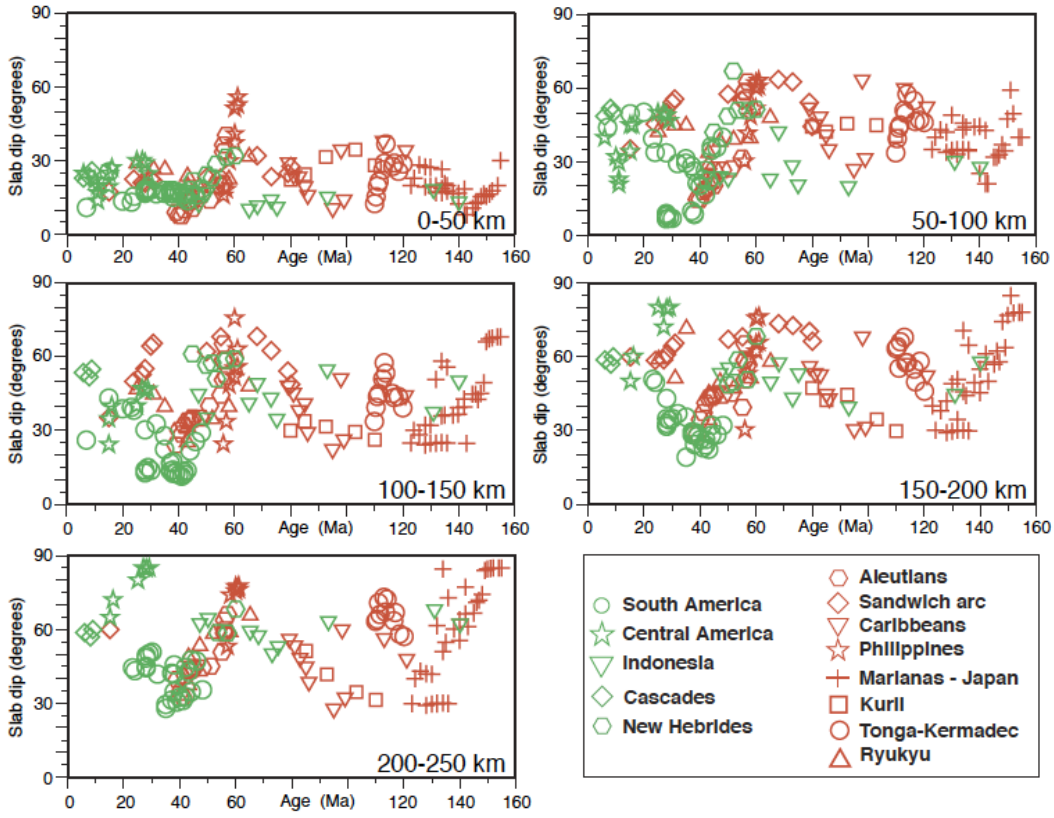

Fig. 9b. Age vs. slab dip plots for 5 different depth ranges, with data measured along sections parallel to the plate convergence vector.

These examples show that the geographic polarity of the subduction rather than any other parameter constrains the different characters of the two classes. This poses the question whether subductions can be ascribed only to mantle convection and slab pull or

whether they are also influenced by the relative westward drift of the lithosphere with respect to the upper mantle postulated by several authors (Le Pichon, 1968; O'Connell et al., 1991; Ricard et al., 1991). Polarization of the seismic waves in the mantle far away from the subduction zones, e.g., beneath the Nazca plate (Russo and Silver, 1994), the Tyrrhenian back-arc basin (Margheriti et al., 1996) and the South Victoria Land and the Ross Sea coast, Antarctica (Barklage et al., 2009), provide evidences for a relative E-ward mantle flow. The mantle polarization would be able to differentiate the opposite behavior of the decollement planes along the W- (or SW-) directed and E- (or NE-) directed subduction zones and to determine the differences on the orogenic belts (Doglioni, 1992) which may be analyzed also in terms of the ratio between convergence rate and retreat rate of the subduction hinge (Waschbusch and Beaumont, 1996). One could argue that the two classes of subduction zones are simply sensible to the thickness and composition of the hangingwall and footwall plates. However, the two classes persist independently from the age and nature of the involved lithospheres, and they are strictly constrained by the geographic polarity (Harabaglia and Doglioni, 1998).

In summary, W- (or SW-) directed subductions are zones where there is a negative volume balance of lithosphere, in other words, the lithosphere is almost entirely lost in subduction and replaced by the uprising asthenosphere in the back-arc region. Along E- (or NE-) directed subduction zones, the volume balance of the lithosphere is more positive because the hangingwall lithosphere is thickened from the footwall plate which is sliding below and following the shape of the upper plate. This could provide an explanation for their higher structural and morphologic elevation (Fig. 6).

On the origin of W- (or SW-) directed subduction zones.

W- (or SW-) directed subduction zones are marked by east-verging arcs a few thousand km long (1500 km - 3000 km). They form very fast and are short lived, usually younger than 50 Myr, and are characterized by a frontal accretionary wedge and back-arc basin propagating together toward E. A summary of the main characteristics of W-directed subduction zones is given in Fig. 10 (Doglioni et al., 1999a). The main known, presently active or preserved W- (or SW-) directed subduction zones of the world are: Apennines, Carpathians, Barbados, Sandwich, Aleutians, Kurile, Japan, Nankai, Ryukyu, Izu-Bonin, Marianas, Tonga, Kermadec, Banda, Philippines. The Aleutian slab dips northwestward, but the Pacific plate travels WNW oblique to the trench, thus it is W- (or SW-) directed. The accretionary wedge scrapes off superficial layers of the downgoing plate (thin-skinned tectonics) whereas

the back-arc extension cross-cuts the entire subduction hanging wall (thick-skinned tectonics). The slab of this type of subduction is steep to vertical and the hanging wall of the subduction has a mean elavation of 1 km below sea level.

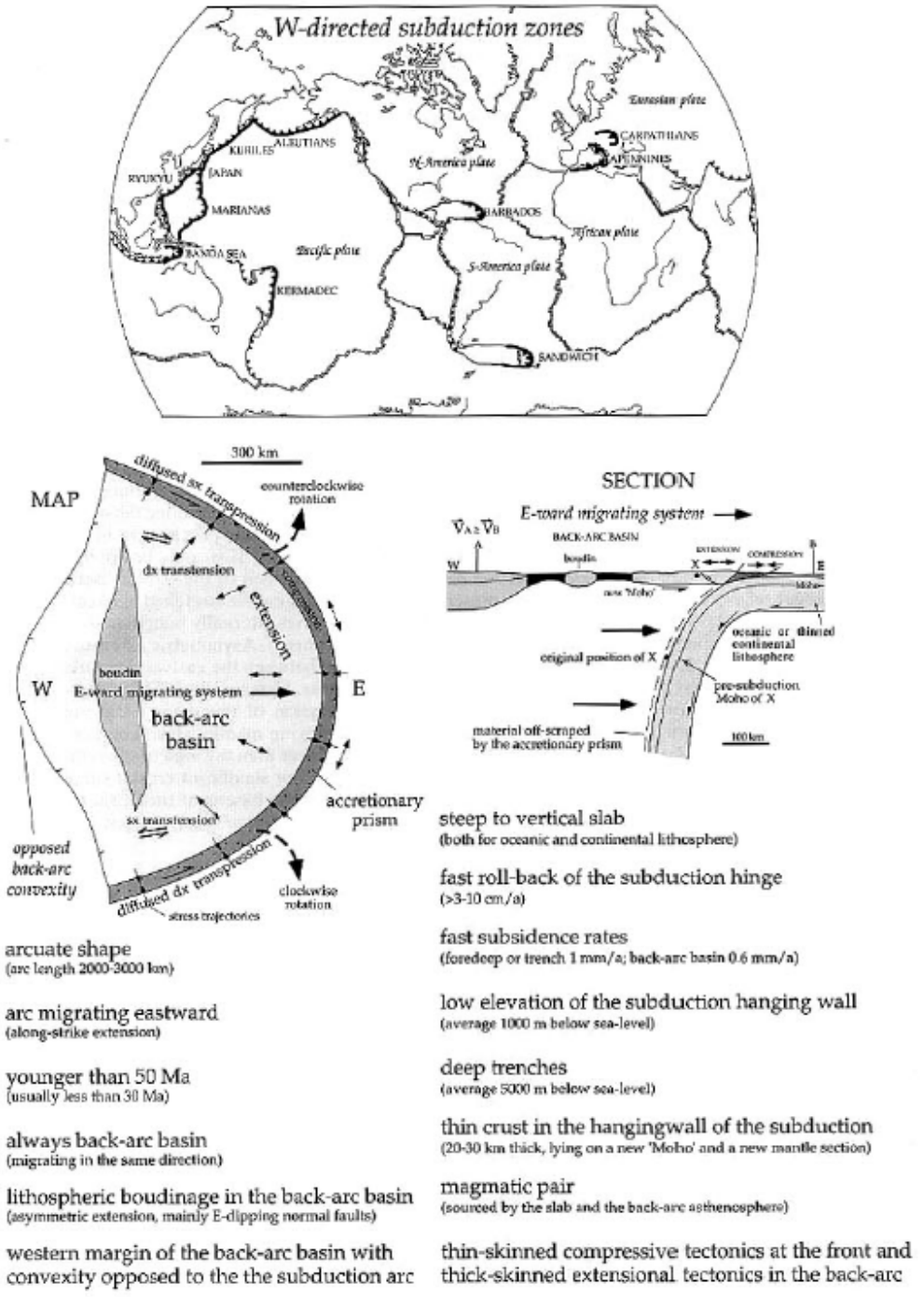

Fig. 10. Summary of the main characteristics of W- (or SW-) directed subduction zones. Plate boundaries in the uppermost figure are after Fowler (1990). For more details see Doglioni et al. (1999a)

Trenches and foredeeps are the deepest basins of the Earth and their mean depth is of 5 km below sea level. W- (or SW-) directed subduction occurs both in the case of the highest E-W convergence rates

among plates (e.g. W-Pacific examples) and no or very low convergence (e.g. Carpathians). In the Mediterranean, the Adriatic continental lithosphere (e.g. Venisti et al., 2005; Panza et al., 2007) and the Ionian oceanic (?) lithosphere (e.g. de Voogd et al., 1992; Cernobori et al., 1996; Nicolich et al., 2000; Panza et al., 2007a,b) are subducting both under the Apennines (steep W-directed subduction) and under the Dinarides-Hellenides (shallow NE-directed subduction) (e.g. Christova and Nokolova, 1993; Selvaggi and Chiarabba, 1995; Brandmayr et al., 2010) and with very scarce seismic activity (deformation) in the horizontal part of the plate (Fig. 11; see also Fig. 8).

The two related thrust belts follow the east and west Pacific rules, without age and thickness variations of the subducting lithosphere. In the Pacific, the W- (or SW-) directed subductions are the fastest in the world and the slab is steep, while the AS (E- or NE-directed) is active since the Mesozoic and the slab inclination is less than about 25° (Riguzzi et al., 2010). This behaviour cannot be explained in terms of slab pull (the tectonic plate motion due to higher densities) and age of the subducting lithosphere.

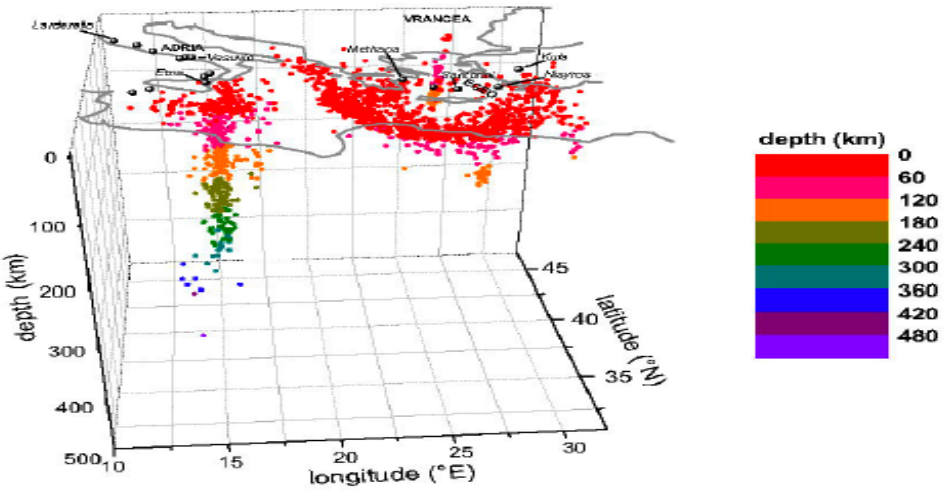

Fig. 11. The Mediterranean is characterized by four deep-earthquake zones: Tyrrhenian, Aegean, West Turkey, Vrancea, modified from Scalera (2008a). The shown seismicity evidences absence or very low seismic activity in correspondence of the horizontal part of the plate (see also Fig. 7)

Following Atlantic W- (or SW-) directed subduction examples, the W- (or SW-) directed subductions seem to develop along the back-thrust belt of former E- (or NE-) directed subduction zones, where oceanic lithosphere occurs in the foreland to the east, with the narrowing of the American continents. This applies to the onset of the Apennines subduction along the back-thrust belt of the Alpine-Betic orogen where

Tethys oceanic crust was present. The Alpine orogen was stretched and scattered in the Apennines back-arc basin. The back-arc extension is internally punctuated by necks (sub-basins) and boudins, horsts of continental lithosphere, well visible in recent absolute models of the lithosphere-asthenosphere system, based on non-linear inversion of surface waves tomographic maps (e.g. Brandmayr et al., 2010). Asymmetric extensions in the back-arc basin appears controlled by differential drag between the eastward mantle flow and the overlying, passively transported, crustal remnants. Compression in the accretionary prism may be interpreted as the superficial expression of the shear occurring between the down going lithosphere and the horizontally moving mantle which compensates the slab roll-back. The area of the Apennines appears lower than the area of the sedimentary cover before subduction: this supports the idea that not significant crustal slices have been involved in the Apenninic accretionary prism, and the basement thrust sheets included in the western part of the belt are mainly relics of the Alpine-Betic orogen.

The tectonic equator

Global flow lines drawn along the axes of Cenozoic (65.5-0 Myr ago) stretching and shortening show a smooth and gradual variation. The flow lines may approximate the path of the eastward mainstream mantle flow relative to the overlying lithosphere, the long-wavelength undulation being due to instability of the rotation axis. The westward delay of the lithosphere with respect to the mantle (see also Panza et al., 2010) could be due to a minor angular velocity of the lithosphere relative to the underlying mantle, as a result of the deceleration of the Earth's rotation or, in a toroidal field, due to lateral heterogeneities within the lithosphere and the underlying upper mantle. Variations in the upper-mantle Low Velocity Layer (LVL) (e.g. Panza et al., 2010) allow variable decoupling between lithosphere and asthenosphere and plate-tectonic process may be driven by differential plate velocities. When there is compression or transpression (compression with a transcurrrent component), the eastern plate is moving faster westwards, while if there is stretching or transtension (stretching with a transcurrrent component) the western plate moves faster westwards. Relative plate motions are allowed by horizontal and vertical viscosity and density gradients both in the lithosphere and the underlying mantle (e.g. Forte and Peltier, 1987).

Tectonics and plate rotations of first order are localized along the global flow lines while those of second order are induced by localized body forces, therefore tectonic structures of the first order form perpendicular or with a great angle with respect to the mantle flow, while,

for example, local rotations of plates may generate tectonic structures of the second order (e.g. Pyrenees).

Lithospheric subduction into the mantle, particularly W- (or SW-) directed subduction, strongly enhances the coupling between the lithospheric plate and the underlying eastward mantle flow. Hence, subduction zones act as "nails" into the mantle, which strongly modify the relative plate velocities. The E- (or NE-) directed subduction zones have shallower dip than W- (or SW-) directed subductions and provide a much lower obstacle than the latter to the mantle flow, whose existence is naturally consistent with the ubiquitous asthenospheric LVZ (global circuit) detected below the TE-perturbed (TE-pert) (Panza et al., 2010), where no relevant obstacle is present against the global relative E-ward mantle flow.

The concept of tectonic mainstream defined on the basis of geological evidences is consistent with space geodesy data, which supplies a new unified way to describe plate motions with respect to the underlying mantle (Crespi et al., 2007).

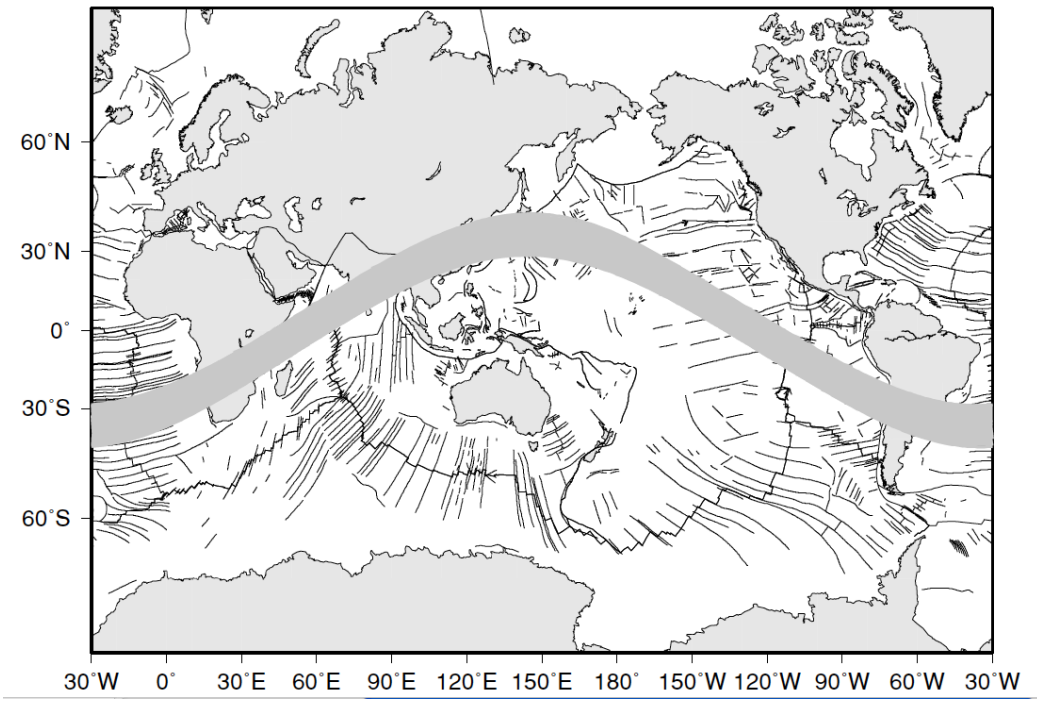

Fig. 12. The tectonic mainstream latitude band according to the solution (S20) by Crespi et al. (2007) that is the most consistent solution with the polarization of tectonic structures and global asymmetry (Riguzzi et al., 2010; Panza et al., 2010).

A parametric function in the form of a third-order Fourier series has been used to define the tectonic mainstream, based on the estimation of plate kinematics consistent both with velocities from space geodesy and geological evidences used as constraints (Fig. 12). Three possible solutions under different hypotheses about the depth of the

Pacific hotspot source, the velocity of the Pacific plate increasing with decreasing depth of the asthenospheric source, are confirming (i) the tectonic mainstream and (ii) the net rotation of the lithosphere.

The shear wave splitting technique (e.g. Savage, 1999) is an independent tool for detecting the seismic anisotropy in the asthenosphere, that is considered the result of the preferential orientation of olivine crystals in a sheared flowing mantle (Silver and Holt, 2002). The direction of the anisotropy between lithosphere and underlying mantle (e.g. Fischer et al., 1998; Montagner, 2002; Debayle et al., 2005; Barklage et al., 2009) aligns quite consistently with the absolute plate motions reconstructions, apart along subduction zones or other mantle anomalies.

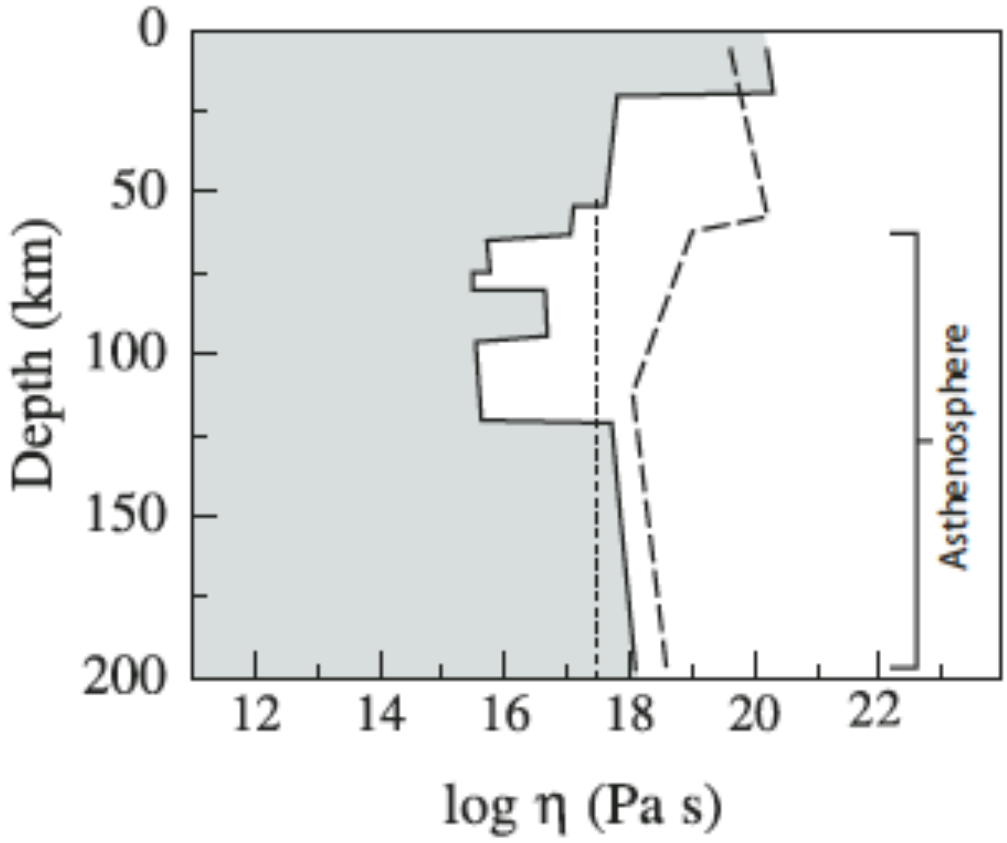

Fig. 13. Viscosity profiles of lithospshere and asthenosphere mantle. The solid line is after Mei et al. (2002), whereas the dashed line is after Hirth and Kohlstedt (1996). These two curves have been calculated using flow laws and information on water content and melt fraction obtained from laboratory experiments. The dotted line is from Pollitz et al. (1998), and is the results of numerical modeling of earthquake long-range interaction, modiefed from Scoppola et al. (2006).

The level at which radial anisotropy is low, e.g., <1%, may represent the decoupling level between the lithosphere and the underlying asthenospheric low-velocity layer, due to the presence of a relevant fraction of melt that inhibits the formation of preferential orientations in

the texture of mantle rocks (Panza et al., 2010). A decoupling at the lithosphere base has been postulated in order to satisfy the geoid anomaly across transform zones by Craig and McKenzie (1986) who considered the existence of a thin low-viscosity layer beneath the lithosphere in their two-dimensional numerical models of convection in a fluid layer overlain by a solid conducting lid. Water content in the asthenosphere can drastically lower its viscosity to 10^{15} Pa·s (Karato et al., 2008; Korenaga and Karato, 2008). Moreover, the viscosity in the asthenospheric LVZ can be orders of magnitude lower when measured under horizontal shear with respect to the viscosity computed by vertical unloading due to post-glacial rebound (Scoppola et al., 2006). Jin et al. (1994) have shown how the intra-crystalline melt in the asthenospheric peridotites under shear can generate a viscosity of about 10^{12} Pa·s (Stevenson, 1994), a value compatible with the plate tectonics driven by the Earth's rotation (Scoppola et al., 2006). Therefore the presence of an ultra-low viscosity layer in the upper asthenosphere can be considered as a possibility consistent with the present available techniques of mantle sampling and laboratory experiment.

Therefore, even if the occurrence of a westerly polarized lithosphere motion cannot be considered at present a controversial phenomenon (Ricard et al., 1991; Gripp & Gordon, 2002, and reference therein), we feel that its origin is not yet completely clear, because it may be due to different combined effects hard to single out. A mean lithospheric rotation could be preferred to a global phenomenon (e.g. Ricard et al. 1991) since the former preserves the angular momentum of the Earth without rapidly decelerating its rotation speed. However, Scoppola et al. (2006) have shown that a global lithospheric rotation is physically feasible, although with variable velocities of the different plates. According to this model, plate tectonics would occur with the concurring contributions of the planet rotation under tidal torque, and lateral viscosity variations at the lithosphere-mantle interface, where, hosted in the LVZ asthenospheric layer, are supposed to occur thin hydrate layers with very low viscosity (Fig. 13 and 14). These layers are beyond the reach of standard tomography due to the limitations of the theoretical framework employed; ray theory does not handle diffraction and frequency dependence, whereas normal mode perturbation theory requires weak and smooth lateral variations of structure (Waldhauser et al., 2002; Romanowicz, 2003; Anderson, 2007a,b; Panza et al., 2007b; Boschi et al., 2007; Boyadzhiev et al., 2008). The viscosity of the upper asthenosphere is still unknown, but, as shown in Fig. 13 and 14, the effective viscosity should be about 1000 times lower when measured for a horizontal shear with respect to vertical loading as simulated in classical postglacial rebound studies (Scoppola et al., 2006).

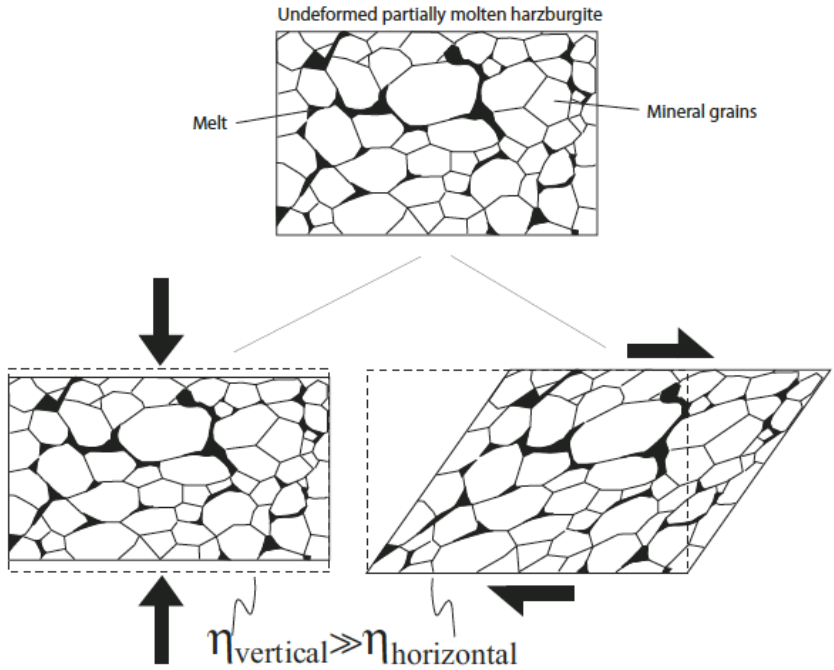

Fig. 14A. The effective viscosity in a granular layer with intervening melt in the pores is much smaller when measured for a shear parallel to the bedding (i.e. induced by horizontal plate motion) with respect to vertical load (e.g. induced by ice formation or melting), modiefed from Scoppola et al. (2006).

This possibility is not contradicted by petrological and geophysical evidences about a very low viscosity between 100 - 150 km of depth, within the LVZ of the upper asthenosphere (Panza, 1980; Hirth & Kohlstedt, 1996; Holtzman *et al.,* 2003; Rychert *et al.,* 2005; Panza et al., 2010). A 50-100 km thick layer with low viscosity remains invisible to post-glacial rebound modelling (the channel flow model of Cathles, 1975). This layer, probably because well beyond the reach of standard tomography, is usually neglected and considered as a whole with the underlying higher viscosity lower asthenosphere and it is not included in current rheological models because of the real difficulty to handle numerically high viscosity contrasts, as it is well described by Tackley (2008) and Ismail-Zadeh and Tackley (2010). A global net rotation is more coherent with the geological and geophysical asymmetries (Riguzzi et al., 2010; Panza et al., 2010), which favor a complete rotation of the lithosphere rather than only a mean rotation (see Fig. 14B).

Relevant evidence about the tidal role for the existence of a net rotation is that the latitude range of the estimated tectonic *mainstream* is about the same as the Moon maximum declination range (± 28◦) during the nutation period (≈18.6 yr). Further indications come from the fact that the induced geopotential variations and the solid Earth tide modeling (McCarthy and Petit, 2004) generate extreme amplitudes of the Earth bulges (≈ ±30 cm) propagating progressively within the same latitude

range (Biagi et al., 2006). In particular, the track of the semi-diurnal bulge crest is roughly directed from E to W, as small circles moving from latitudes 28◦ to 18◦, when the Moon moves from maximum to minimum declinations (the same happens at negative latitudes for the opposite bulge), thus corroborating the role, within plate tectonics, of rotational and tidal drag effects (Bostrom, 1971).

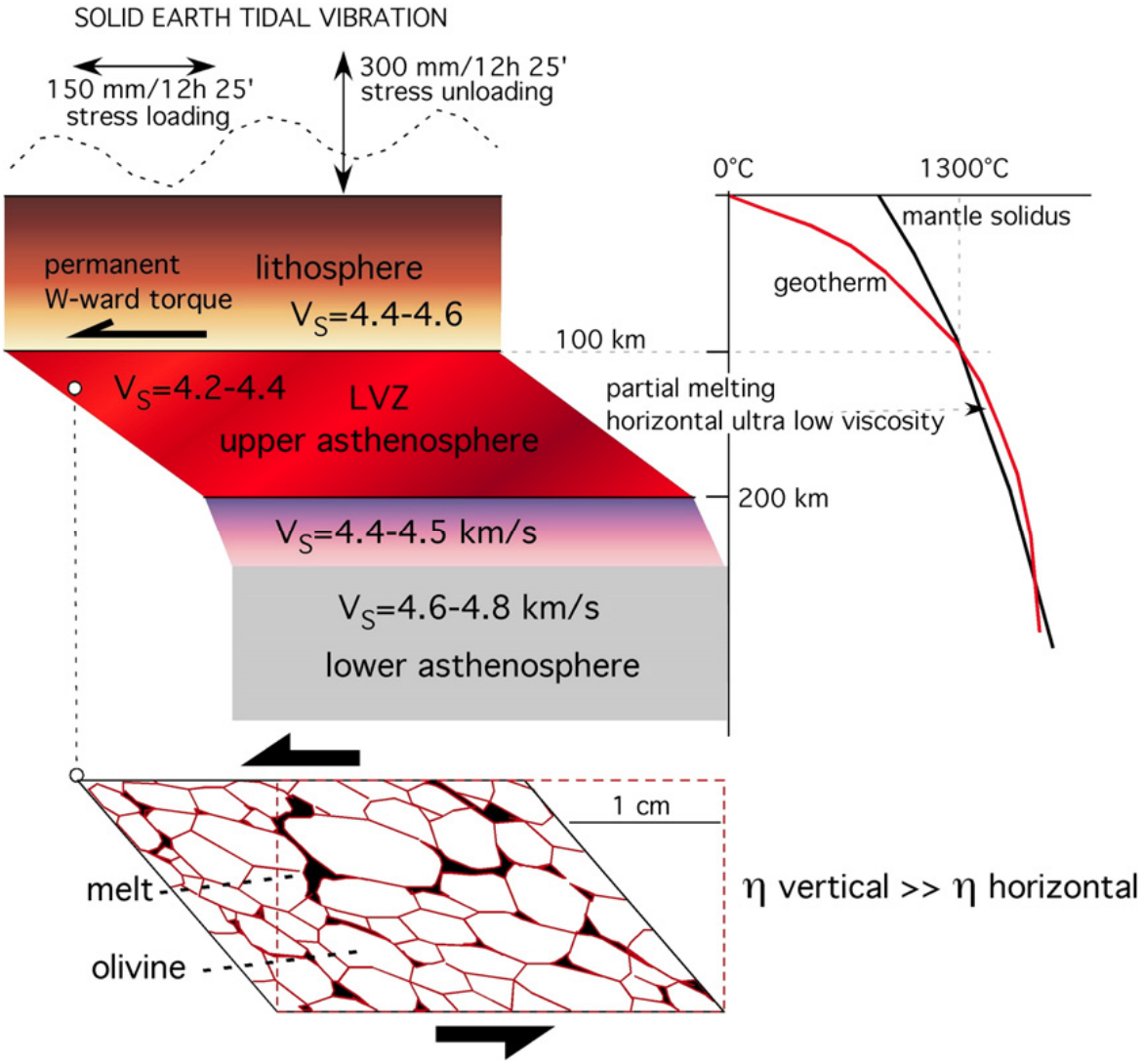

Fig. 14 B. In the asthenosphere, where the geotherm is above the temperature of mantle solidus, small pockets of melt can induce a strong decrease of the viscosity in the upper part of the asthenosphere. The viscosity in this layer, the LVZ of the asthenosphere, can be much lower than the present-day estimates of the asthenosphere viscosity based on the post-glacial rebound, because the horizontal viscosity under shear can be several orders of magnitude lower than the vertical viscosity computed averaging the whole asthenosphere. This should be the basic decoupling zone for plate tectonics, where the lithosphere moves relative to the underlying mantle. Tidal waves are too small to generate plate tectonics. However, their horizontal polarized movement, might determine a fundamental consequence. The lithosphere, being swung horizontally by the solid tide of say 150 mm/semidiurnal, may, under a permanent torque, retain a small but permanent strain (e.g., a shift of 0.1 mm/semidiurnal). At the end of the year this slow restless deformation amounts to a cumulative effect of several centimeters which is consistent with the observed plate motion and thus could be what we consider the net rotation of the lithosphere. After Riguzzi et al. (2010).

The tectonic equator (TE) is the ideal line (great circle) along which plates move over the Earth's surface with the fastest mean angular velocity toward the west relative to the mantle (Crespi et al., 2007). Consistently with the present-day Vs resolution, the TE-pert (which is not a great circle) describes the trajectory along which a global circuit, formed by an ubiquitous LVZ about 1000 km wide and about 100 km thick, occurs in the asthenosphere, where the most mobile mantle LVZ is located. The existence of a continuous global flow within the Earth is thus granted by the existence of the perturbed equator (Panza et al., 2010).

Shallow and deep hot spots reference frameworks

The so-called hot spots are a misleading reference framework for measuring plate motion relative to the mantle, because they are not fixed and they may partly originate in the lower lithosphere or the asthenosphere (Anderson, 1999; Smith and Lewis, 1999; Harpp et al., 2002; Doglioni et al., 2005; Panza et al., 2007b). Intraplate migrating hotspots, which are unrelated to rifts or plate margins in general, regardless of their origin in the mantle column, indicate relative motion between the lithosphere and the underlying mantle in which the hotspot source is located.

Pacific plate hotspots are sufficiently fixed relative to one another to represent an independent reference framework to compute plate motions. However, the interpretation of the middle asthenosphere (shallow hot spot reference framework) rather than the deep lower mantle (deep hot spot reference framework) as the source for intraplate Pacific hotspots has several implications. First, the decoupling between the lithosphere and the sub-asthenospheric mantle is greater than that recorded by hotspot volcanic tracks (>100 mm/yr) due to undetectable shear (Waldhauser et al., 2002; Romanowicz, 2003; Anderson, 2007a,b; Panza et al., 2007b; Boschi et al., 2007; Boyadzhiev et al., 2008) in the lower asthenosphere below the magmatic source. The shallower the source, the larger the décollement is.

The computation of the westward drift is linked to the Pacific plate and assumes that the deep lower mantle, below the decoupling zone, is the source for the hotspots above. The Pacific plate is the fastest plate in the hotspots reference framework and dominates the net rotation of the lithosphere. Therefore, if decoupling with respect to the subasthenospheric mantle is larger, the global westward drift of the lithosphere must be faster than the estimates made so far, and may possibly vary between 50 and 90 mm/yr. In this case, all plates, albeit moving at different velocities, move westward relative to the subasthenospheric mantle. Finally, faster decoupling can generate more

shear heating in the asthenosphere (even >100 °C).

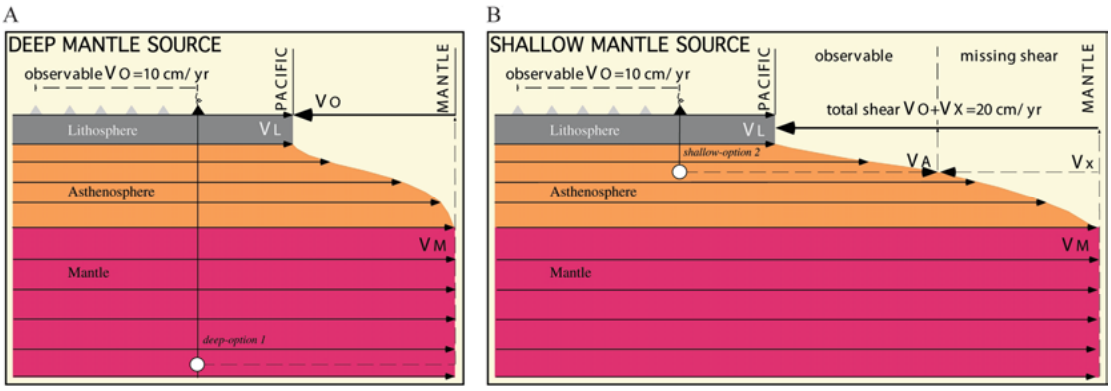

Fig. 15. The Hawaiian volcanic track indicates that there is decoupling between the magma source and the lithosphere, which is moving relatively toward the WNW. (A) If the source is below the asthenosphere (e.g., in the subasthenospheric mantle), the track records the entire shear between lithosphere and mantle. (B) In the case of an asthenospheric source for the Hawaiian hotspot, the volcanic track does not record the entire shear between the lithosphere and subasthenospheric mantle, because part of it operates below the source (deep, missing shear). Moreover, the larger decoupling implies larger shear heating, which could be responsible for the scattered point-like Pacific intraplate magmatism, after Doglioni et al. (2005) and Cuffaro and Doglioni (2007). Following the hypothesis of deep-fed hotspots, after assuming that shear is distributed throughout the asthenospheric channel (Fig. 15A), and providing the velocity **VL** of the Pacific lithosphere toward the ESE (110–120°) is slower than that of the underlying subasthenospheric mantle **VM** (**VM** > **VL**), the relative velocity **VO** corresponding to the WNW delay of the lithosphere is: **VO** = **VL** – **VM** (1). For the case of Hawaii, the observed linear velocity is **VO** = 103 mm/m.y. and it corresponds to the propagation rate of the Hawaiian volcanic track (Fig. 15A). If the location of the Hawaiian melting spot is in the middle of the asthenosphere (Fig. 15B) instead of the lower mantle (Fig. 15A), it would imply that the shear recorded by the volcanic track at the surface is only that occurring between the asthenospheric source and the top of the asthenosphere, i.e., in the hypothesis of a rough linear increase of **VA** as shown in the figure, of only half of the total displacement, if the source is located in the middle of the asthenosphere. Under this condition, the velocity recorded at the surface is: **VO** = **VL** – **VA** (2), with **VA** = **VX** + **VM** (3), where **VO** = 103 mm/year is still the observed propagation rate of the volcanic track (e.g., Hawaii), **VA** is the velocity recorded at the shallow source of the hotspot, and **VX** is that part of the velocity that is not recorded, due to the missing shear measurement. Substituting equation (3) in equation (2), we have: **VO** = **VL** – **VM** – **VX** (4) and **VO** + **VX** = **VL** – **VM** (5). The observed velocity **VO** = 103 mm/year of Hawaii is the velocity of the total displacement if the magmatic source is located in the deep mantle, whereas it represents only half of the total shear if the source is located in the middle of the asthenosphere. In that case, to refer plate motions again with respect to the mesosphere, the velocity **VX** has to be added to the observed velocity **VO** (Fig. 15B), as in equation 5. If the source of Pacific hotspots is in the middle of the asthenosphere, half of the lithosphere–subasthenospheric mantle relative motion is unrecorded, which means that the total relative displacement of the Hawaiian hotspot would amount to about **VO** + **VX** = 200 mm/year (Fig. 15B).

If the viscosity of the asthenosphere is locally higher than normal, this amount of heating, in an undepleted mantle, could trigger the scattered intraplate Pacific volcanism itself. The Emperor-Hawaiian bend can be reproduced assuming a local bend of the viscosity anisotropy in the asthenosphere. Variations in depth and geometry in the asthenosphere of these regions of higher viscosity could account for the irregular migration and velocities of surface volcanic tracks. This type of volcanic chain has different kinematic and magmatic origins from the Atlantic

hotspots or wetspots, which migrate with or close to the oceanic spreading center and are therefore related to the plate margin.

The preferred location of hotspots in a shearing asthenosphere would seem to discount the existence of hotspot reference frameworks that include both intraplate and ridge-centered hotspots. A hotspot reference framework using only Pacific hotspots seems to be more reliable due to their relative inertia. However, in every hotspot reference framework, the Pacific plate is the fastest-moving plate in the world, and it contains the most diffuse intraplate magmatism, regardless of its margins. Fastest velocity implies largest potential shear heating at its base.

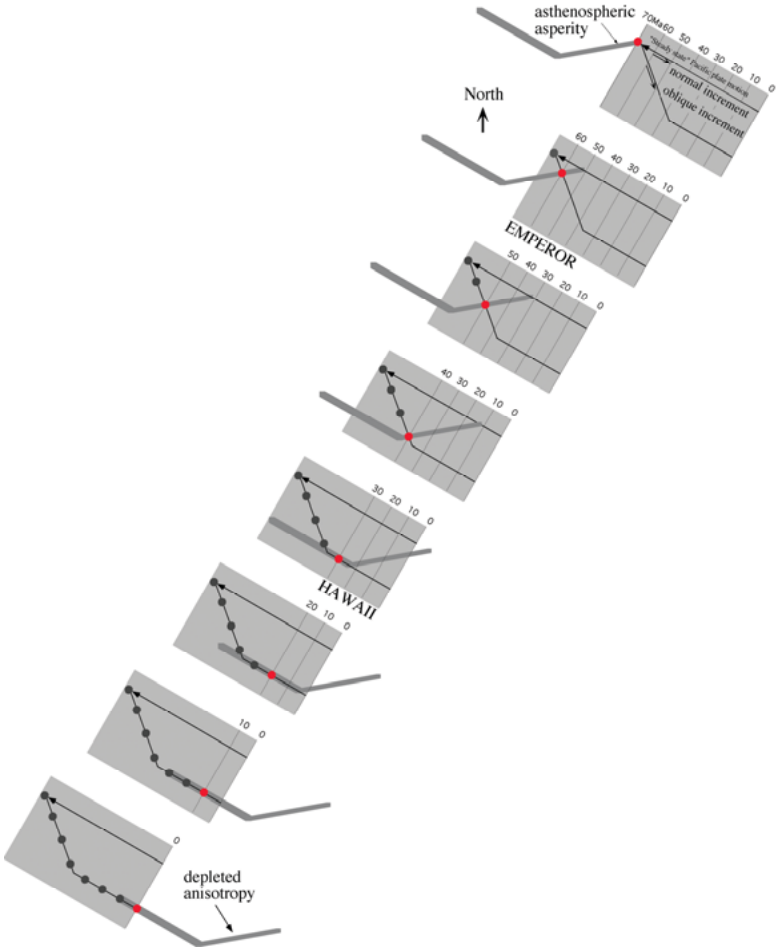

Fig. 16. Kinematic map view model for the bending of the Emperor-Hawaiian chains, maintaining stable the Pacific plate motion. The bend can be reproduced by introducing a bent, mirror like anisotropy in the décollement zone (i.e., the asthenosphere), where locally higher viscosity generates shear heating and related magmatism. The shaded area is a part of the Pacific plate progressively moving to the west-northwest and overriding the asthenosphere. The asthenosphere is assumed to have a typical viscosity of 10^{17} Pa·s apart from the gray line, where it rises to ~10^{20} Pa·s. In each panel, the red spot indicates the active magmatism. In the top panel, while the oblique Emperor seamount chain formed, the velocity of the southeastward propagating volcanic ridge is faster because it is oblique to the Pacific plate motion (the longer oblique arrow in the incremental 10 Myr interval).

Classic, deep lower mantle sources (Morgan, 1971) for Pacific

intraplate hotspots imply ~103–118 mm/yr shearing between the lithosphere and subasthenospheric mantle, as indicated by the age progression of the volcanic tracks. In this view, hotspots are generated either by fluid jets or anomalously high temperatures in the deep mantle (e.g., Schubert et al., 2001). Alternatively, an asthenospheric mantle source for the same hotspots is supported by petrological, geochemical, and kinematic data. A model in which the source of the magma is the asthenosphere (e.g., Smith, 1993; Anderson, 2000) allows for two important deductions: (1) Shear heating generated in the asthenosphere by the motion of the overlying Pacific plate is large enough to generate the scattered and diffuse intraplate magmatism observed, and (2) the velocity recorded in volcanic chains is a function of the depth to the source of the magmatism in the asthenosphere (Fig. 15) and its trend relative to plate motion direction (Figs. 16 and 17) (Doglioni et al., 2005).

The shear between the lithosphere and subasthenospheric mantle is expected to be greater than 103–118 mm/yr, because of the missing shear in the asthenosphere below the hotspot source.

This estimate provides a global net rotation of the lithosphere towards W that is larger than the present estimate of 49 mm/yr (Gripp and Gordon, 2002). In this interpretation, all plates on Earth move westward relative to the subasthenospheric mantle, although at different velocities, and with a sinusoidal trend (Doglioni, 1993a). Therefore, in contrast with the predictions of the classic hotspot reference framework (Fig. 18, option 1), the subasthenospheric mantle beneath the Nazca plate would move eastward relative to the lithosphere (Fig. 18, option 2), thus providing a mechanism that makes continuously available new fertile asthenosphere that melts beneath the westward-migrating East Pacific Rise (EPR) (Fig. 19).

With these velocities relative to the subasthenospheric mantle, the net rotation of the entire lithosphere at its “equator” could be faster than 90 mm/yr. Most of the Pacific asthenosphere has an average viscosity around $5 \cdot 10^{17}$ Pa·s (Pollitz et al., 1998). However, lateral variations in geochemistry and fluid depletion can result in local increases in viscosity. Greater shear between the lithosphere and subasthenospheric mantle could generate excess heating exceeding 100 °C if the asthenosphere contains local anomalies in which the viscosity is higher ($4 \cdot 10^{19}$ to 10^{20} Pa·s). For the maximum temperature increases, extra melting can be generated, which may be responsible for scattered superficial magmatism. An increase of ~100 °C would shift the adiabat curve of the uprising mantle to the right (Doglioni et al., 2005), shifting the asthenospheric mantle to the field of more extensive melting (Green, 2003).

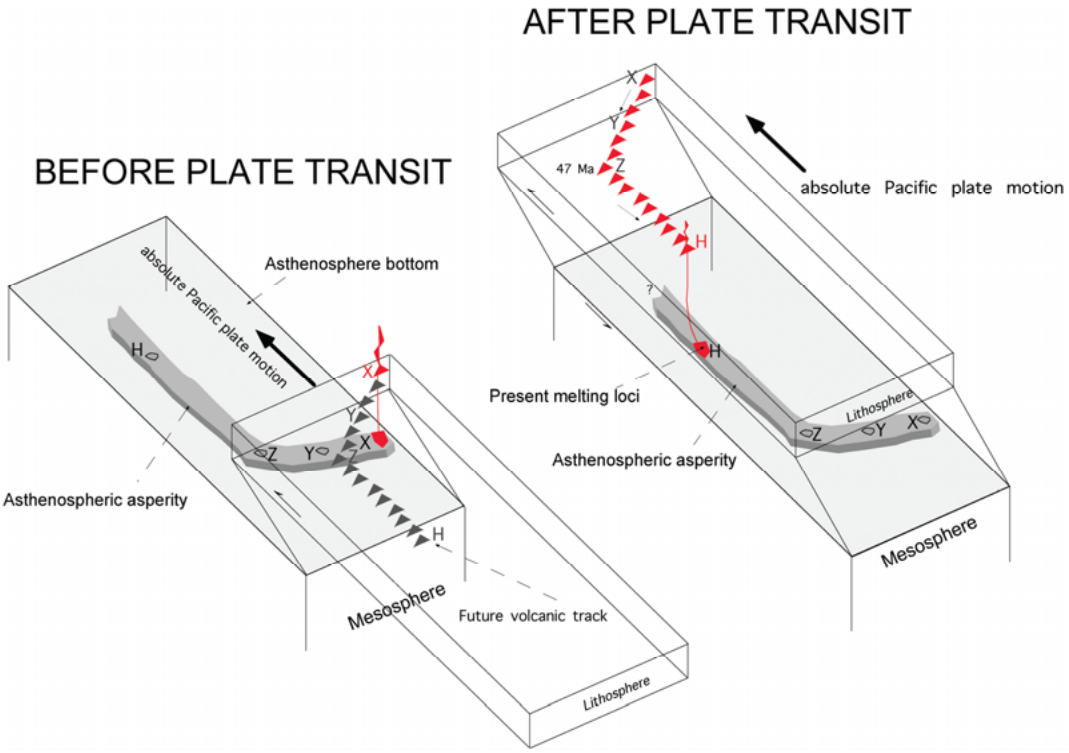

Fig. 17. The irregular distribution of an area of higher viscosity (e.g., 10^{20}–10^{21} Pa·s) in the Pacific asthenosphere (viscosity, 10^{17} Pa·s), such as that shown by the curved gray band in the pre-transit cartoon, could account for the bend in the Emperor-Hawaiian track, in spite of a stable absolute Pacific plate motion direction. The pre-transit geometry mirrors the resulting volcanic chain shown in the post-transit cartoon. X, Y, Z, and H in the asthenospheric asperity correspond to similarly labeled volcanoes in the surface trail. Red letters show the active magmatism. The gray volcanic track in the left panel indicates inferred, not yet existing volcanoes.

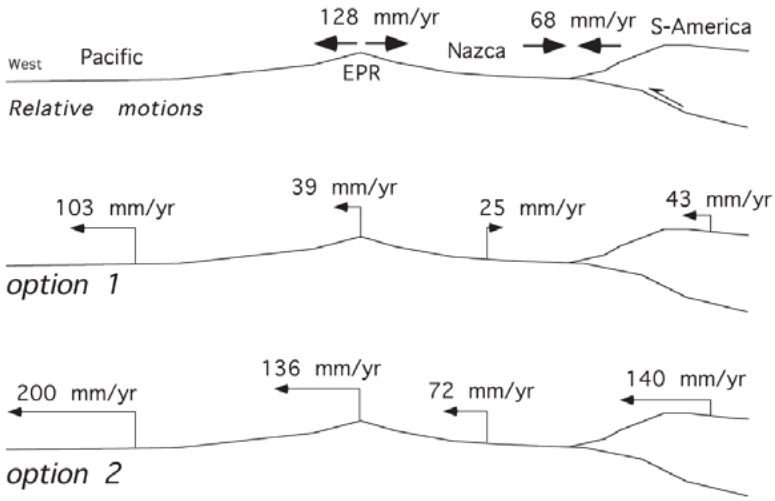

Fig. 18. Simple kinematic relation between the Pacific, Nazca, and South America plates. Relative motion vectors (top) after Heflin et al. (2007). Option 1 (middle) indicates the absolute motions when referred to the Hawaiian hotspot moving at ~103 mm/yr (Gripp and Gordon, 2002). Option 2 (bottom) is the case for which the hotspot source is located in the asthenosphere and relative motion between the Pacific plate and the subasthenospheric mantle is assumed to be 200 mm/yr (see also Doglioni et al., 2005). In this last configuration, all three plates move westward relative to the mantle. EPR (East Pacific Rise); S-America (South America plate).

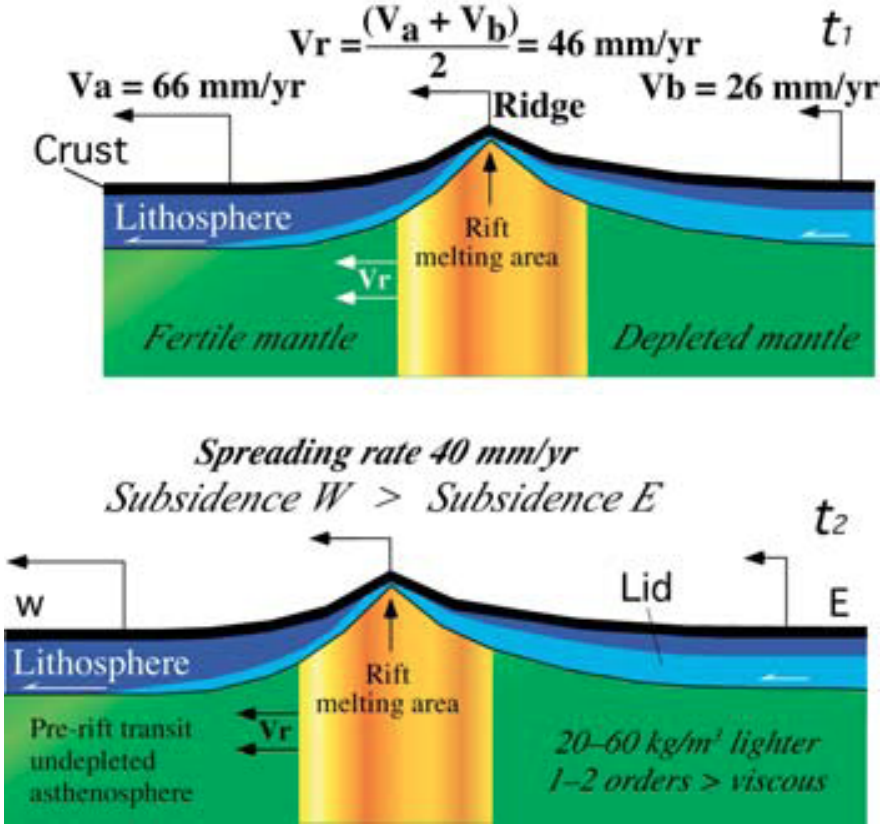

Fig. 19. Oceanic rift with hypothetic velocities of plates a and b relative to fixed mantle (e.g. in the case where the Pacific plate is on the W and Nazca plate on the E, the Pacific lithosphere moves W faster than the Nazca plate does, because the asthenosphere underlying the Pacific plate is less viscous and therefore decoupling is more efficient; due to the increase in viscosity and decrease in temperature along the rifting area, which is also moving westward, the asthenosphere below the eastern plate is more viscous, causing stronger coupling and a lower steady-state velocity for the Nazca plate). Ridge moves west at velocity of ridge (Vr). Separation between plates triggers uplift of undepleted mantle previously located to west. In melting area, mantle loses Fe, Mg, and other minerals to form oceanic crust, while residual mantle is depleted. Since melting area moves west it gradually transits toward undepleted mantle, releasing depleted mantle to the east. This can explain slightly shallower bathymetry of eastern limb, but it should also generate asymmetry of seismic wave velocity seen in Fig. 26. In this model, differential velocity among plates is controlled by low-velocity layer viscosity variations generating variable decoupling between lithosphere and mantle (see text). *t*1 and *t*2 are two time stages. Lid is lithospheric mantle. This kinematic model implies that new fertile mantle is continually supplied to the oceanic ridge (Doglioni et al., 2005; Panza et al., 2010).

This model resurrects the work of Shaw and Jackson (1973) and can explain Pacific hotspots often attributed to deep mantle plumes as stress-generated intraplate melt anomalies in the asthenosphere. The model also explains the observed periodicity and variability in magma segregation, because strong shear heating decreases viscosity and therefore also inhibits melting until a higher viscosity is regained and shear heating recommences.

The origin of such hotspots would therefore be different from those persistently located on oceanic ridges and sourced in the

asthenosphere, where abundant water in the mantle (wetspots) strongly affects the extent of melting (Bonatti, 1990; Asimov and Langmuir, 2003).

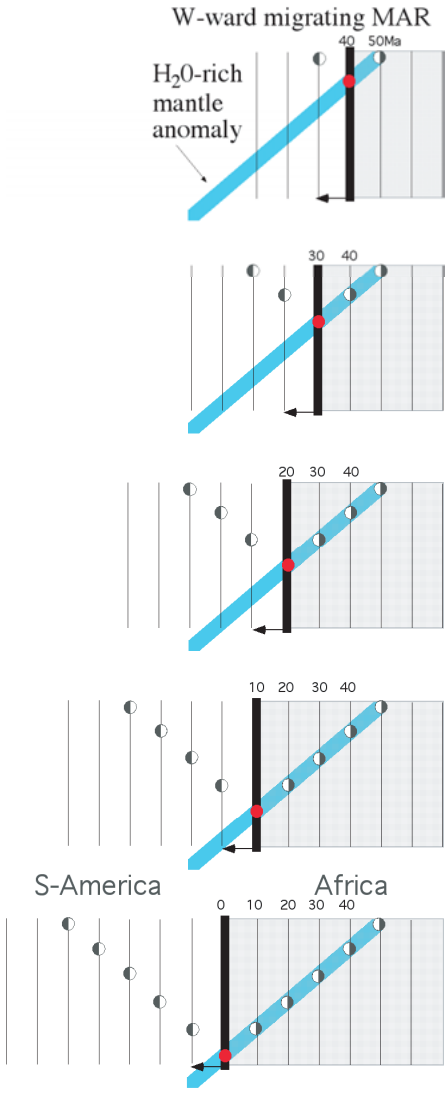

Fig. 20. Hypothetical reconstruction of the south-Atlantic–type migrating volcanic ridges. An anomalously water-rich asthenospheric mantle, or wetspot (sensu Bonatti, 1990), oriented oblique to absolute African plate motion and the mid-Atlantic Ridge (MAR) migration could generate a southwest-oriented rejuvenated volcanic track. A similar, mirror like track (northwest trending, southeast propagating) could form in the South America plate. This model explains why the age progression of the volcanic trail is oblique to the transform faults.

The main differences between hotspots and wetspots (e.g., Hawaii versus Ascension) may be summarized in terms of 3D kinematics and petrology, as follows.

The source of the hotspot is in or below the asthenospheric décollement. The plate moves relative to a deeper source and the volcanic trail is independent of any plate margin. The age of the trail is much younger than the host lithosphere. The melting temperature is higher (1400–1500 °C, possibly caused by shear heating).

The wetspot moves with the oceanic ridge, and has an age close

to that of the host oceanic crust (i.e., a speed close to that of the plate boundary). The source of the wetspot is above the asthenospheric décollement. The melting temperature and pressure are lower (perhaps <1300 °C, possibly caused by more water in the mantle). Because wetspots are sourced above the plate-tectonic décollement and do not move with the mantle but rather migrate at the same velocity as the oceanic ridge, they exhibit different surface kinematics. For example northeast-trending, water-rich, parallel anomalies in the asthenospheric mantle generate surface volcanic trails with the same northeast-trending orientation but propagating to the southwest (e.g., Walvis and Cameroon ridges, Fig. 20).

Similar but NW-trending and SE-propagating volcanic trails can be generated in the paired plate to the west (e.g., Rio Grande Rise). The north-northwest-trending Emperor hotspot track can be generated by a north-northeast-trending asthenospheric anomaly located in the décollement surface, and the resulting magmatism propagates toward the south-southeast. In both these cases, there is an angle between the absolute plate motion and the mantle structural anisotropy, but the resulting volcanic tracks are trending in the opposite directions (compare Figs. 16 and 20). In the case of the Hawaiian track, the directions of plate motion and mantle anisotropy seem to coincide. There exist traces that extend from intraplate to ridge-centered locations and vice versa (e.g., Foundation, Nazca-Easter-Tuamotu, Cobb), plus ridge-crossing traces (e.g., New England–Great Meteor, Réunion, Kerguelen). Is each of these tracks really linked to the same source (e.g., is Réunion really connected to the Chagos-Laccadive system), or are they two independent magmatic systems? Are some of these tracks related to transtensional tectonics along transform zones? Could shear heating and wet melting occur along the same trail? Can shear heating persist beneath a ridge, or is there a switch to a water-driven process? These are questions that remain to be answered.

Global kinematics in deep versus shallow hotspot reference frameworks

Plume tracks at the Earth's surface probably have various origins, such as wet spots, simple rifts, and shear heating. Because plate boundaries move relative to one another and relative to the mantle, plumes located on or close to them cannot be considered reliable for the definition of a reference framework. Considering the intraplate Pacific hotspots, the plate motions with respect to the mantle in two different reference frameworks, one fed from below the asthenosphere, and one fed by the asthenosphere itself, provide different kinematics and stimulate opposite dynamic speculations. Plates move faster relative to the mantle

if the source of hotspots is taken to be the middle-upper asthenosphere (shallow-fed hot spots), because the hotspot tracks would then not record the entire decoupling occurring in the low-velocity zone. The shallow intra-asthenospheric origin for the hotspots would raise the Pacific deep-fed velocity from a value of ~10 cm/year to a faster hypothetical velocity of ~20 cm/year. In this setting, the net rotation of the lithosphere relative to the mesosphere would increase from a value of 0.4359°/m.y. (deep-fed hotspots) to 1.4901°/m.y. (shallow-fed hotspots). In this framework, all plates move westward along an undulated sinusoidal stream (see Section "Tectonic Equator"), and plate rotation poles are largely located in a restricted area at a mean latitude of 58°S. This reference framework seems quite consistent with the persistent geological asymmetry that suggests a global tuning of plate motions due to Earth's rotation. Another significant result is that along E- (or NE-) directed subduction zones, slabs move relative to the mantle in the direction opposed to the subduction, casting doubts on slab pull as the first-order driving mechanism of plate dynamics (Cuffaro and Doglioni, 2007; Doglioni et al, 2007).

The computation of plate motions with respect to a shallow hotspot reference framework shows that shallow sources for hotspots produce different plate kinematics, compared with the HS3-NUVEL1A results (Gripp and Gordon, 2002), i.e., new and faster plate motions with respect to the mesosphere than those previously calculated; in the deep hotspot framework, rotation poles are largely scattered, and most of the plates move toward the west, except for Nazca, Cocos, and Juan de Fuca plates (Cuffaro and Doglioni, 2007). On the contrary, relative to the shallow hotspot framework, all plates move westerly, and rotation poles are mostly located in a restricted area at a mean latitude of 58°S. Furthermore, the net rotation of the lithosphere is faster with respect to the shallow-fed hotspot framework, which is useful to compute plate motions in the mean-lithosphere reference framework, No Net Rotation (NNR) reference framework (Jurdy, 1990).

The mean lithosphere is also the framework for space geodesy applications to plate tectonics (Heflin et al., 2007). Most of the geodesy plate-motion models are referred to the NNR framework (Sella et al., 2002; Drewes and Meisel, 2003). The International Terrestrial Reference Frame (ITRF2000) (Altamimi et al., 2002) is the framework in which site velocities are estimated. The ITRF2000 angular velocity is defined using the mean lithosphere.

As suggested by Argus and Gross (2004), it would be better to estimate site positions and velocities relative to hotspots, continuing first to estimate velocity in the ITRF2000 and then adding the net-rotation angular velocity.

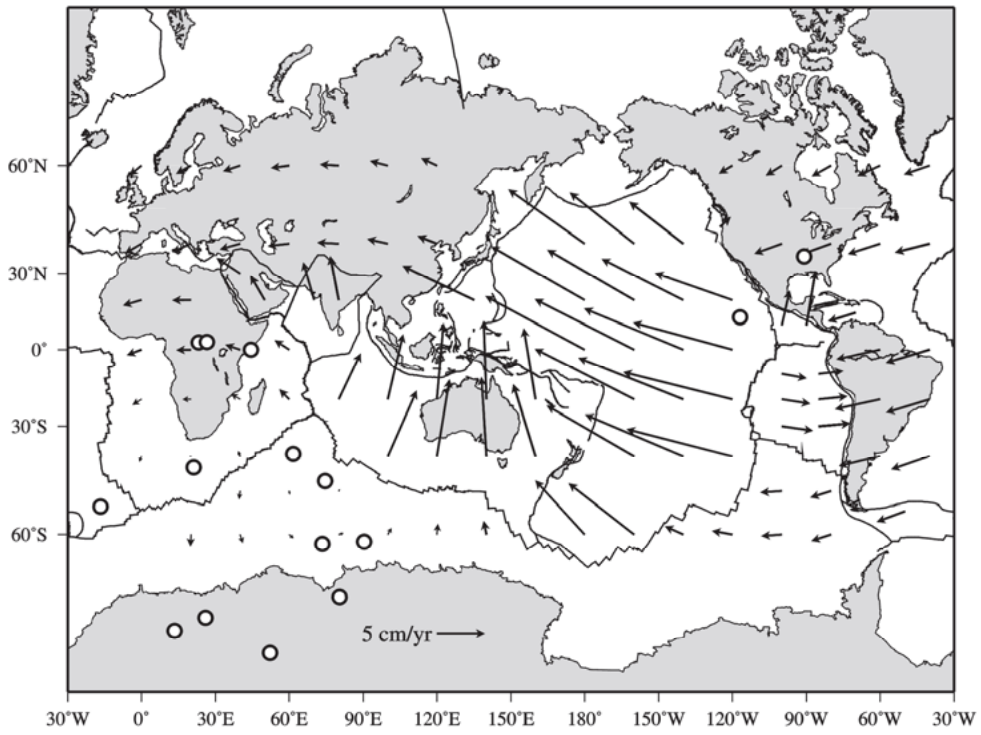

Fig. 21. Current velocities with respect to the deep hotspot reference frame. Open circles are the rotation poles. Data from HS3-NUVEL1A (Gripp and Gordon, 2002).

The deep and shallow hotspot interpretations generate two different hotspot reference frameworks. In the case of deep-mantle sources for the hotspots, there are still a few plates moving eastward relative to the mantle (Fig. 21), whereas in the case of shallow mantle sources, all plates move "westward," although at different velocities (Fig. 22). The kinematic and dynamic consequences of the shallow reference framework are so unexpected that it could be argued that they suggest that plumes are instead fed from the deep mantle.

However, the shallow reference framework (see Sections "Shallow and deep hot spots reference frameworks" and "Global kinematics in deep versus shallow hotspot reference frameworks") fits better the observed geological and geophysical asymmetries (described in Sections "Accretionary prisms", "Rifts", "Thrust belts, foredeep and subduction zones"). This fact indicates a global tuning (i.e., a complete "westward" rotation of the lithosphere relative to the mantle) rather than a simple average of plate motions (i.e., where the westward drift is only a residual of plates motion both westward and eastward relative to the mantle). In fact, geological and geophysical signatures of subduction and rift zones independently show a global signature, suggesting a complete net westward rotation of the lithosphere and a relative eastward motion of the mantle that can kinematically be inferred only from the shallow hotspot reference framework.

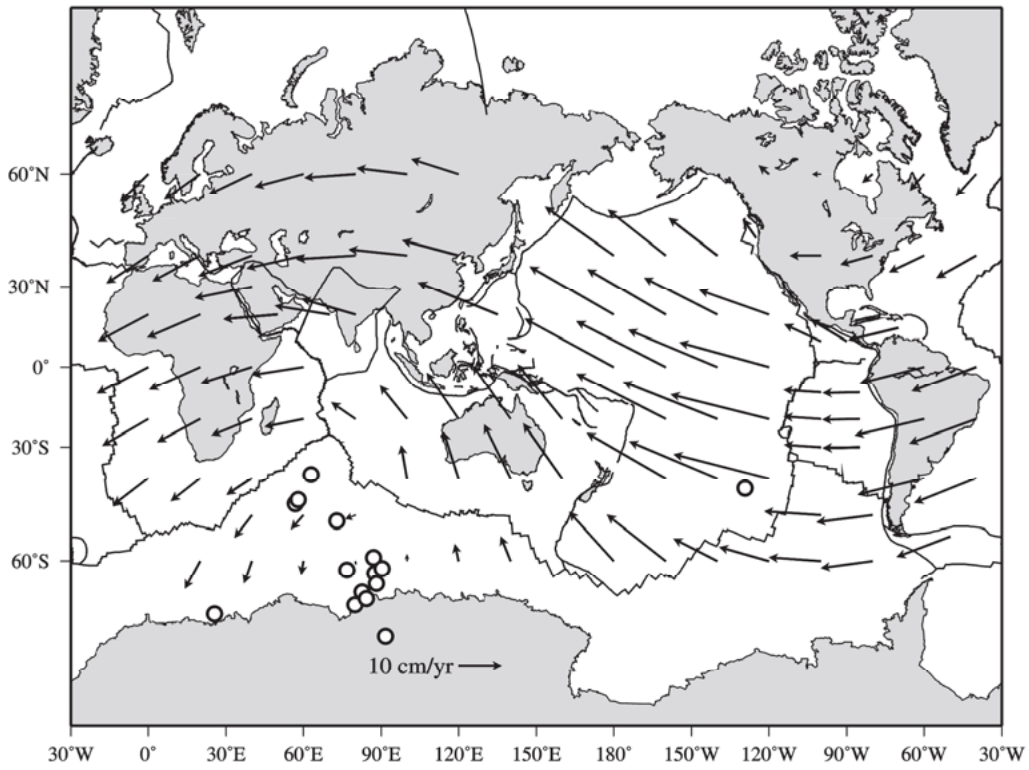

Fig. 22. Present-day plate velocities relative to the shallow hotspot reference framework, incorporating the NUVEL-1A relative plate-motion model (DeMets et al., 1990, 1994). With respect to this reference framework, all plates have a westward velocity component. Open circles are the rotation poles.

Plates move along a sort of mainstream depicting a sinusoid (Doglioni, 1990, 1993a; Crespi et al., 2007), the Tectonic Equator (Fig. 12), which is nicely confirmed by present-day space geodesy plate kinematics (e.g., Heflin et al., 2007). Global shear-wave splitting directions (Debayle et al., 2005) are quite consistent with such undulate flow and naturally deviate from it at subduction zones, which represent obstacles to the relative mantle motion. In fact, along this flow, W- (or SW-) directed subduction zones are steeper than those that are E- (or NE-) directed, and associated orogens are characterized by lower structural and topographic elevations, backarc basins, or by higher structural and morphological elevation and no back-arc basins (see Section "Thrust belts, foredeeps and subduction zones" and Doglioni et al., 1999a,b). The asymmetry is striking when comparing western and eastern Pacific subduction zones, and it has usually been interpreted as related to the age of the down going oceanic lithosphere, i.e., older, cooler, and denser on the western side. However these differences persist elsewhere, regardless of the age and composition of the down going lithosphere (see Section "Thrust belts, foredeeps and subduction zones"), e.g., in the

Mediterranean Apennines and Carpathians versus the Alps and Dinarides, or in the Banda and Sandwich arcs, where even continental or zero-age oceanic lithosphere is almost vertical along west-directed subduction zones. Rift zones are also asymmetric, with the eastern side more elevated by ~100–300 m worldwide (Doglioni et al., 2003) and this asymmetry extends to mantle depths. Based on a surface wave tomographic three-dimensional model of the Earth's upper 300 km, a global cross section parallel to the equator of the net rotation of the lithosphere, the TE, shows that shear wave velocities are different at the western when compared to those of the eastern flanks of the three major oceanic rift basins (Pacific, Atlantic, and Indian ridges). In general, the western limbs have a faster velocity and thicker lithosphere relative to the eastern or northeastern one, whereas the uppermost asthenosphere is faster in the eastern limb than in the western limb. The difference between the two flanks can be the combination of mantle depletion along the oceanic rifts and of the westward migration of the ridges and the lithosphere relative to the mantle. The low-velocity layer in the upper asthenosphere at the depth of 120–200 km represents the decoupling between the lithosphere and the underlying mantle, as it is well defined by the distribution of radial anisotropy that reaches minimum values close to the rifts, but with an eastward offset (Panza, et al. 2010).

The westward drift of the lithosphere implies that plates have a general sense of motion and that they are not moving randomly. If we accept this postulate, plates move along this trend at different velocities, relative to the mantle, toward the west along the flow line of the TE. In this view, plates would be more or less dragged by the mantle, as a function of the decoupling at their base, the degree of decoupling being mainly controlled by the thickness and viscosity of the asthenosphere.

Lateral variations in decoupling could control the variable velocity of the overlying lithosphere (Fig. 23). When a plate moves faster westward with respect to an adjacent plate to the east, the resulting plate margin is extensional; when it moves faster westward with respect to the adjacent plate to the west, their common margin will be convergent (Fig. 23).

The kinematic framework of shallow Pacific hotspots (Fig. 22) constrains plate motions as entirely polarized toward the west relative to the deep mantle. This framework provides a fundamental observation along E- (or NE-) directed subduction zones. In fact, with this reference framework, the slab tends to move out relative to the mantle (upduction), but apparent subduction occurs because the upper plate overrides the lower plate faster (see Section "Subduction kinematics and dynamic constraints", in particular Fig. 42). This scenario argues against slab pull as the main mechanism for driving plate motions, because the slab does

not penetrate into the mantle. In this view, slabs are rather passive features (Fig. 24).

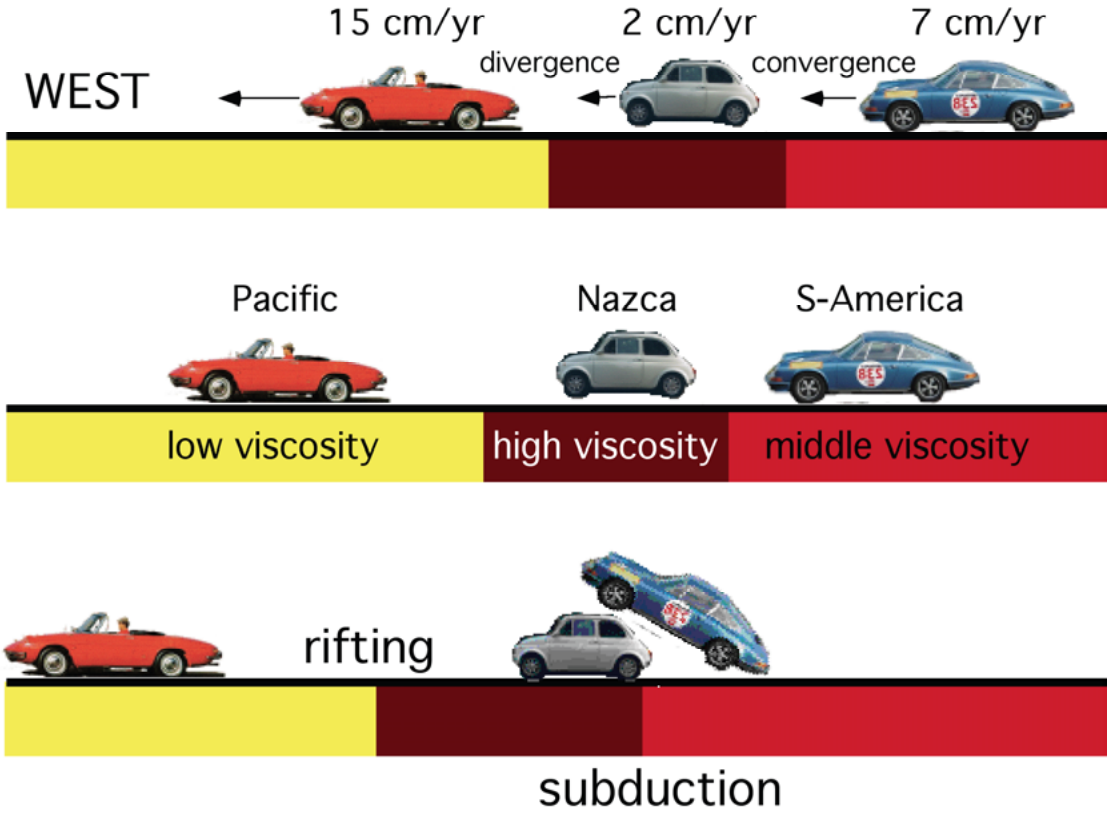

Fig. 23. Cartoon illustrating that plates (cars) move along a common trail (the TE) but with different velocities toward the W, as indicated by the westward drift of the lithosphere relative to the mantle. The differential velocities control the tectonic environment and result from different viscosities or topography of the decoupling surface (Panza et al 2010) within the asthenosphere. There is extension when the western plate moves westward faster with respect to the plate to the east, whereas convergence occurs when the plate to the east moves westward faster with respect to the plate to the west. When the car in the middle is "subducted," the tectonic regime switches to extension, because the car to the west moves faster, e.g., the Basin and Range. After Doglioni (1990).

This kinematic reconstruction is coherent with the frequent intraslab down-dip extension earthquake focal mechanisms that characterize east or northeast-directed subduction zones (e.g., Isacks and Molnar, 1971). It is generally assumed that oceanic plates travel faster than plates with large fractions of continental lithosphere. However, Gripp and Gordon (2002), even in the deep hotspot reference framework, have shown that the South American plate is moving faster than the purely oceanic Nazca plate. Another common assumption is that plates move away from ridges, but again, in the deep reference framework, Africa is moving toward the mid-Atlantic ridge, although slower than is South America. Moreover, Africa is moving away from the Hellenic subduction zone.

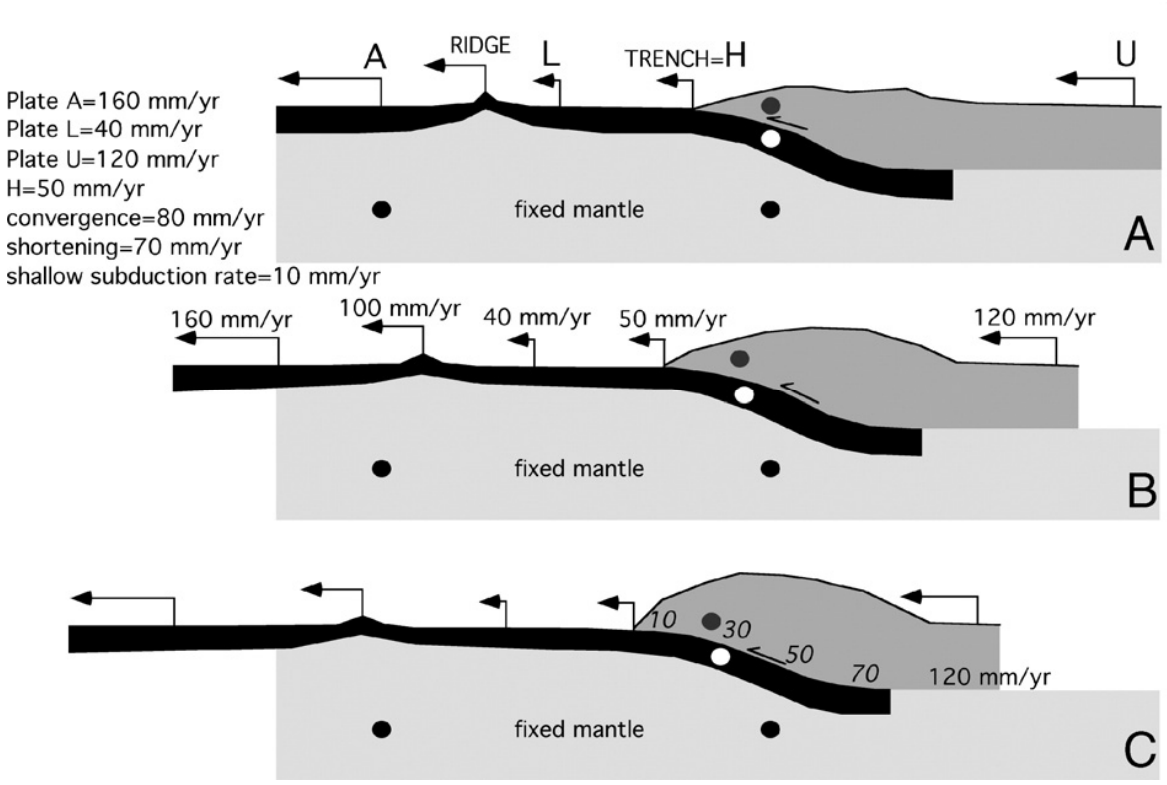

Fig. 24. Cartoon assuming a Pacific plate (plate A) moving at 16 cm/year. When plate motions are considered relative to the shallow hotspot reference framework, i.e., assuming fixed the mantle, the slabs of E- (or NE-) directed subduction zones may move out of the mantle. This scenario is clearly the case for Hellenic subduction and, in the shallow hotspot reference framework, also for Andean subduction (AS). The white circle moves leftward relative to the underlying black circle in the mantle. Subduction occurs because the upper plate dark gray circle moves leftward faster than the white circle in the slab. In this model, the slab moves west at 40 mm/yr relative to the mantle. The subduction rate is the convergence minus the orogenic shortening. With different velocities, this scheme applies to the Hellenic subduction and, in the shallow hotspot reference framework, also to the AS. In the lower section, the numbers in italic from10 through 70 indicate the relative velocity in mm/yr between the upper and the lower plate. The subduction rate should increase with depth, where the upper plate shortening is decreasing. This is consistent with the down-dip tension seismicity of this type of subduction (see Fig. 8). This kinematic evidence of slabs moving out of the mantle (upduction) casts doubts on the slab pull as the main driving mechanism of plate motions.

In the shallow reference framework, these observations are enhanced and thus unequivocal. Another typical assumption is that plates with attached slabs (the subducting portions of plates) move faster, but the Pacific plate moves at ~1.06°/m.y., much faster in terms of absolute velocity than the Nazca plate (~0.32°/m.y.). The Pacific and Nazca plates have roughly the same percentage of attached slab (37% and 34%, respectively).

Therefore, in the case of a shallow origin for Pacific hotspots, westward drift implies a generalized counterflow of the underlying mantle (Fig. 25). With such an asymmetric flow, upper mantle circulation is possible in correspondence of TE-pert and disturbed by subduction and rift zones along TE (Doglioni et al., 2006a,b; Panza et al., 2010).

The fertile asthenosphere coming from the west melts and

depletes along the ridge. Continuing its travel to the east, the depleted asthenosphere is more viscous and lighter (Doglioni et al., 2005; Panza et al., 2010). Subduction zones directed to the E (or NE), along the mantle counterflow, might refertilize the upper mantle, whereas W- (or SW-) directed subduction zones would penetrate deeper into the mantle.

Net westward rotation of the lithosphere relative to the underlying mantle is a controversial phenomenon first attributed to tidal effects, and later to the dynamics of mantle convection. In spite of a number of independent geological and geophysical arguments for westward tectonic drift, this phenomenon has received little attention in the recent past.

The global-scale asymmetry of tectonic features and the westward drift of the lithosphere support a rotational component for the origin of plate tectonics (Scoppola et al., 2006). The westward drift could be the combined effect of three processes (see also Fig. 27): (1) tidal torques acting on the lithosphere and generating a westerly directed torque that decelerates Earth's spin; (2) down welling of denser material toward the bottom of the mantle and in the core, slightly decreasing the moment of inertia and speeding up Earth's rotation and only partly counterbalancing tidal drag; and (3) thin (3- to 30-km) layers of very-low-viscosity hydrate channels in the asthenosphere. These layers are beyond the reach of tomography due to the limitations of the theoretical framework employed (Waldhauser et al., 2002; Romanowicz, 2003; Anderson, 2007a,b; Panza et al., 2007; Boschi et al., 2007; Boyadzhiev et al., 2008).

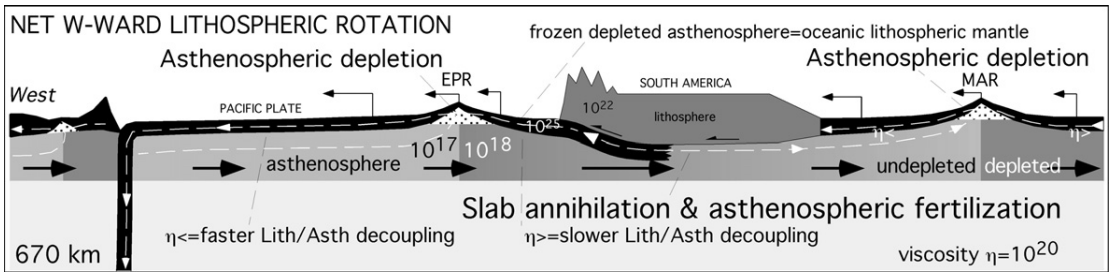

Fig. 25. Model for the upper mantle cycle, in the case of the shallow Pacific hotspot reference framework. The lower the asthenospheric viscosity, the faster the W-ward displacement of the overlying plate is. The asthenospheric depletion at oceanic ridges makes the layer more viscous and decreases the lithosphere/asthenospheric decoupling, and the plate to the east is then slower. The oceanic lithosphere subducting E-ward enters the asthenosphere where it is molten again to refertilize the asthenosphere. W- (or SW-) directed subductions provide deeper circulation. The E- (or NE-) directed subduction (the Andes) tends to escape out of the mantle, but it is overridden by the upper plate (South America, after Doglioni et al., 2006a); similar observation applies to the Adria plate (E- (or NE-) directed subduction) under the Hellenides (the upper plate) (see Section "Subduction kinematics and dynamic constraints", in particular Fig. 40 and 42)

Shear heating and the mechanical fatigue may self-perpetuate one or more channels of this kind, within the TE and the TE-pert (Panza et al.2010), which provide the necessary decoupling zone of the lithosphere.

Consistently with the present-day Vs resolution, the TE-pert (which is not a great circle) describes the trajectory along which a ubiquitous LVZ about 1000 km wide and about 100 km thick occurs in the asthenosphere, where the most mobile mantle LVZ is located. The existence of TE-pert is necessary for the existence of a continuous global flow within the Earth (Panza et al., 2010).

The westward drift of the lithosphere

The essential points supporting a net westward drift of the lithosphere are: (1) the observed net westward drift of the lithosphere with respect to the hotspot reference framework (both shallow and deep) of 50–90 mm/year; (2) the tidal torque provides a sufficiently energetic mechanism to drive this motion, but requires a mechanical decoupling between the lithosphere and the deeper mantle that is well possible along the TE and TE-pert, even if incompatible with current understanding of upper-mantle viscosity and mathematical models for Navier-Stokes laminar flow; (3) a thin, low-viscosity layer (shear zone) could accommodate this motion; and (4) such a layer might not be detectable using classical analysis of postglacial rebound nor of tomography (Scoppola et al., 2006; Romanowicz, 2003).

Mei et al. (2002) recently give estimates of the viscosity of the asthenosphere lower than 10^{16}Pa▪s in thin intra-asthenospheric layers. These ultralow-viscosity layers could enable decoupling of the lithosphere relative to the mantle induced by rotational drag. The contribution of Earth's rotation to the relative westward motion of the lithosphere accounts for the inadequate kinematics of mantle convection on plate tectonics (e.g., Anderson, 1999), and it provides an explanation of where most of the large amount of energy related to rotation is dissipated and of the balance of forces that are controlling the length of the day (e.g., Lambeck, 1980; Varga et al., 1998; Krasinsky, 1999; Denis et al., 2002; Riguzzi et al., 2010). The net rotation of the lithosphere associated with lateral variations of the viscosity-controlled coupling between lithosphere and underlying mantle can determine variable relative velocities between plates, i.e., extension or convergence, or in other words, plate tectonics. According to this model, shear zones within the asthenosphere should be detected. Recently, based on migrated stacked seismic receiver functions, Zandt et al. (2004) identified the occurrence of low-velocity shear zones in the upper mantle underneath the Sierra Nevada. The generalized presence of low-velocity shear zones in the upper mantle can be inferred in correspondence of the low radial anisotropy (<1%) mantle level shown in Fig. 26.

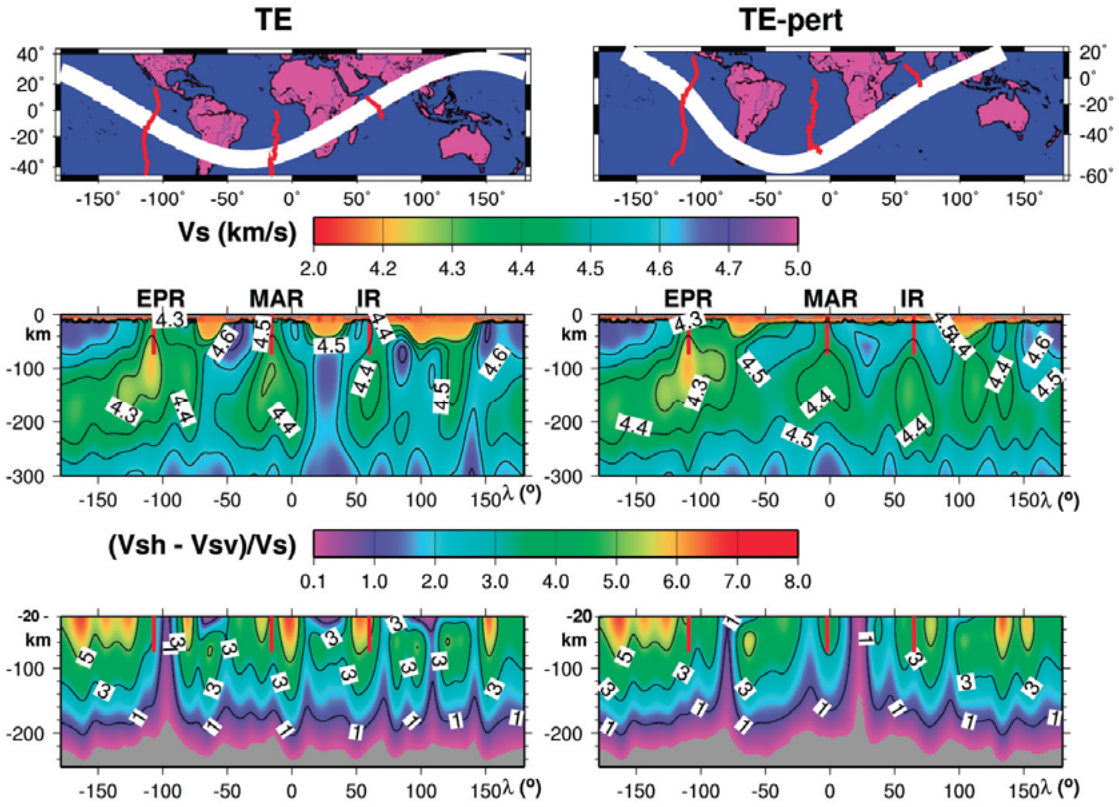

Fig. 26. Shear wave (Earth's) section along tectonic equator (TE) proposed by Crespi et al. (2007) to left, and along perturbed path (TE-pert), a global circuit of partially molten, low velocity material. There is a generalized asymmetry across oceanic ridges: lithosphere (0–100 km) in western side of rift is faster than in eastern or northeastern side, whereas the upper asthenosphere (low-velocity layer, 100–200 km) is slower in the western side with respect to the conjugate counterpart. Red lines correspond to elements of Eastern Pacific (EPR), Mid-Atlantic (MAR), and Indian Ridges (IR). Lower panels show radial anisotropy along these sections. Vs is taken here as average of Vsv and Vsh (see Panza et al., 2010 for more details) along section covering 10° width. Radial anisotropy sections are without crust, since crust is assumed to be isotropic.

In this view, plate tectonics is the result of the combination of the tidal torque effect on a rotating planet, efficient internal convection and lateral viscosity variations at the lithosphere-mantle interface. Here thin hydrate layers are supposed to occur with very low viscosity, far lower than the average estimates predicted by postglacial rebound, and well consistent with the globally observed minimum in the mantle radial anisotropy (Debayle et al., 2005; Panza et al., 2010). This minimum is located at a depth, which varies in the range from 20 km to 200 km as shown in Fig. 26. The permanent, although low, tidal drag and the fatigue could determine the "westward" drift of the lithosphere relative to the mantle (Fig. 27).

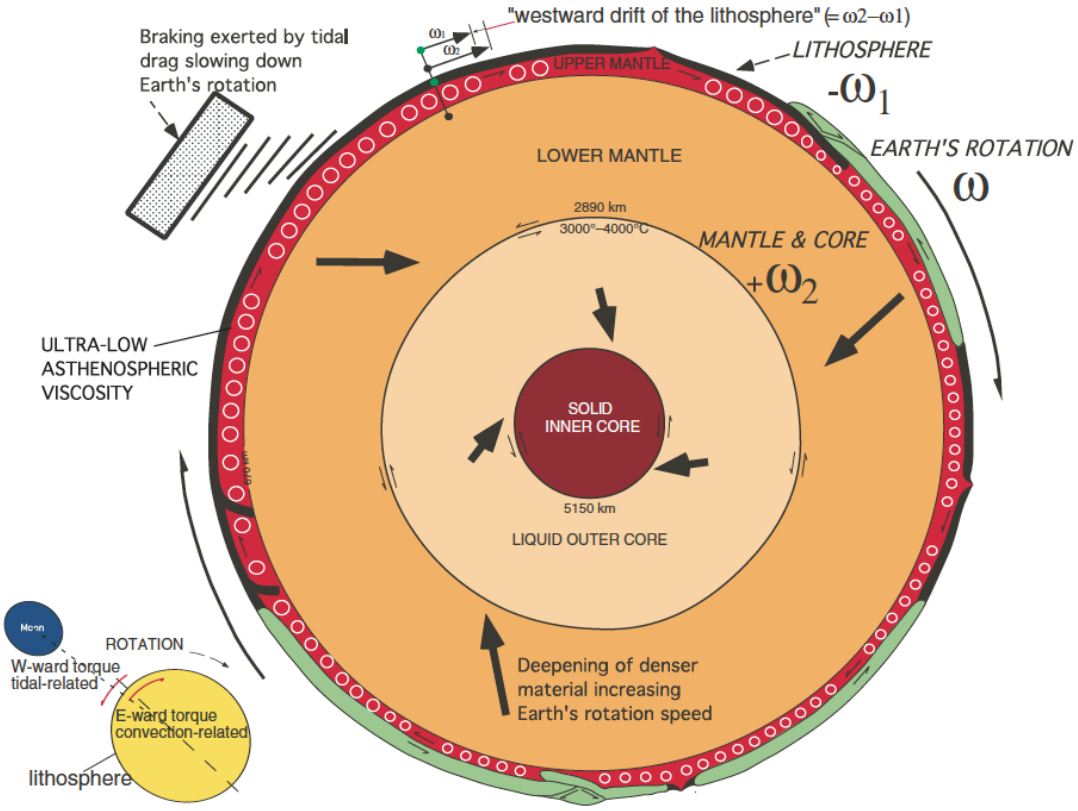

Fig. 27. Cartoon showing how the Earth, viewed from the southern pole, is undergoing two opposite torques. The tidal torque is opposing Earth's rotation, whereas convection is speeding up the spinning due to the accumulation of heavier material toward the inner parts of the planet, growing the inner core and making the lower mantle denser. Very low viscosity, hydrated layers are inferred in the nonlinear rheology asthenosphere where the tides perform mechanical fatigue. The mixing of these different issues could allow for decoupling between the lithosphere and underlying upper mantle.

There is not yet a final positive answer to the question if the westward drift is related to Earth's rotation, however, it cannot be neglected on the basis of the results of very simple mechanical and rheological models. This model explains why, unlike Earth, satellites where stronger gravitational tides operate (e.g., the Moon, the four largest of Jupiter's satellites, Io, Europa, Ganymede, Callisto) and internal convection is low or absent have moved to the orbital resonance condition (Boccaletti and Pucacco, 2002), or tidal locking, where the time of rotation equals the time of revolution around the main planet, and plate tectonics do not occur. On the other hand, moonless planets do not show plate tectonics similar to Earth, while recently (Kobayashi and Sprenke, 2010) have shown that the crustal magnetic anomalies on Mars may represent hot spot tracks resulting from lithospheric drift on ancient Mars. The lineations in the magnetic anomalies on Mars are hot spot tracks representing an east–west drift of the lithosphere over fixed mantle plumes on ancient Mars. Most of the giant impact basins on Mars that probably were formed while the dynamo was active lie along three paleo-

equators delineated from magnetic anomalies, suggesting that fragments from former satellites of Mars formed these impact basins. These ancient martian moons could have provided the tidal force to create a rotational drag on the ancient martian lithosphere, resulting in the east–west hot spot tracks.

The re-evaluation of the possibility that Earth's rotation contributes to plate tectonics shows that, if a very-low viscosity layer is present in the upper asthenosphere, the horizontal component of the tidal oscillation and torque would be able to slowly shift the lithosphere relative to the mantle. This conclusion is supported by the following observations: 1) plates move along a westerly polarized flow that forms an angle relative to the equator close to the revolution plane of the Moon; 2) plate boundaries are asymmetric, being their geographic polarity the first order controlling parameter; 3) the global seismicity depends on latitude and correlates with the decadal oscillations of the excess length of day (LOD); 4) the Earth's deceleration supplies energy to plate tectonics comparable to the computed budget dissipated by the deformation processes; 5) the Gutenberg–Richter law supports that the whole lithosphere is a self-organized system in critical state, i.e., a force is acting contemporaneously on all the plates and distributes the energy over the whole lithospheric shell, a condition that can be naturally satisfied by a force acting at the astronomical scale (Riguzzi et al 2010).

What moves slabs?

When considering a migrating subduction hinge, the kinematics of convergent geodynamic settings shows that subduction zone rates can be faster or slower than convergent rates as a function of whether the subduction hinge migrates away or toward the upper plate.

This (opposite) behaviour occurs in particular along W- (or SW-) directed and E- (or NE-) directed subduction zones, respectively.

Along W- (or SW-) directed slabs, the subduction rate is the convergence rate plus the slab retreat rate, which tends to equal the backarc extension rate. Along E- (or NE-) directed slabs, the subduction rate is decreased by the shortening in the upper plate. Relative to the mantle, the W- (or SW-) directed slab hinges are fixed, whereas they move west or southwest along E- (or NE-) directed subduction zones.

Therefore, subduction zones appear as passive features controlled by the far field plate velocities and their motion relative to the underlying “eastward” mantle flow, rather than by the negative buoyancy alone of the down going plate (Doglioni, et 2006b). The convergence/shortening ratio is regularly higher than 1 in E- (or NE-) directed subduction zones (Fig. 28). This value is sensitive to the viscosity of the upper continental lithosphere. Higher ratio means higher

viscosity of the lithosphere, i.e., it is stiffer and it sustains the convergence, while most of it is absorbed by subduction (Fig. 29).

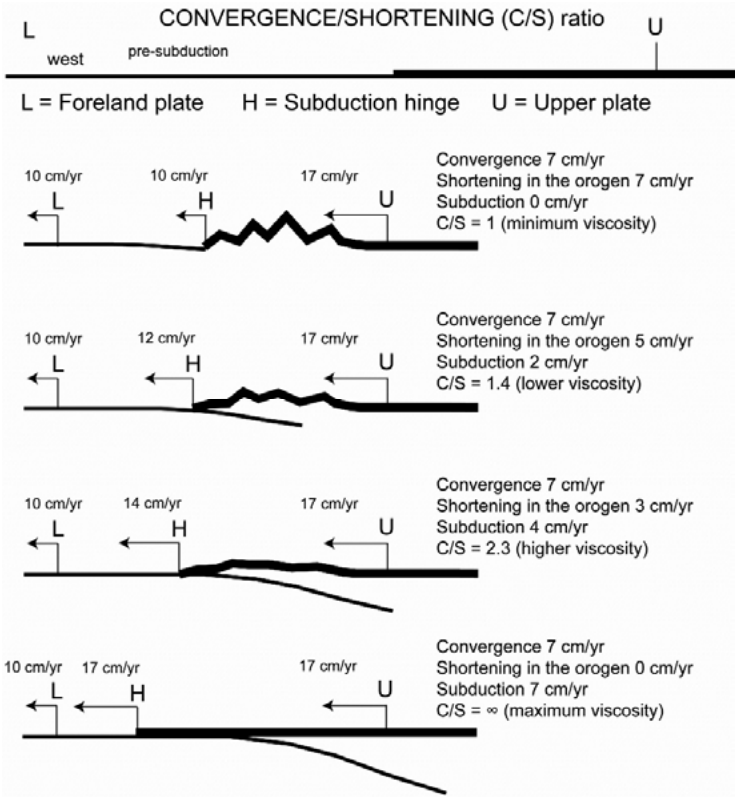

Fig. 28 - Four hypothetical cases of an oceanic subduction, where the shortening is confined to the continental upper lithosphere and varies as a function of its viscosity. The larger the shortening, the smaller the subduction rate, and the lower the viscosity (upper case). The convergence/shortening ratio can vary from 1 to ∞.

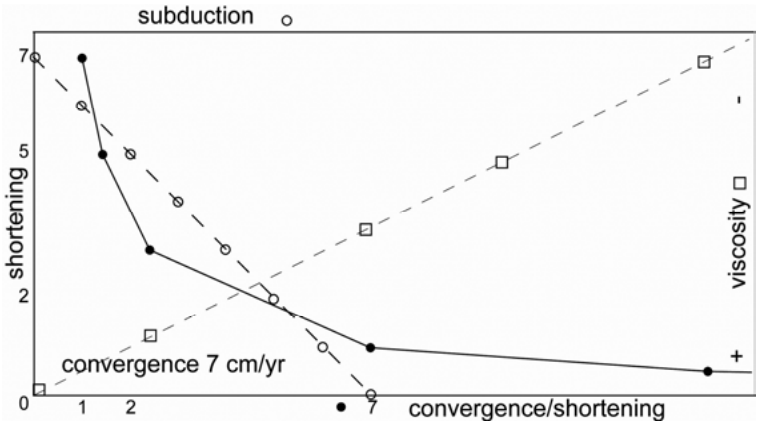

Fig. 29 - Diagram with the relations between shortening rate, convergence/shortening ratio, subduction rate and viscosity of the upper plate along an E- NE-directed subduction zone, at a convergence rate of 7 cm/yr.

The observation that the convergence is faster than the shortening

supports the notion that the plate boundary (subduction and related orogen) is a passive feature, and does not provide relevant driving energy for plate motions. Kinematically, when plate motions are analyzed relative to the shallow hotspots reference framework the slab is moving out of the mantle along E- (or NE-) directed subduction zones, i.e., moving in the direction opposite to the one predicted by the pull of the slab (see Section "Subduction kinematics and dynamic constraints" and Doglioni et al., 2007). Mantle convection is also inadequate to explain the Earth's surface kinematics.

What is moving the lithosphere relative to the mantle? The only reasonable mechanisms are the slab pull and the tidal friction. However, the slab pull model is affected by a number of inconsistencies, which have been described in Sections "Thrust belts, foredeeps and subduction zones", "On the origin of W- (or SW-) directed subduction zones" and "Global kinematics in deep versus shallow hotspot reference frameworks". Slab pull does not seem to be able to determine plate motions in general, although it could enhance subduction once started. An alternative and/or complementary source of energy for plates motion is the tidal drag exerted by the Moon and the Sun while the Earth rotates. Plate motions driven by the Earth's rotation seem to be the simplest and natural explanation for the asymmetry along the subduction and rift zones (Panza et al., 2010; Riguzzi et al, 2010).

Subduction kinematics and dynamic constraints

The kinematics of subduction zones shows a variety of settings that can provide clues for the understanding of Earth's dynamics. Two reference frameworks can be used to describe the simple 2D kinematics of subduction zones. In the first, the upper plate is assumed fixed, whereas in the second framework upper and lower plates move relative to the mantle (Doglioni et al., 2007).

Relative to a fixed point in the upper plate U, the transient subduction hinge H can converge, diverge, or be stationary. Similarly, the lower plate L can converge, diverge or be stationary. The subduction rate V_S is given by the velocity of the hinge H (V_H) minus the velocity of the lower plate L (V_L) ($V_S=V_H-V_L$). The subduction rate 1) increases when H diverges, and 2) decreases when H converges. Combining the different movements, at least 14 kinematic settings can be distinguished along the subduction zones. Variable settings can coexist even along a single subduction zone. Apart from few exceptions, the subduction hinge converges towards the upper plate along E- (or NE-) directed subduction zone, whereas it diverges from the upper plate along W- (or SW-) directed subduction zones accompanying backarc extension.

Before collision, orogen growth occurs mostly at the expenses

of the upper plate shortening along E- (or NE-) directed subduction zones, whereas the accretionary prism of W- (or SW-) directed subduction zones increases at the expenses of the shallow layers of the lower plate. The convergence/shortening ratio is >1 along E- (or NE-) directed subduction zones, whereas it is <1 along accretionary prisms of W- (or SW-) directed subduction zones.

Backarc spreading forms in two settings: along the W- (or SW-) directed subduction zones it is determined by the hinge divergence relative to the upper plate, minus the volume of the accretionary prism, or, in case of scarce or no accretion, minus the volume of the asthenospheric intrusion at the subduction hinge. Since the volume of the accretionary prism is proportional to the depth of the decollement plane, the backarc rifting is inversely proportional to the depth of the decollement. On the other hand, along E- (or NE-) directed subduction zones, few backarc basins form (e.g., Aegean, Andaman) and can be explained by the velocity gradient within the hangingwall lithosphere, separated into two plates.

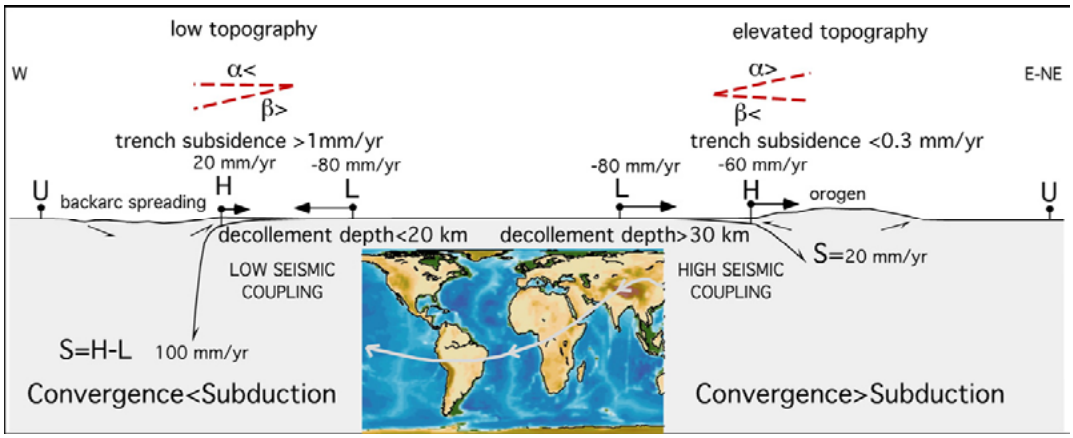

Fig. 30. Assuming fixed the upper plate U, along west-directed subduction zones the subduction hinge H frequently diverges relative to U, whereas it converges along the opposite subduction zones. L, lower plate. The subduction S is larger than the convergence along W-directed slabs, whereas S is smaller in the opposite case. The two end-members of hinge behavior are respectively accompanied in average by low and high topography, steep and shallow foreland monocline, fast and slower subsidence rates in the trench or foreland basin, single vs. double verging orogens, etc., highlighting a worldwide subduction asymmetry along the flow lines of plate motions indicated in the insert (modified after Lenci and Doglioni, 2007).

When referring to the mantle, the kinematics of subduction zones can be computed either in the deep or in the shallow hotspot reference frameworks. The subduction hinge is mostly stationary being the slab anchored to the mantle along W- (or SW-) directed subduction zones, whereas it moves W- (or SW-) ward along E- (or NE-) directed subduction zones. Along E- (or NE-) directed subduction zones, the slab moves “out” of the mantle, i.e., the slab slips relative to the mantle

opposite to the subduction direction. Kinematically, this subduction occurs because the upper plate overrides the lower plate, pushing it down into the mantle. As an example, the Hellenic slab moves out relative to the mantle, i.e., SW-ward, opposite to its subduction direction, both in the deep and shallow hotspot reference frames. In the shallow hotspot reference frame, upper and lower plates move "westward" relative to the mantle along all subduction zones. This kinematic observation casts serious doubts on the slab negative buoyancy as the primary driving mechanism of subduction and plate motions.

Orogens and related features show marked asymmetries (Fig. 30 and 31). The topography and the foreland monocline are lower and

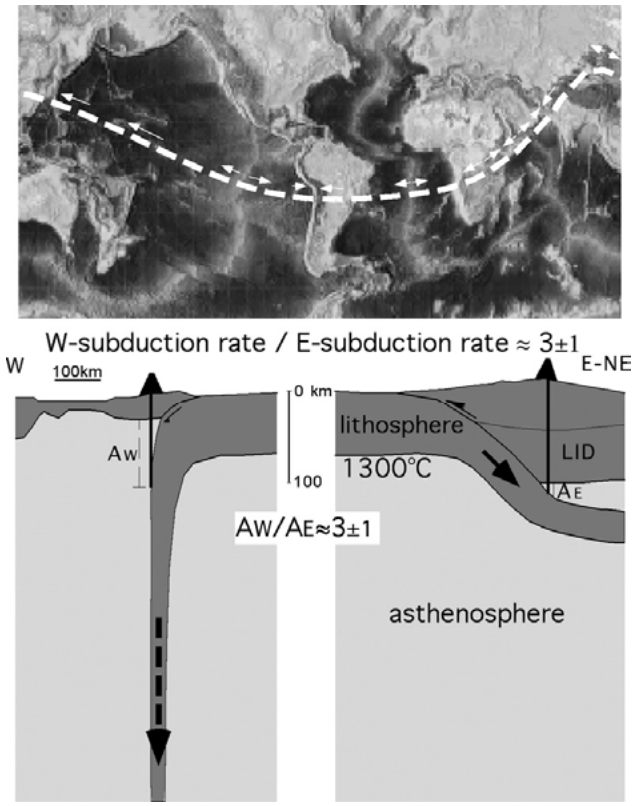

Fig. 31a. The main differences between orogens are a function of the subduction polarity along the tectonic mainstream (Doglioni, 1993a; Crespi et al., 2007). The volumes recycled along W-directed subduction zones is about 2–3 times higher than along the opposite settings due to the aforementioned kinematic constraints. The asthenospheric wedge above slabs is thicker along W- (or SW-) directed subduction zones (AW) with respect to the E- (or NE-) directed subductions (AE), modified after Doglioni et al. (2007)

steeper for the W- (or SW-) directed subduction zones (Fig. 32) and the area above sea level is remarkably higher for the opposite E- (or NE-) directed subduction zones (Fig. 33).

All types of tectonic-geodynamic settings at plate boundaries show 10–100 times faster horizontal velocity with respect to the vertical one (Cuffaro et al., 2006).

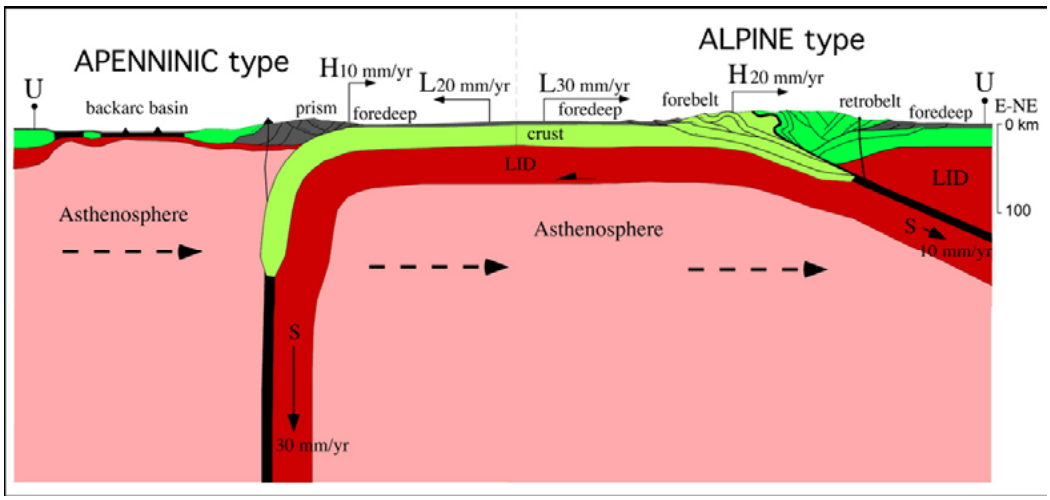

Fig. 31b. In an Alpine setting, the subduction rate is decreased by the migration of the hinge H toward the upper plate U, and the orogen in the final collision stage is composed both by the upper and lower plate L rocks. In the opposed Apenninic setting, the subduction rate is rather increased by the migration of H away from U, and the accretionary prism is made of shallow rocks of the lower plate. Typical of W-directed subduction zones, the asthenosphere is shallower in the hanging wall than in the footwall.

Is this a trivial observation, or is it rather telling us something fundamental on the dynamics of plate tectonics? Does slower vertical motion imply strain partitioning and passive role of plate boundaries, as suggested, for example, by the gradual decrease in shortening from the subduction hinge to the fixed upper plate (Fig. 34)?

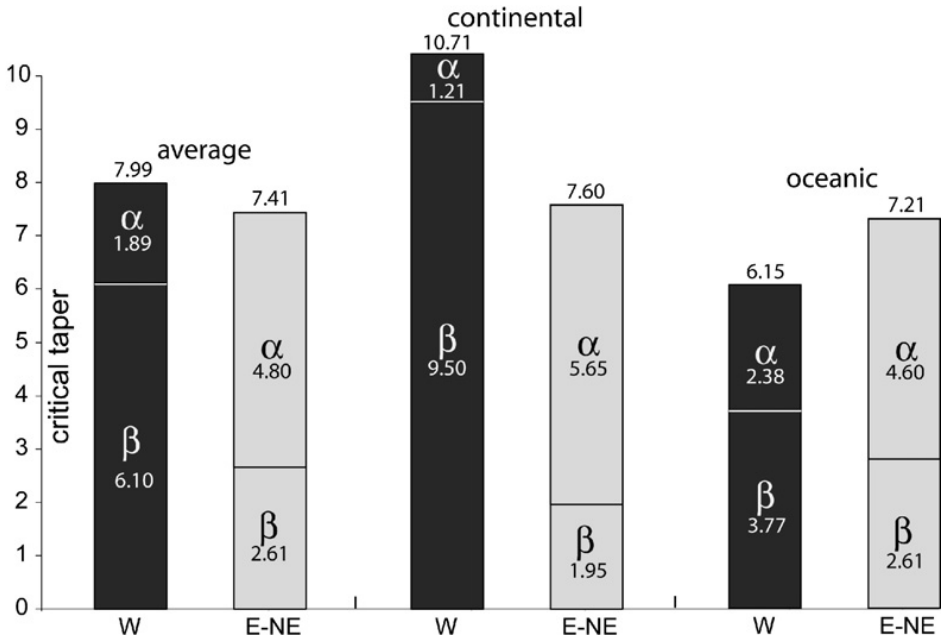

Fig. 32. Average values of the topographic envelope (α), dip of the foreland monocline (β), and critical taper (= α+β) for the two classes of subduction zones, i.e.,W-directed and E- orNE-directed.Note that the "western" classes showlower values α and steeper values of β (after Lenci and Doglioni, 2007).

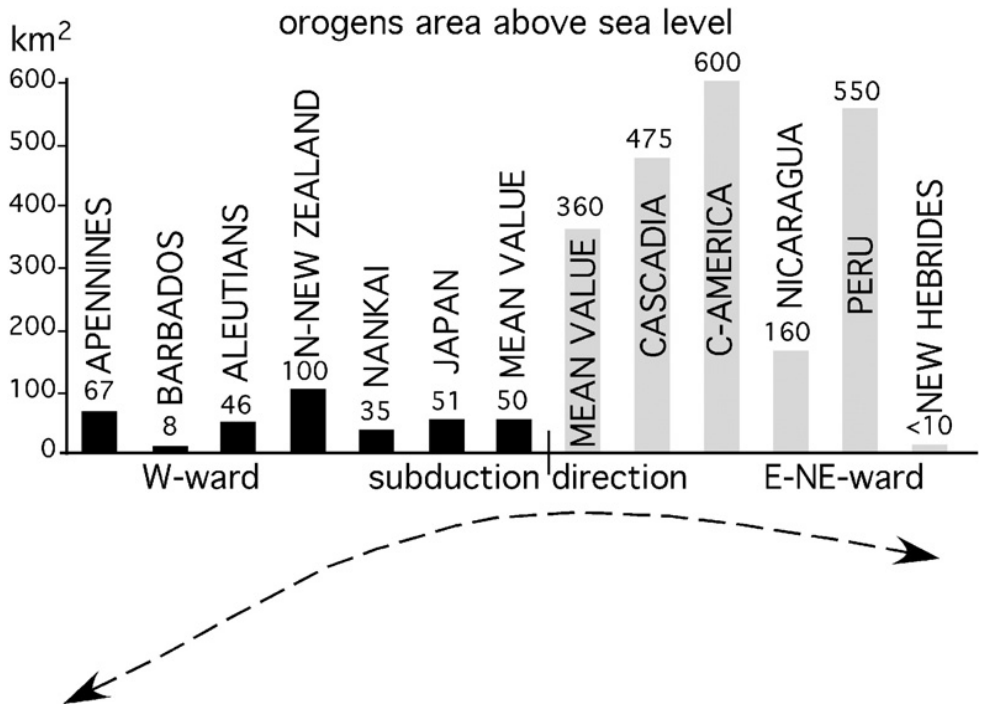

Fig. 33. Average values of the area above sea-level of the main subduction zones, showing how orogens above E- or NE-directed subduction zonesare about 6–8 times larger than the W-directed subduction zones-related accretionary prisms. After Lenci and Doglioni (2007).

The mechanisms driving plate motion, e.g., plates driven by 'the boundary forces', slab pull and ridge push (Forsyth and Uyeda, 1975) vs. plates actively dragged by the asthenosphere flow (e.g., Bokelmann, 2002) seems not relevant with respect to the difference of horizontal vs. vertical motion rates, because the rates themselves do not provide evidence for or against any particular mechanism.

Both 'active plates and passive asthenosphere' and 'an active asthenospheric flow dragging passive plates' may be consistent with faster horizontal motions. The inertia of plates is negligible, and each plate must be in dynamic equilibrium, so the sum of the torques acting on a plate must be zero (Forsyth and Uyeda, 1975). This circumstance allows for relatively small energy sources to influence global tectonic processes and therefore the tidal despinning can contribute to plate tectonics through the westward lithospheric drift (Bostrom, 1971; Knopoff and Leeds, 1972). The main forces acting on the lithosphere can be subdivided into coupled and uncoupled forces (Fig. 35).

Mantle drag and trench suction (e.g., Bercovici, 1998; Conrad and Lithgow-Bertelloni, 2003) need high coupling (higher viscosity) between the lithosphere and the asthenosphere to be effective. The ridge push, the slab pull and the tidal drag rather need low coupling (lower viscosity) to be efficient (Fig. 35). The down-dip extension along E- (or NE-) directed slabs can be generated either by the slab pull from below, and/or by the tidal drag acting on the surface plate.

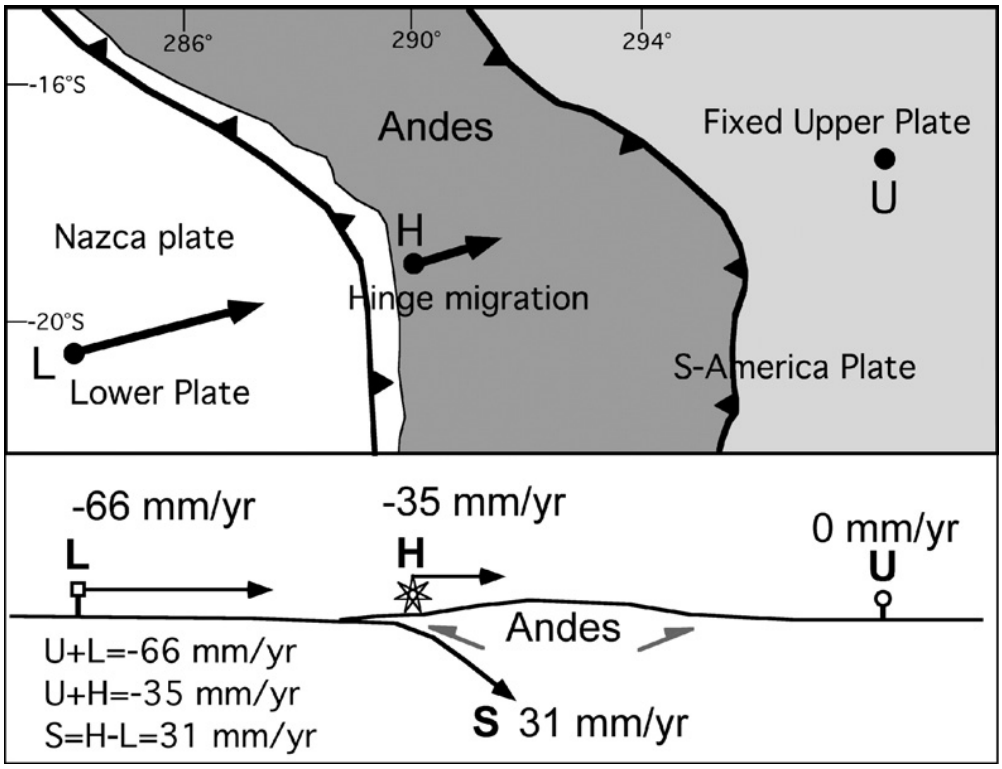

Fig. 34. The convergence between Nazca and South America plates is faster than the shortening in the Andes. The upper plate shortening decreases the subduction rate. The convergence/shortening ratio is about 1.88. GPS data are after Liu et al. (2000).

Among the uncoupled forces, the ridge push is at least one order of magnitude lower than the slab pull (e.g., Ranalli, 1995). The dissipation of energy by tidal friction is even larger ($1.6 \cdot 10^{19}$ J/yr) than the energy released by tectonic activity ($1.3 \cdot 10^{19}$ J/yr) (Denis et al., 2002). The tidal drag can effectively move plates only if very low viscosity intra-astenospheric layers occur (Scoppola et al., 2006). In this case, tidal forces, combined with mantle convection, could trigger plate tectonics, as in ancient Mars (Kobayashi and Sprenke, 2010).

A very low velocity layer, with a sizable fraction of melting which allows for very low viscosity in the uppermost asthenosphere (100–150 km), has been recently revealed in the Mediterranean (Panza et al., 2007a,b). Consistently with the present-day Vs resolution, Panza et al. (2010) have identified along the TE-pert an ubiquitous LVZ circuit, about 1000 km wide and about 100 km thick, in the asthenosphere, that allows for the persistence of a continuous global flow within the Earth. Therefore the viscosity of the upper layers of the asthenosphere plays a crucial role in controlling plate tectonics. Moving from the highest viscosity (10^{19}-10^{20} Pa·s) to the lowest (10^{12}-10^{14} Pa·s), the most likely mechanisms able to move plates are, in the order: the mantle drag, the trench suction,

the slab pull, the ridge push and the tidal drag. Relatively small forces can move a floating plate easily horizontally, because no work has to be done against gravity, whereas non-isostatic vertical motions require work to be done against gravity and this can be true when at the base of the lithosphere there is a very low viscosity in the decoupling layer, i.e., the weaker low velocity zone in the upper asthenosphere, like the TE-pert defined by Panza et al. (2010). If the viscosity of the asthenosphere is not low, relatively larger forces are required to move the lithosphere with respect to the underlying asthenosphere. On the other hand, if the lithosphere is not moved by lateral forces such as the slab pull, but rather passively dragged by the mantle, this requires a relatively higher viscosity (see Fig. 35 for more details)

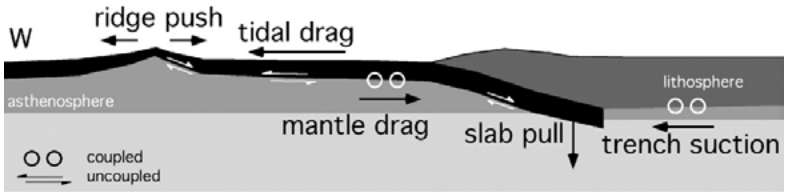

Fig. 35. Main forces acting on the lithosphere. Mantle drag and trench suction need high coupling (higher viscosity) between lithosphere and asthenosphere to be effective. Ridge push, slab pull and tidal drag should rather need low coupling (lower viscosity) to be efficient. Since the lithosphere is decoupled with respect to the asthenosphere, possibly more than one force is actively forcing plate motions. Circles indicate coupled forces, white half arrows show the uncoupled forces.

Then, what is generating the decoupling of the lithosphere (Fig. 36)? Are there external tangential forces acting on the lithosphere? There are lines of evidence that the lithosphere is partly decoupled from the mantle as suggested for example by the hotspot tracks and by the asthenosphere anisotropy and asymmetry of the lithosphere-astenosphere system (Silver and Holt, 2002; Panza et al., 2010). Assuming a shallow origin of the Pacific plumes used as reference framework (Fig. 36), a super fast net rotation of the lithosphere relative to the mantle has been proposed by Crespi et al. (2007). If so, where does the energy providing this torque come from? What is moving plates relative to the mantle? The net westerly directed rotation of the lithosphere has been attributed either to lateral variations in the asthenosphere viscosity (Ricard et al., 1991), or to the Earth's rotation (Scoppola et al., 2006). The westward drift (Le Pichon, 1968) is consistent with the asymmetry of subduction and rift zones worldwide along an undulated plate motions flow (Doglioni et al., 2006a; Panza et al. 2010). A number of authors (e.g., Dickinson, 1978; Uyeda and Kanamori, 1979; Doglioni, 1990) proposed a shear at the lithosphere base driven by mantle drag or relative mantle flow. Plate motions are driven either by coupled or uncoupled forces. A comparison between horizontal and vertical motions does not allow to sort out which

plate tectonics driving mechanism prevails. However, the steady 1 or 2 order of magnitude faster horizontal with respect to vertical motion at plate boundaries points to a major tangential component in plate tectonics.

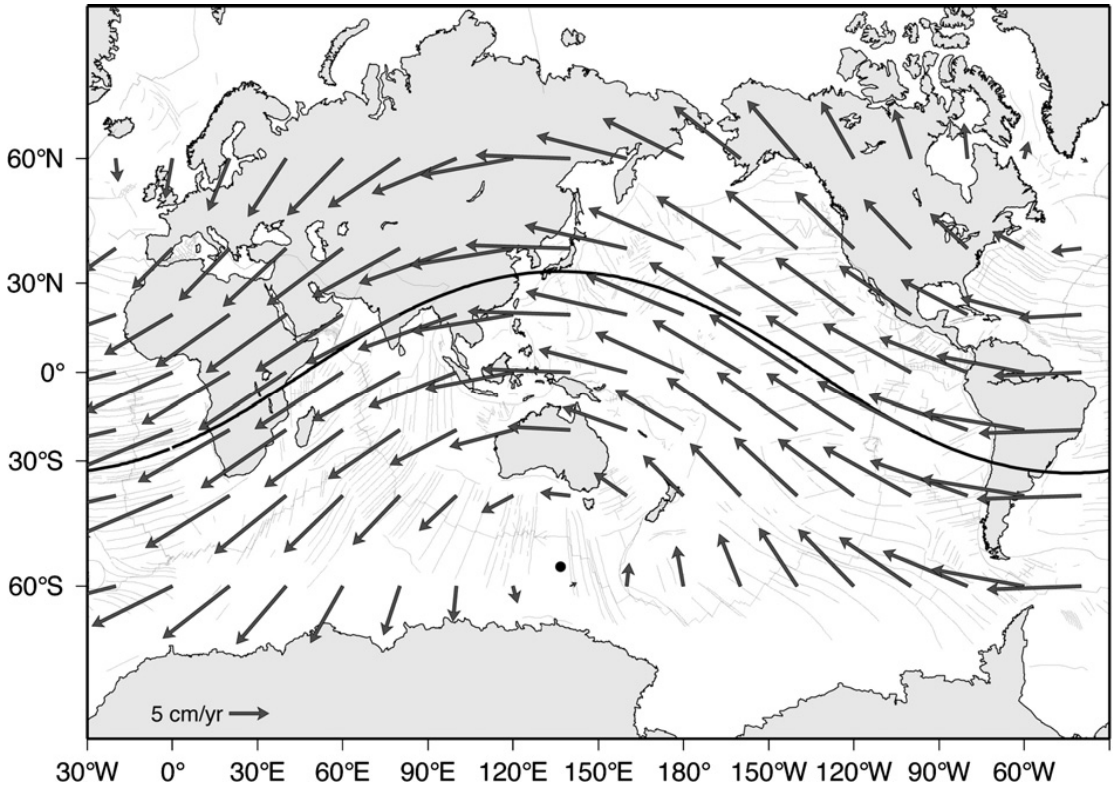

Fig. 36. Global lithospheric net rotation relative to the mantle assuming a mid-asthenospheric source of the Pacific plumes, after Crespi et al., 2007. Subduction asymmetries should not be considered as E–W related, but following or opposing the absolute tectonic mainstream.

If ridges and subduction zones trigger convection, but are nevertheless still passive features, what does move plates? Whatever the mantle convection works, it cannot explain the lithosphere decoupling alone. Therefore the uncoupled forces appear to dominate, but we cannot exclude that possibly more than one force, both coupled and uncoupled, is responsible of plate motions. Earth's rotation cannot work alone because mantle convection is required to maintain the mantle fertile and the low viscosity in the asthenosphere. Moreover density gradients (e.g. slab pull) allow for differential sinking of plates at convergent margins.

Further studies on the composition, water content and viscosity of the asthenosphere might significantly contribute to answer the following basic unanswered questions: (1) are plates dragged horizontally by mantle convection (e.g., Bercovici, 1998)? (2) Are they dragged and sheared at the base by a faster moving mantle (Bokelmann, 2002)? (3) Are they rather pulled by slab pull forces (Forsyth and Uyeda, 1975; Anderson, 2001)? (4) Could they be driven by Earth's rotation and tidal

drag (Scoppola et al., 2006; Riguzzi et al., 2010)?

Subduction, obduction and upduction (exumation)

Subduction zones may initiate when two basic parameters concur: i) the two plates have at least an initial convergent component of relative plate motion and ii) one of the two plates is sufficiently denser, thinner, stronger and wider to be overridden.

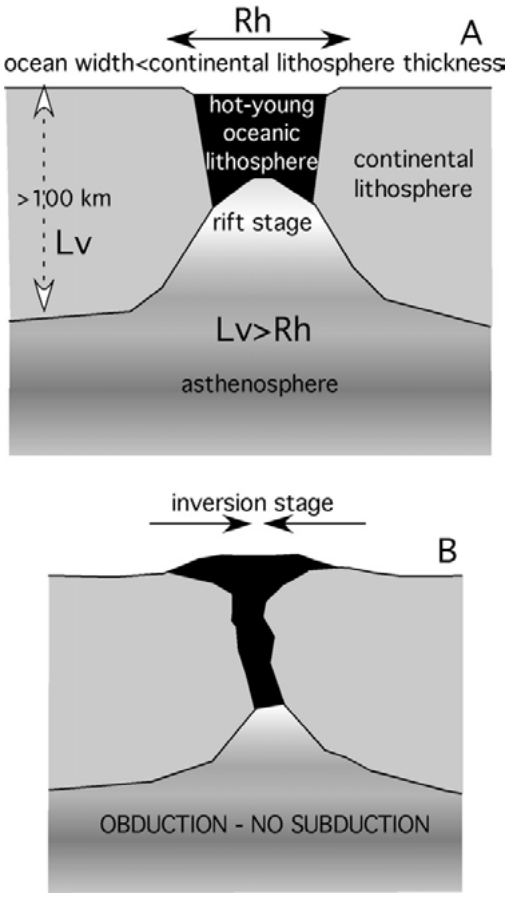

Fig. 37. An ocean basin that has a width (Rh) smaller than the thickness of the continental lithosphere (Lv) at its margins as in the upper panel A cannot evolve to a complete subduction, lower panel B. In this setting the ophiolites can be more easily obducted (after Doglioni et al. 2007).

As a counter example, when an oceanic rift opens to a width equal or smaller than the thickness of the adjacent continental lithosphere, a complete subduction cannot develop (Fig. 37). In other words, small oceans (150–200 km wide) cannot generate normal, steady state, subduction systems. This setting can rather evolve to obduction, where ophiolitic slices of the oceanic realm are buckled and squeezed on top of the continental lithosphere. One example could be the Oman ophiolite complex (Nicolas et al., 2000; Garzanti et al., 2002), even if it is unclear whether this ocean was a narrow independent basin, or rather part of a wider Tethyan branch (Stampfli and Borel, 2002). The obduction process

should not be confused with the new concept of upduction (exumation) introduced in Section "Global kinematics in deep versus shallow hotspot reference frameworks" and discussed later in this Section.

A subduction zone should be analyzed considering at least three points, specifically, two located in stable areas of both the upper and the lower plate, and one located at the plate boundary, along the subduction hinge. Two main types of subduction zones can be distinguished: 1) those where the subduction hinge migrates away from the upper plate, and 2) those in which the subduction hinge migrates towards the upper plate (Fig. 31b). This distinction recalls what Laubscher (1988) defined as pull arc and push arc respectively. Apart few exceptions, this distinction seems to be particularly appropriate for W- (or SW-) directed and E- (or NE-) directed subduction zones, respectively (e.g., Apennines, Marianas, Tonga and Carpathians for the W-directed, Andes, Alps, Dinarides and Hellenides for the opposite case). In either W- (or SW-) and E- (or NE-) directed subduction zones, the hinge migrates eastward or northeastward relative to the upper plate (Table 2). In the literature the expressions retreating or advancing slab are often used. However this terminology might generate confusion because a retreating hinge or slab retreat in the upper plate reference framework might become a fixed hinge in the mantle reference framework (e.g., Barbados). On the other hand, an advancing hinge relative to the upper plate is a retreating hinge relative to the mantle (e.g., Andes). The rate of subduction is generally larger than the convergence rate along W- (or SW-) directed subduction zones, whereas it is smaller along E- (or NE-) directed subduction zones. Therefore the subduction rate decreases or increases whether the subduction hinge converges or diverges relative to the upper plate. Along W- (or SW-) directed slabs, the subduction rate is the convergence rate plus the slab retreat rate, being the latter close to the backarc extension rate, if no accretion occurs in the upper plate, which is a rare case. As a result, in the eastern Pacific subduction zones, and in the E- (or NE-) directed subduction zones in general, such as the Alps or Himalayas, the subduction rate should be lower than the convergence rate. On the other hand, along the western Pacific subduction zones and the W- (or SW-) directed subduction zones in general, such as the Apennines, the subduction rate has to be faster than the convergence rate since it is incremented by the hinge retreat. In this interpretation, the far field velocities of the upper and lower plates control the subduction rate, and the subduction is a passive process. In fact, the rates of subduction do not determine plate velocities, but are rather a consequence of them.

The convergence/shortening ratio along W- (or SW-) directed subduction zones is instead generally lower than 1. Along E- (or NE-) directed slabs, the shortening in the upper plate decreases the subduction

rate, and typically no backarc basin forms. The convergence/shortening ratio in this type of orogens is higher than 1 and is inversely proportional to the strength of the upper plate and it is directly proportional to the coupling between upper and lower plates. The higher the strength and lower the coupling, the smaller the shortening, and faster is the subduction rate.

Table 2
Few main geometric, kinematic and dynamic differences between orogens and subduction zones following or opposing the tectonic mainstream. Subduction zones parallel to the mainstream (e.g., Pyrenees) have similar characters as the subduction zones following it

	Subductions opposing the tectonic mainstream (W-directed)	Subductions following the tectonic mainstream (E–NE–NNE-directed)
Elevation average	−1250 m	+1200 m
Foreland monocline average dip	6.1°	2.6°
Trench or foredeep subsidence rate	>1 mm/yr	<0.3 mm/yr
Prism envelope average dip	1.9°	4.8°
Orogen-prism vergence	Single verging	Mostly Double verging
Type of prism rocks	Mostly sedimentary cover & volcanics	Largely basement, sedimentary cover & volcanics
Prism decollement depth	0–10 km; (rarely up to 20 km) offscraping the top of the lower plate	>30 km; Oceanic subduction, affecting mostly the whole section of the upper plate; continental subduction affecting also the lower plate
Seismic coupling	Mainly low	Mainly high
Moho	Shallow (<30 km) new upper plate Moho	Deep (>40 km) doubled old Mohos
Asthenosphere depth	Shallow (<20–50 km) beneath the arc	Deep (>70–100 km) beneath the arc
Seismicity	0–670 km; intra-slab mostly down-dip compression and horizontal shear	0–250 km and scattered 630–670 km; intra-slab mostly down-dip extension
Slab dip	25°–90°	15°–50°, steeper up to 70° along oblique subductions and thicker upper plate
Subduction hinge motion relative to upper plate	Mainly diverging Eastward (except Japan where subduction started to flip)	Mainly converging Eastward or northeastward
Subduction hinge motion relative to mantle	Fixed	Westward or southwestward
Subduction rate	S=H−L, faster than convergence rate; mainly slab retreating and entering the mantle	S=H−L, slower than convergence rate; slab "escaping" relative to the mantle, overridden by the upper plate
Backarc spreading rate	H(>0), — prism accretion, — hinge asthenospheric intrusion	Differential velocity between two hangingwall plates
Slab/mantle recycling	About 3 times higher than opposite	About 3 times lower than opposite
Subduction mechanism	Slab-mantle wind interaction+far field plate velocities+slab density gradient relative to the country mantle	Far field plate velocities+slab density gradient relative to the country mantle

Along both W- (or SW-) and E- (or NE-) directed subduction zones, the hinge migrates eastward relative to the upper plate, apart few exceptions like Japan. Therefore, most frequently along the W- (or SW-) directed subduction zones, the hinge migrates away with respect to the upper plate, whereas the hinge migrates toward the upper plate along E- (or NE-) directed subduction zones. In this interpretation, the far field velocities of the upper and lower plates control the subduction rate, and the subduction is a passive process. Along E- (or NE-) directed subduction zones, the convergence rate is partitioned between upper plate shortening and subduction. The shortening is mainly concentrated in the upper plate until it is continental and less viscous than the lower oceanic plate. At the collision stage even the lower plate is extensively shortened. However, the observation that, say 80 mm/yr convergence are transferred to 60 mm/yr shortening in the upper plate and 20 mm/yr only are reserved to subduction, points out a fundamental result: the lower values of shortening and subduction rates with respect to the convergence rate are

hierarchically a consequence of the far field plate motion. This means that the driving primary source of energy for determining the convergence is neither within the slab, nor in the related orogen.

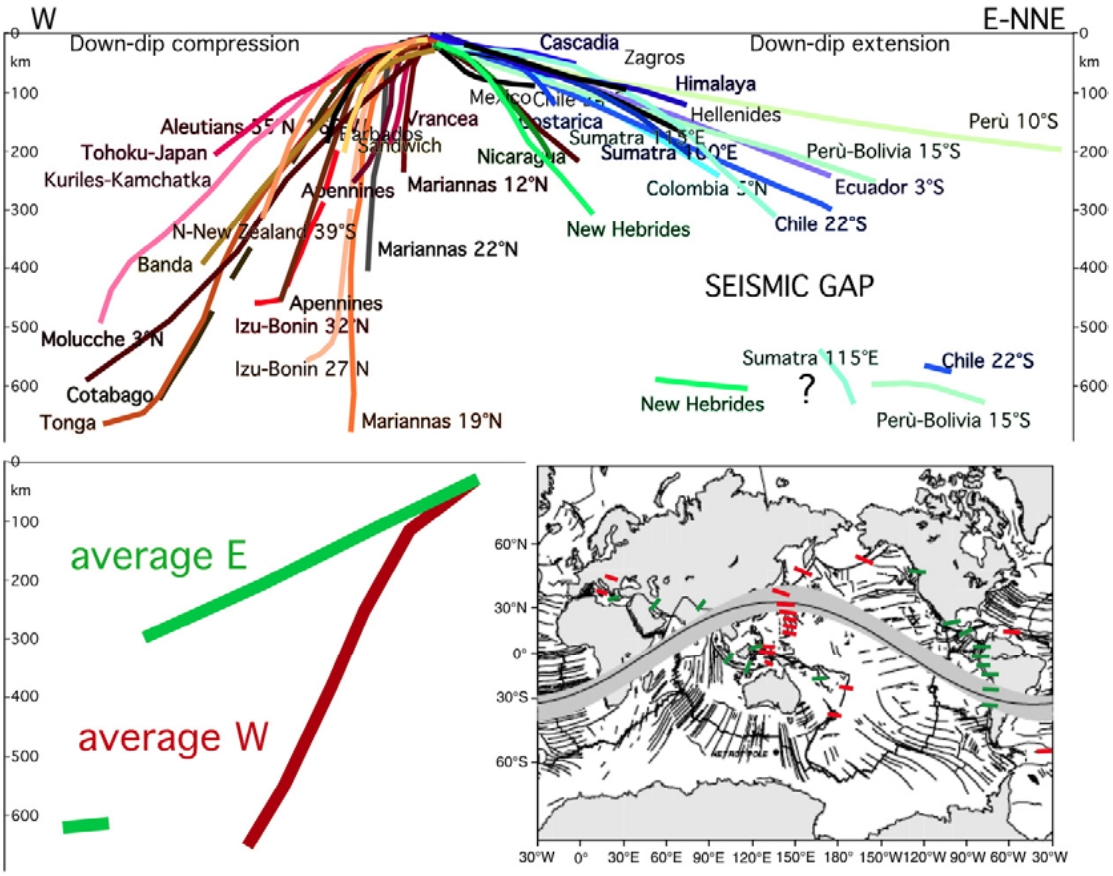

Fig. 38. Compilation of the slab dip measured along cross-sections perpendicular to the trench of most subduction zones. This is a generalization of Fig. 7. Each line represents the mean trace of the distribution of hypocenters, and not the axis of the velocity anomalies that can be found in tomographic images, along every subduction. The asymmetry is also marked by the seismic gap between around 300–550 km occurring only along the E- or NE-directed subduction zones, that are, in general, shorter than the W-directed slabs. Some E- or NE-subduction zones present a deeper scattered cluster of hypocenters between 550–670 km which may be interpreted either as a detached fragment of the slab, or as a portion of lower mantle sucked from below, in the wake left by the slab in its upduction (exumation) motion (Doglioni et al., 2009). The dominant down-dip compression occurs in the W- (or SW-) directed intraslab seismicity, whereas down-dip extension prevails along the opposed E- or NE-directed slabs. The W-directed slabs are, on average, dipping 65.6°, whereas the average dip of the E- (or NE-) directed slabs, to the right, is 27.1° (see Table 3). The motion towards E of the mantle relative to the lithosphere explains in a natural way not only (a) the fact that the edges of continental mantle are found under an oceanic crust located to the east and (b) the asymmetry of the subduction zones, at low angle (15°-40°) those E-directed, since they follow the mantle flow, more steep (40°-90°) those W-directed, since they tend to oppose the mantle flow, but also (c) the global E-ward migration of magmatism (Doglioni et al. 2009).

A paradigm of plate tectonics is that the negative buoyancy of slabs drives plate motions (e.g., Conrad and Lithgow-Bertelloni, 2003), as suggested by the steeper dip of the slab bearing old oceanic crust (Forsyth and Uyeda, 1975), and the convergence rate at subduction zones

related to the age of the oceanic crust at the trench (e.g., Carlson et al., 1983).

However a number of aforementioned counterarguments makes the slab pull a plate motion ingredient much weaker than so far accepted. For example the energy required to pull the plates is far higher than the strength that plates can afford under extension. At the Earth's surface, the oceanic lithosphere has low strength under extension (e.g., $8 \cdot 10^{12}$ Nm^{-1}, Liu et al., 2004) and it is able to resist a force smaller than that requested by slab pull ($3.3 \cdot 10^{13}$ N m^{-1}, Turcotte and Schubert, 2002). If the slab pull is the cause for the motion of the Pacific plate, this observation argues for a stretching of the Pacific lithosphere before slab pull is able to move the plate. In other words, the plate cannot sustain the tensional stresses eventually due to slab pull.

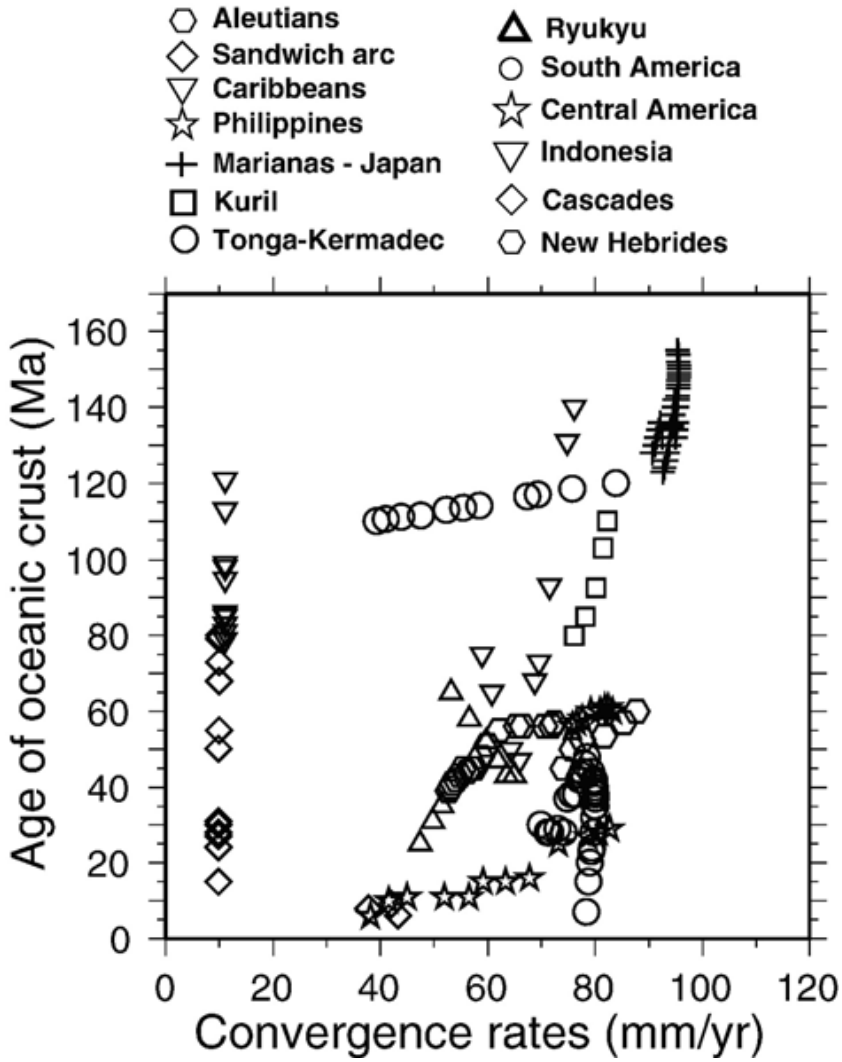

Fig. 39. Age of oceanic lithosphere entering the trench (after Mueller et al., 1997) vs. velocity of convergence calculated using the NUVEL1A (DeMets et al., 1994) rotation poles. The diagram shows a plot obtained for 13 subduction zones. The absence of correlation suggests no significant relation between plate motions speed and negative slab buoyancy. Data form Cruciani et al. (2005).

The low lithospheric strength problem could be, however, partly counterbalanced by the mantle flow and viscous tractions acting on the plates induced by slab sinking (e.g., Lithgow-Bertelloni and Richards, 1998). Due to low temperature and high pressure, the strength of subducted oceanic lithosphere rises to some $2 \cdot 10^{13}$–$6 \cdot 10^{13}$ N m^{-1} (Wong A Ton and Wortel, 1997) and would make sustainable the pull eventually induced by density anomalies related to phase changes at depth. In summary the subducted slab is probably able to sustain the load induced by slab pull but probably this load cannot be entirely transmitted to the unsubducted portion of the plate without breaking it apart. Moreover the asymmetry which is evident when comparing the western and the eastern Pacific subduction zones occurs also in the Mediterranean subductions, regardless the age and composition of the downgoing lithosphere (Doglioni et al., 1999b) as shown in Fig. 7, 11 and 38.

Table 3. Dip of the slab of the W- and E- (or NE-) directed subduction zones

W-directed	Slab dip >100 km	E- or NE-directed	Slab dip >70 km	Deep cluster
Tohoku-Japan	35°	Nicaragua	50°	
Kuriles-Kamchatka	45°	Cascadia	18°	
Molucche 3°N	50°	Molucche 3°N	45°	
Aleutians 55°N/160°W	50°	New Hebrides	50°	yes
N-New Zealand 39°S	65°	Zagros	18°	
Banda	55°	Himalaya	15°	
Tonga	58°	Perù 10°S	10°	
Cotabago	63°	Perù-Bolivia 15°S	18°	yes
Mariannas 22°N	84°	Chile 22°S	21°	yes
Izu-Bonin 32°N	72°	Chile 24°S	21°	
Izu-Bonin 27°N	83°	Ecuador 3°S	20°	
Apennines	72°	Costarica	50°	
Sandwich	69°	Colombia 5°N	25°	
Barbados	68°	Hellenides	23°	
Mariannas 12°N	85°	Mexico	10°	
Mariannas 19°N	84°	Sumatra 100°E	32°	
Vrancea	78°	Sumatra 115°E	35°	yes
Average	65.6°	Average	27.1	

Data after Caputo et al. (1970; 1972) Sacks and Okada (1974); Isacks and Barazangi (1977); Baranzangi and Isacks (1979); Pilger (1981); Vassiliou et al. (1984); McGeary et al. (1985); Garfunkel et al. (1986); Jarrard (1986); Oncescu and Trifu (1987); Bevis (1988); Cahill and Isacks (1992); Frepoli et al. (1996), Castle and Creager (1998), Engdahl et al. (1998), Gudmundsson and Sambridge (1998), Gutscher et al. (1999), Chen et al. (2001), Karato et al. (2001), Engdahl and Villaseñor (2002), Pardo et al. (2002), Rivera et al. (2002), Billen et al. (2003), Hirth and Kohlstedt (2003), Das (2004), Lallemand et al. (2005), Milsom (2005), Reyners et al. (2006), Syracuse and Abers (2006), Billen and Hirth (2007), Vinnik et al. (2007), Ammon et al. (2008), Chiarabba et al. (2008), Espurt et al. (2008), Pérez-Campos et al. (2008), Scalera (2008b).

Lallemand et al. (2005) and Cruciani et al. (2005) have

demonstrated that there is no correlation between the slab dip and the age of the subducting lithosphere. As can be seen from Fig. 39, there is no correlation between convergence rate and age of the oceanic lithosphere at the trench (Fig. 39). This is a further evidence suggesting that the negative buoyancy cannot be the primary driving force of plate tectonics.

In the hotspot reference framework, the Africa plate moves westward (Gripp and Gordon, 2002), without any slab in its western side, and opposite to a hypothetic Atlantic ridge push. The only slabs attached to Africa are in its northern margin, i.e., the Hellenic–Cyprus and Apennines subduction zones. Although problematic, another small, finger-like, E-directed slab has been supposed beneath the Gibraltar arc (Gutscher et al., 2002). The Hellenic–Cyprus slab is also directed NE-ward, opposite to the direction of motion of the Africa plate, providing a kinematic evidence of no dynamic relationship. The Apennines slab is retreating and westward directed. These northern Africa subduction zones are a small percentage of the plate boundaries surrounding Africa, and they dip in opposite directions with respect to the absolute motion of the plate.

Therefore they cannot be the cause of its motion. The Apennines–Marianas and the Alps–Andes (continental and oceanic subduction zones) are representative of the two major classes of orogens where the subduction hinge migrates away from, and toward the upper plate respectively (Fig. 30).

However, it has been shown that in the Apennines, a number of sub-settings can be described, and in the southern side of the arc the hinge migrates towards the upper plate, while in the rest of the arc the hinge migrates away from it (Doglioni et al., 2007). The orogens of Alpine–Andean type have therefore slower subduction rates than the Apenninic–Marianas type when convergence is constant. The double verging Alpine–Andean type belt is composed mostly by upper plate rocks during the oceanic subduction, being the lower plate more extensively involved during the later collisional stage. The single verging Apennines–Marianas type belt is rather composed primarily by shallow rocks of the lower plate (Fig. 31b). A wide variety of different geophysical, geological and volcanological signatures mark the two end members of orogens and subduction zones (Doglioni et al., 1999b). The two end-members where the subduction hinge migrates away or toward the upper plate largely match the two opposite cases of seismic decoupling or seismic coupling (e.g. Scholz and Campos, 1995). However, along the Apennines subduction zone at least five different kinematic settings coexist, showing how a single subduction can have internal deviations from the standard model and variable velocities as a function of the combination VH and VL. Relative to the mantle, the W-

directed slab hinges are almost fixed, whereas they move west or southwest along E- (or NE-) directed subduction zones. When describing the plate motions relative to the mantle, e.g. in the hotspot reference framework, both Africa and Greece move southwestward with respect to the mantle (Greece faster). This implies that, relative to the mantle, the slab is moving in the opposite direction of the subduction (upduction). The slab sinks because it is overridden by the faster upper plate (Fig. 24 and 42). Therefore the slab pull cannot be the only driving force of neither the Hellenic subduction, nor of E- (or NE-) directed subduction zones in general, because it is moving SW-ward or W-ward relative to the mantle. Along this subduction zone, again, plate motions are not controlled by subduction rates, but vice-versa. Unlike E- (or NE-) directed subduction zones, along W- (or SW-) directed subduction zones, the slab generally sinks faster than the convergence rate. However, the lower plate can converge or diverge from the upper plate. In case the lower plate diverges faster than the hinge, the subduction rate is negative, i.e., the lower plate is escaping from the subduction (Fig. 40, sections 5W and 6W). This setting might represent a final evolution of the subduction zone and could be an alternative cause for the detachment of slab that is generally inferred as related to the sinking of the supposed denser lower part (e.g., Wortel and Spakman, 2000). Alternatively, since once penetrated into the mantle, the slab cannot be re-exhumed, the detachment of the slab could rather occur because the top part of the lower plate L is moving away from the deeper (>100-150 km?) segment (Fig. 40, sections 5W and 6W). Nevertheless it is not necessary to invoke slab detachment to justify the seismic gap in E- (or NE-) directed subductions (Fig. 38).

In other words the deep seismicity along W- or (SW-) directed slabs is regularly connected to the superficial part of the subduction zone (α - $\beta \approx 6°$), while along E- (or NE-) directed subduction zones the large difference between dips (α - $\beta \approx 30°$) rather suggests a different origin for the deep seismicity (Varga et al., 2011). In fact along E- (or NE-) directed subduction zones, the seismicity is, as a rule, very low or absent between 350 km and 550 km of depth (Riguzzi et al., 2010). The deep seismicity may be due rather than to the presence of a detached slab to a mantle suction process and to the shear between upper and lower mantle, due to Venturi effect: the mantle, in correspondence of E- (or NE-) directed subduction zones, can flow through a surface that is significantly reduced, with respect to standard situations, by the subduction plate marked by seismicity, as a rule, not deeper than about 350 km, with consequent reduction in fluid pressure.

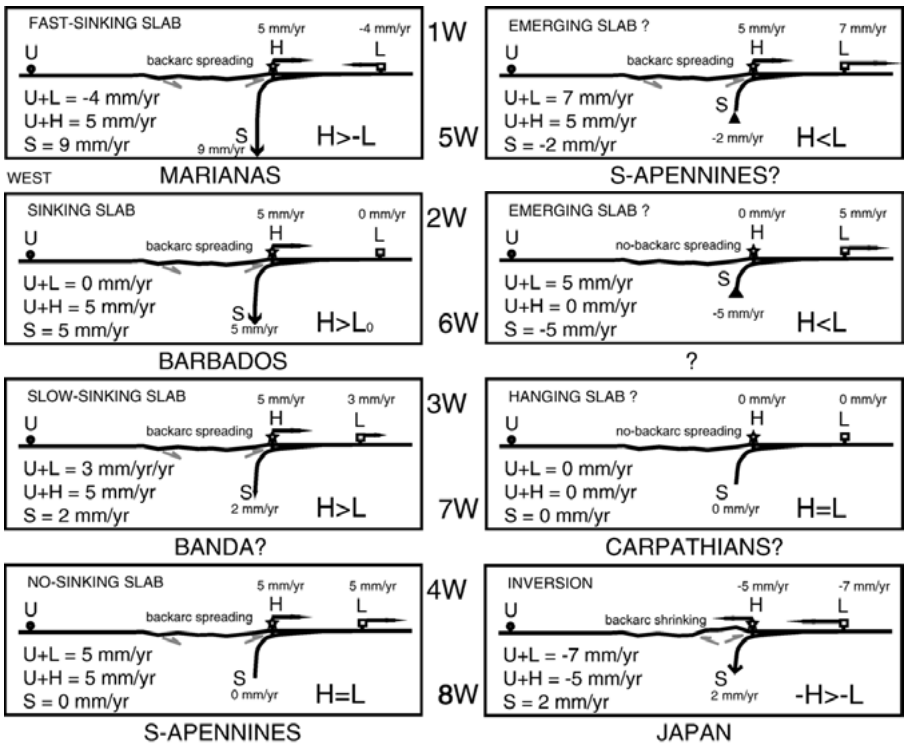

(A)

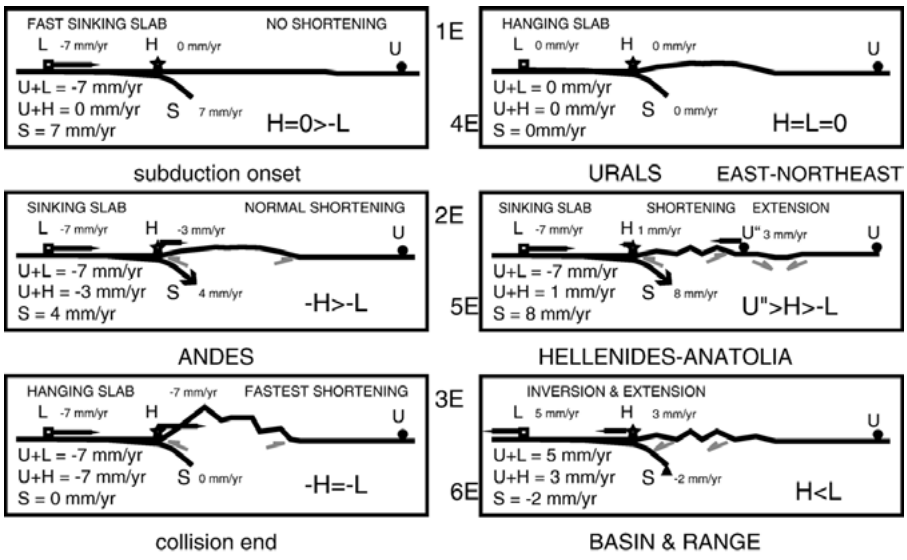

(B)

Fig. 40. (A) Different kinematic settings of W- (or SW-) directed subduction zones. In the 1W to 5 W sections, H is moving away from U, in 6W and 7W sections H is fixed, and in section 8W it is moving towards U. The site L is converging relative to U in sections 1W and 8W; it is fixed relative to U in sections 2W and 7W. In the other cases L is moving away from U, but with different velocity with resepect to H, i.e., faster, slower or equal. (B) Different kinematic settings of E- (or NE-) directed subduction zones. In the sections 1E, 2E, 3E and 5E, L is converging relative to U, whereas L is fixed in section 4E and diverging in section 6E. The hinge H is fixed relative to U in sections 1E and 4E, it is rather converging in sections 2E, 3E and 5E, whereas it is diverging in section 6E. The different regions are interpreted as examples of the variable settings. Both in (A) and (B) Velocities are only for relative comparison and do not apply to the example geographic areas.

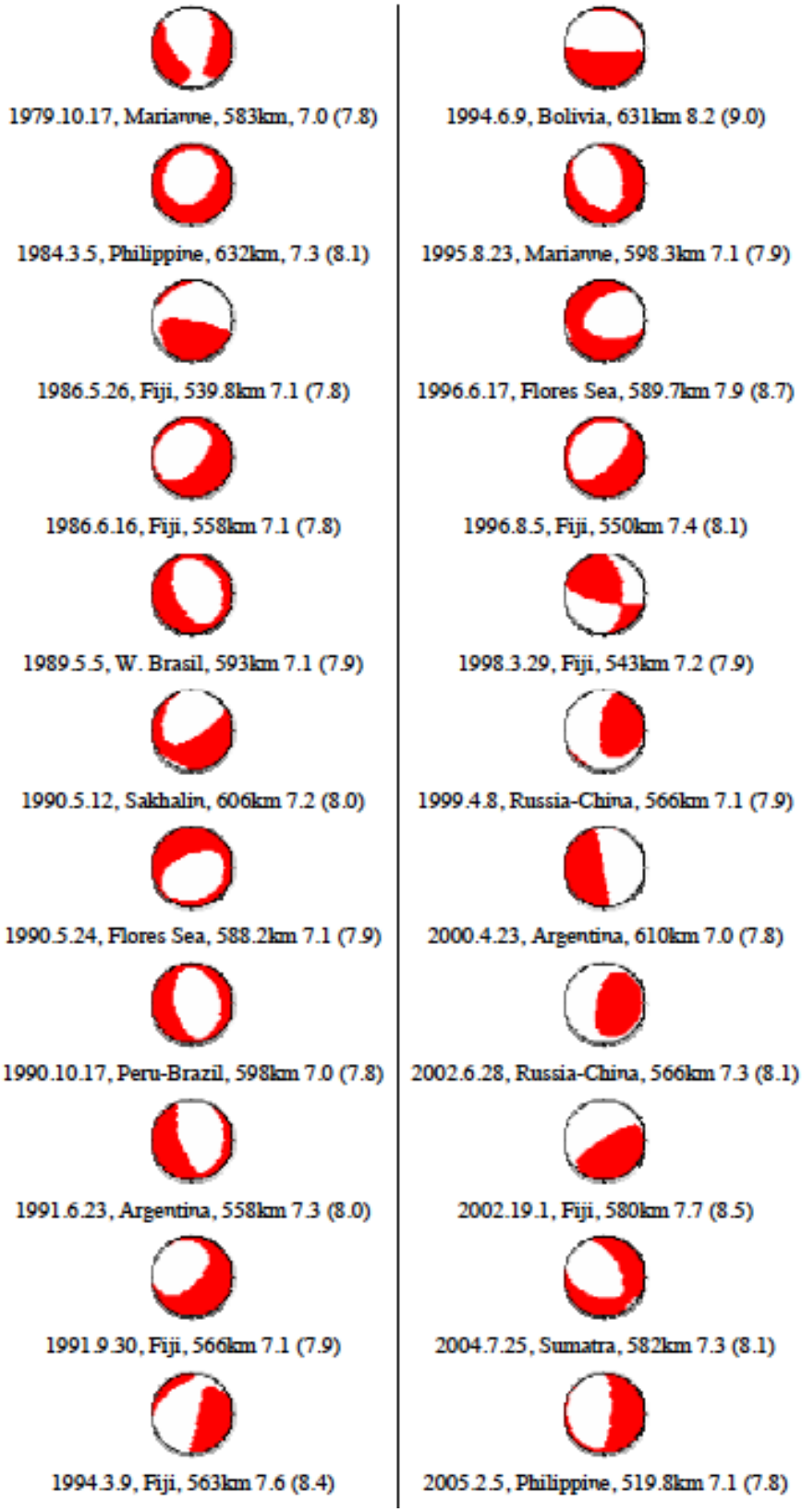

Fig. 41. Focal mechanisms for the earthquakes with MW ≥ 7 for time interval 1979-2005. M_W values of Engdahl and Villaseñor, 2002 (corrected according Herak et al., 2001)

Therefore the deep earthquakes along the E- (or NE-) directed slabs may be related to the subduction system, which is sucking up the mantle, but they occur in the mantle without requiring the presence of any slab fragment (e.g., Doglioni et al., 2009).

Most of the elastic energy radiated by deep events is concentrated in the depth interval between 580 km and 640 km. Green (2007) proposed that deep earthquakes are related to shearing instabilities accompanying high-pressure phase transformations. Most of the 27 focal mechanism given in the Harvard CMT Catalogue for the deep events with $M_W \geq 7.0$ occurred in the time interval 1976-2005 have a major extensional component (Fig. 41), well consistent with an accelerated mantle flow through narrow structures (e.g. Hilst, 1995) across the lower boundary of the C layer. This phenomenon leads to the reduction in pressure (Venturi effect) what is reflected in the extensional character of the focal mechanism of the earthquakes with $M_W \geq 7$ which occurred, in the depth interval from 520 km to 630 km, close to the bottom of the transition zone, below the E- (or NE-) directed subduction zones (see Fig. 44).

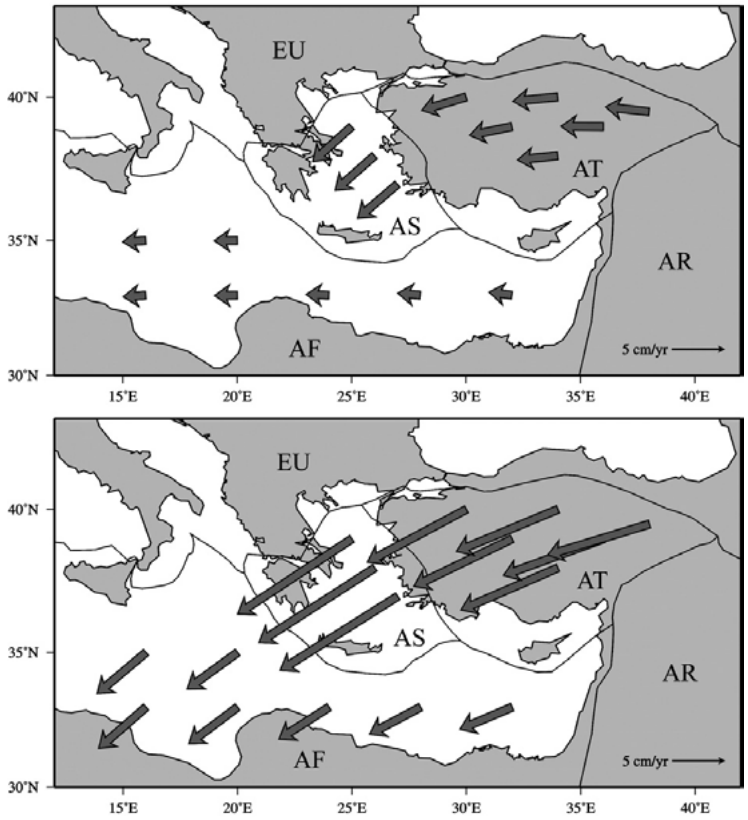

Fig. 42. Plate motions of Africa, Greece and Anatolia relative to the mantle in the deep (above) and in the shallow hotspot reference frames (below). Note that in both reference frames, Africa is moving westward faster than the underlying mantle, escaping from the subduction, i.e. upducting This setting refers to the case of the panel 5E of Fig. 40B, after Doglioni et al. (2007). See also Fig. 8, 11 and 24.

Let us consider, for example, the case schematized in section 5E of Fig. 40B. The plate motion of Africa, Greece and Anatolia relative to the mantle in the deep (above) and in the shallow hotspot reference frameworks (below) (see Section "Shallow and deep hot spot reference frameworks) is shown in Fig. 42. In both reference frameworks, Africa is moving westward faster than the underlying mantle (Fig. 42), escaping from the subduction, i.e. upducting (Doglioni et al., 2007).

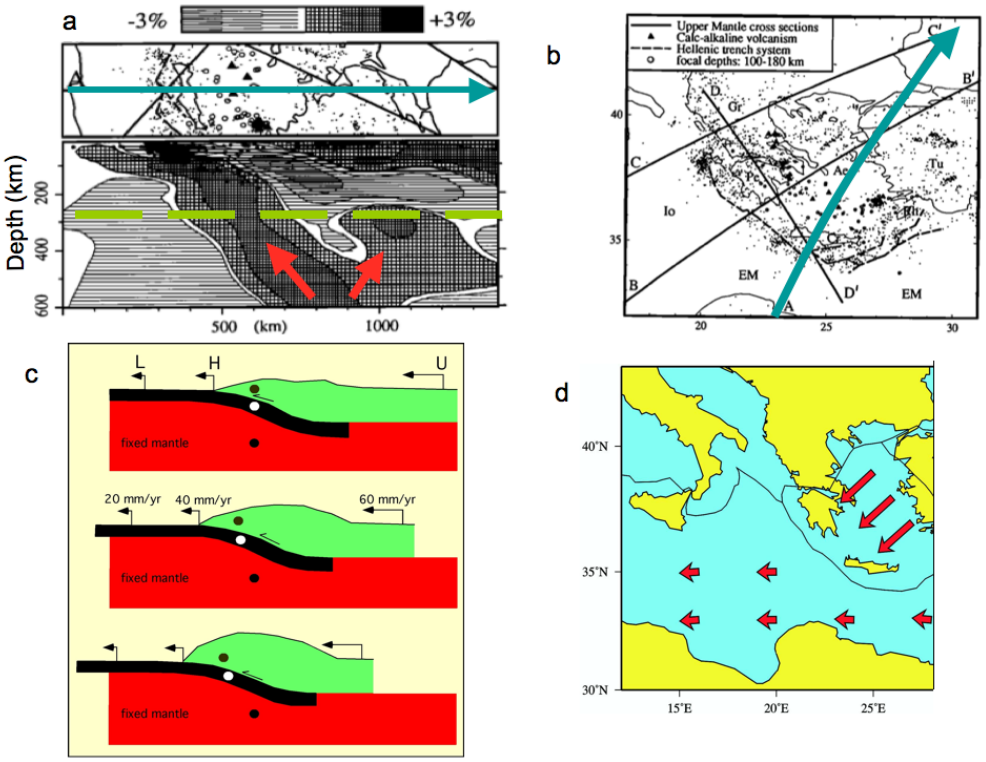

Fig. 43. (a) Tomographic image of the Aegean/Eastern Mediterranean upper mantle for the section shown in (b); the contouring is in percentages of the ambient Jeffreys-Bullen upper mantle velocity (see legend); cross (horizontal) hatching indicates positive (negative) anomalies; regions with poor spatial resolution are not contoured (large white areas); the interval -0.1%/+0.1% is also indicated in white; horizontal and depth axes are given without vertical exageration. Black symbols are the projection of hypocenters with M>4 located within 100 km from the plane (see also Fig. 7); the long dashed horizontal line delimits the maximum depth of hypocenters and the width of the location map is 3 degrees (Spakman et al., 1988); the short inclined arrows indicate a possible flow of a portion of lower mantle sucked from below made possible by the wake left by the slab in its upduction (exumation) motion (Doglioni et al., 2009); this interpretation seems more consistent with the tomo image than the presence of a subductiong slab, with rather complex shape. In the location map of the Eastern Mediterranean and Aegean area (b), the solid lines indicate the location of the upper mantle cross sections considered by Spakman et al. (1988) and the solid arrow indicates the cross section considered here; full dots indicate the epicenters of earthquakes with M>4 and focal depths less than 100 km that occurred from 1964-1984; Ae=Aegean basin, Cr=Crete, EM=Eastern Mediterranean, Gr=Greece, Io=Ionian basin, Pe=Peleponnesus, Rh=Rhodes, Tu=Turkey. (c) When plate motions are considered relative to the hotspot reference frame, i.e., assuming fixed the mantle, the slabs of E- (or NE-) directed subduction zones, like the Adria/Ionian plate, may move out of the mantle (upduction); in the three stages sketch the white dot moves leftward relative to the underlying black dot in the mantle and subduction occurs because the upper plate dark gray dot moves leftward faster than the white circle in the slab, the subduction rate is the convergence minus the orogenic shortening (in the model, the slab moves west at 20 mm/yr relative to mantle). (d) Plate motions of Africa and Greece relative to the mantle in the deep hotspot reference framework – detail from Fig. 42.

The tomographic image shown in Fig. 43 has been interpreted as a subducting slab reaching depth of about 600 km (Spakman et al., 1988) even if the recorded hypocenters are not deeper than about 300 km (see also Fig. 7) and the shape of the supposed slab is quite far from the simple geometry of Benioff zones (Isacks and Barazangi, 1977).

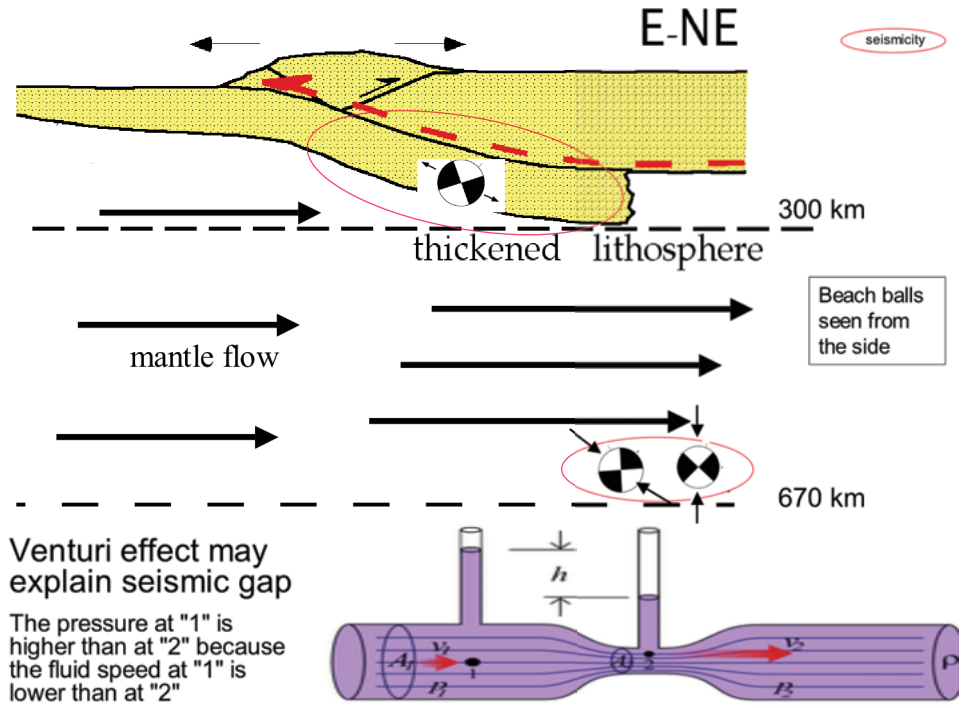

Fig. 44. The deep seismicity maybe naturally explained by a mantle suction process and to the shear between upper and lower mantle, generated by a sort of Venturi effect: the mantle, in correspondence of E- (or NE-) directed subduction zones, can flow through a surface that is significantly reduced, with respect to standard situations, by the subduction plate marked by seismicity, as a rule, not deeper than about 300 km. Therefore the deep earthquakes along the E- (or NE-) directed slabs may be related to the subduction system, which is sucking up the mantle, but they occur in the mantle without requiring the presence of any slab (e.g., Doglioni et al., 2009). Most of the 27 focal mechanism given in the Harvard CMT Catalogue for the deep events with $M_W \geq 7.0$ occurred in the time interval 1976-2005 have a major extensional component (Figure 9), well consistent with the reduction in pressure (Venturi effect) what is reflected in the extensional character of the focal mechanism of the earthquakes with $M_W \geq 7$. Deep earthquakes (h>500km) in E- (or NE-) subducting plates may be linked to (a) phase changes, (b) fast strain rate (Venturi effect), (c) higher rigidity of the uplifted perovskite phase, the last two processes being similar to the shallow-type brittle seismogenic processes.

The short inclined arrows indicate, on the other side, the possible flow of a portion of lower mantle, sucked from below. Such a process is made possible by the wake left by the slab in its upduction (exumation) motion (Doglioni et al., 2009). Therefore the upduction seems a much more natural process, consistent with the tomographic image, than the subduction of a slab, with rather complex shape. Similar conclusion can be reached considering the other sections given by Spakman et al., 1988). In fact, when plate motion is considered relative to

the hotspot reference frameworks, the Adria/Ionian plate moves out of the mantle (upduction) (Fig. 42, 43c and 43d).

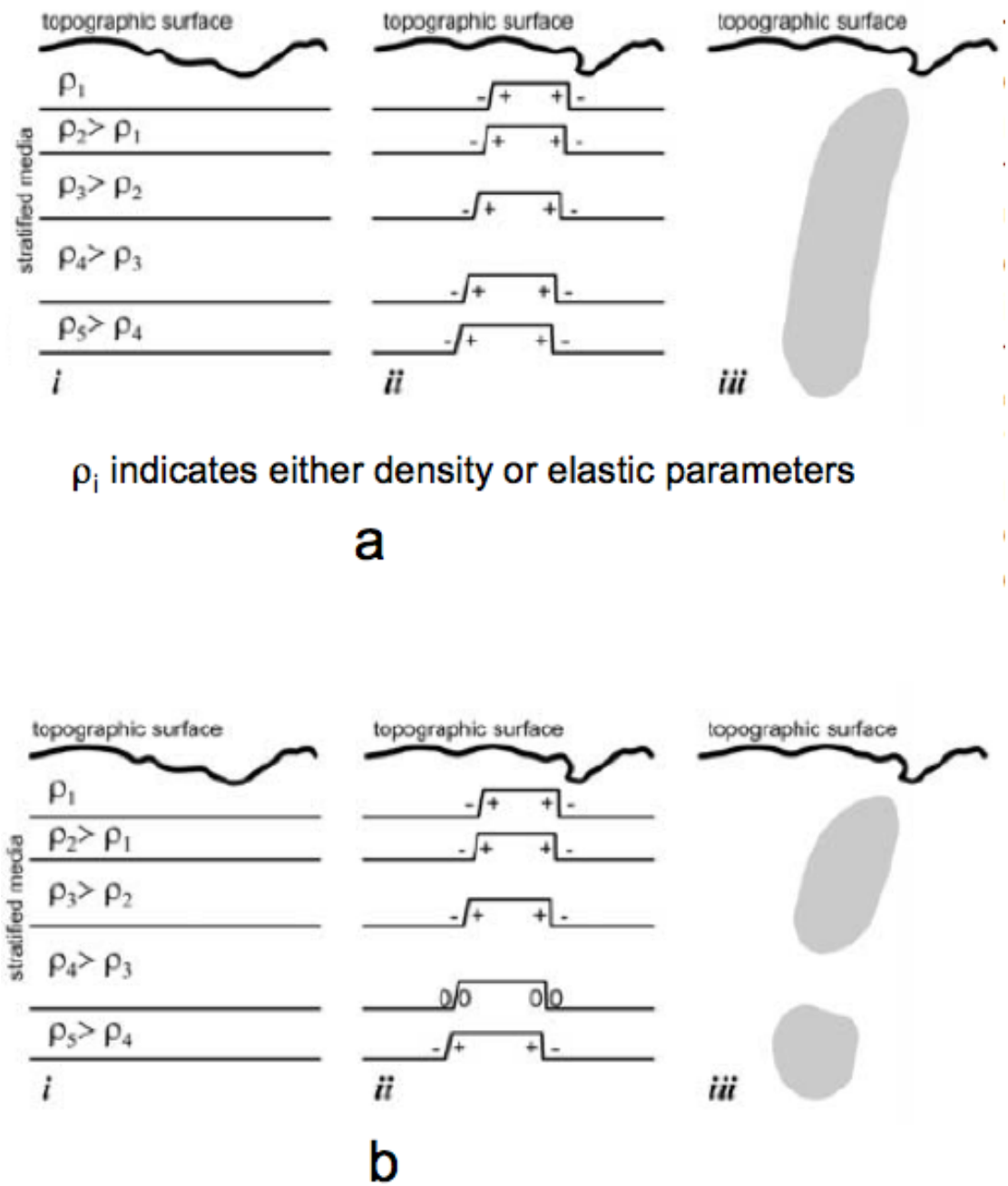

Fig. 45. Schematic model of upducting mantle. The internal pressure and isostasy drives the rising of deep (denser and/or faster) mantle material along the wake left by the upducting slab. (a) If in the previously undeformed stratified media ***i*** the density and velocity functions increase toward the Earth's center, as it is the case at depth greater than 300 km in the Earth, the rising column in ***ii*** produces a contrast (represented as faced '–' and '+' in ***ii***) that the seismic tomography, represented in ***iii***, can interpret erroneously in a different way: a cold down going slab (Fig. 45a). (b) If, for example, in the fourth layer the rising column in ***ii***, reaches a state in which the resulting elastic parameters produce a null velocity contrast (faced '0' and '0' in ***ii***) and consequently the slab-like continuity appears broken in the tomography represented in ***iii***. Such a situation can be erroneously interpreted as a detached slab, which is dropping toward the deep mantle (Fig. 45b), modified after Scalera (2005).

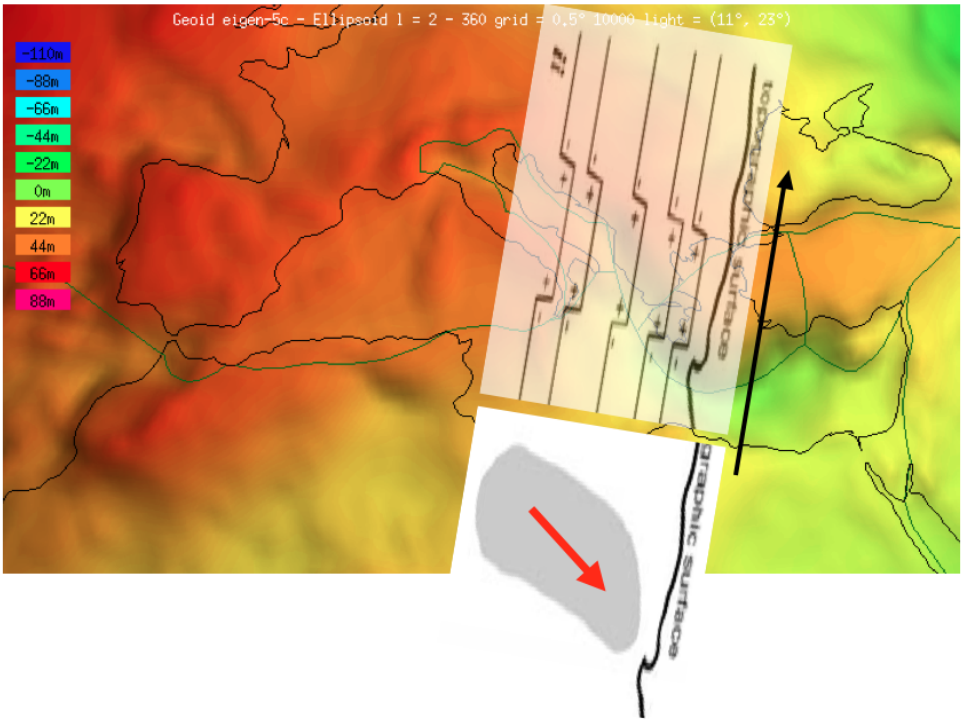

(a)

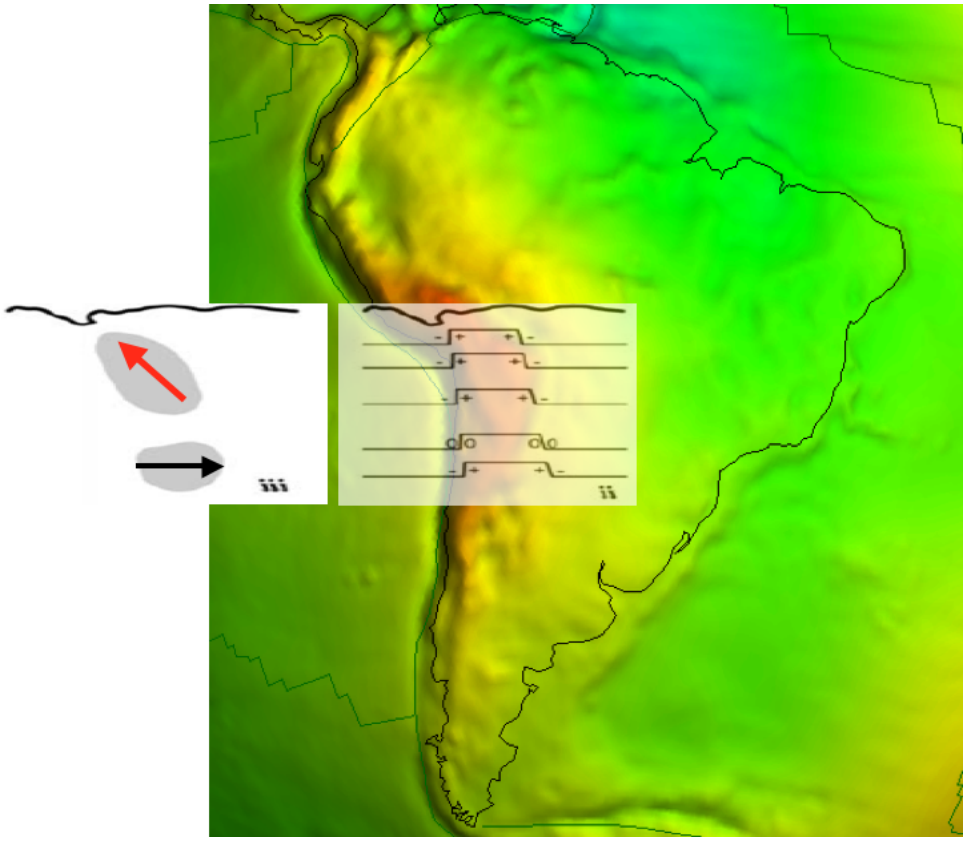

(b)

Fig. 46. Geoid of the Mediterranean area (a) and of South America (b) (see also http://www.iges.polimi.it/pagine/services/repo/by_map.asp) are consistent with the model described in Fig. 45.

As shown in fig. 43c, the white dot moves leftward relative to the underlying black dot in the mantle and subduction occurs because the upper plate dark gray dot moves leftward faster than the white circle in the slab. The subduction rate is the convergence minus the orogenic shortening. With different velocities, this seems to apply, in the shallow hotspot reference framework, also to the Andean subduction (AS). This kinematic evidence of upducting slabs casts serious doubts on the slab pull as the dominant driving mechanism of plate motions.

The internal pressure and isostasy drives the rising of deep (denser) mantle material along the wake left by the upducting slab. If the previously undeformed stratified media ***i*** has density and velocity function increasing toward the Earth's center, as it is the case at depth greater than 300 km in the Earth, the rising column in ***ii*** produces a contrast (represented as faced '–' and '+' in ***ii***) that the seismic tomography, represented in ***iii***, can interpret erroneously in a different way: a cold downgoing slab (Fig. 45a). Furthermore, if in the fourth layer, the rising column in ***ii***, because of a difference in decompression or depletion of fluids, reaches a state in which the resulting elastic parameters produce a null velocity contrast (faced '0' and '0' in ***ii***) the slab-like continuity appears broken in the tomography represented in ***iii*** and this can be erroneously interpreted as a detached slab, which is dropping toward the deep mantle (Fig. 45b).

On the contrary the upduction naturally explains the tomographic images and does not require the introduction of the concept of slab break off. The rise of denser material from below is in quite good agreement with the geoid undulations, as can be see in Fig. 46.Therefore W- (or SW-) directed subduction zones bring larger volumes of lithosphere back into the mantle than the opposite subduction zones. W- (or SW-) directed subduction zones have the rate of sinking controlled by the slab-mantle horizontal "easterly"- directed wind interaction, which mostly determines the retreat of the subduction hinge, plus the far field velocities of the plates, and the value of the negative slab buoyancy. On the other side, E- (or NE-) directed subduction zones have rates chiefly determined by the far field velocity of plates, since the subduction hinge generally advances toward the upper plate and decreases the subduction rate (Table 2).

The analyzed kinematics frameworks suggest that subduction zones have rates of sinking controlled by far field plate velocities, hinge migration direction, and subduction polarity, claiming for a passive behavior of the slabs. This is more reasonable if the net "westward" rotation of the lithosphere is a global phenomenon rather than the simple average of plate motions (Scoppola et al., 2006). Tidal drag (Bostrom,

1971; Moore, 1973) combined with Earth's rotation, mantle convection, and a thin very low viscosity layer in the asthenosphere seem to be at the base of plate motions (Scoppola et al., 2006; Riguzzi et al., 2010).

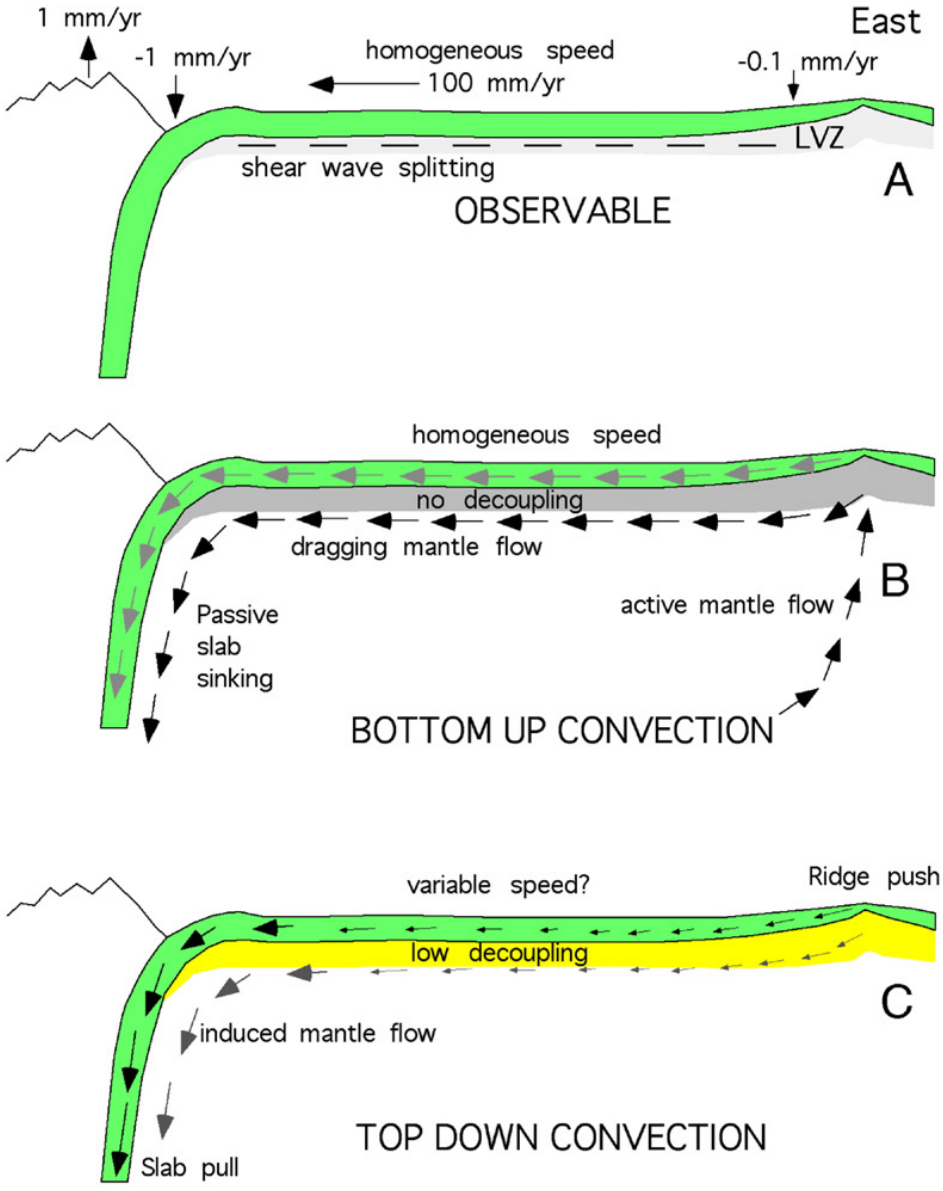

Fig. 47. The surface observables (A) are compared with two models of plate dynamics, where plate motion is induced by classic mantle convection (B) and boundary forces (C). Modified from Doglioni et al., 2007.

The ridge push, related to the topographic excess, should be higher along elevated orogens, where on the contrary, plates converge rather than diverge. Boundary forces such as slab pull and ridge push could in principle generate a deceleration moving away from the energy source, but plates rather show internal homogeneous velocity (Fig. 33). Mantle convection could satisfy a steady state speed of the overlying

lithosphere, assuming low or no decoupling at the asthenosphere interface. However, mantle convection is kinematically problematic in explaining the migration of plate boundaries and the occurrence of a decoupling surface at the lithosphere base. Although a combination of all forces acting on the lithosphere is likely, the decoupling between lithosphere and mantle suggests that a torque acts on the lithosphere independently of the mantle drag. Slab pull and ridge push are candidates for contributing to this torque, but, unlike these boundary forces, the advantage of the Earth's rotation and related tidal drag is to be a volume force, acting simultaneously and tangentially on the whole plates. Tidal drag maintains the lithosphere under a permanent high frequency vibration, polarized and sheared toward the "west" (Fig. 47). Earth's rotation and the break exerted by the lag of the tidal bulge (Bostrom, 1971) can be efficient only if very low viscosity occur at the lithosphere-asthenosphere transition (Jordan, 1974) and growing evidences are emerging on the presence of a very low viscosity layer at the very top of the asthenosphere (e.g., Rychert et al., 2005), possibly related also to very high fluids concentration in the mantle.

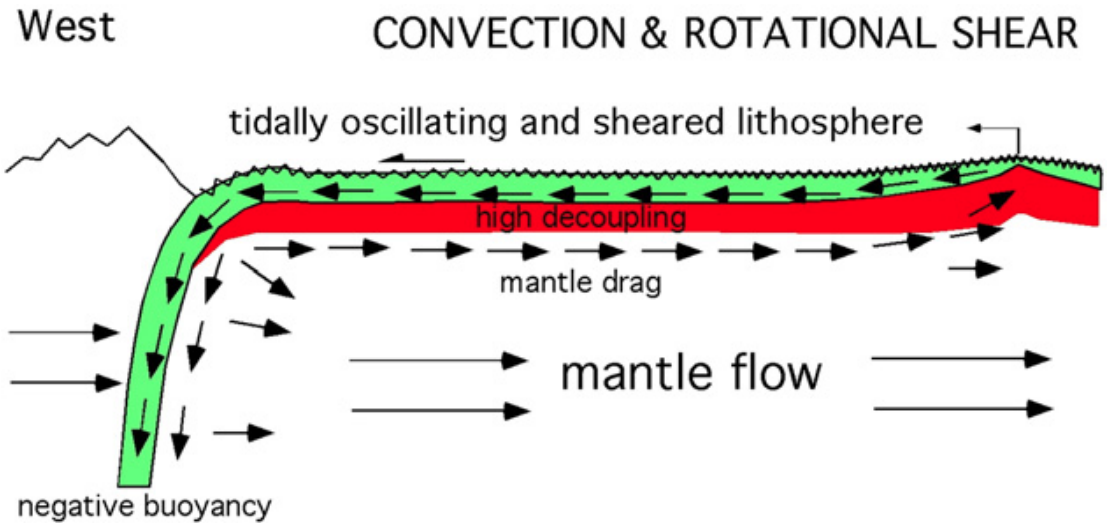

Fig. 48. Schematic plate dynamics resulting from the combination of the mechanisms (B) and (C) shown in Fig. 47 with the rotational drag, where the flow patterns, schematized by arrows, describing the coexistence of Earth's convection and the rotational shear, are shown. The cooling of the Earth, enhancing mantle convection, adds to the shear associated to the horizontal component of the solid Earth tide triggered by the westward drift of the lithosphere.

Lateral variations in the low velocity layer viscosity could control the different velocity of plates. The Earth's rotation contribution to move the lithosphere could account for: i) the homogeneous internal velocity of each plate, ii) the decoupling occurring at the lithosphere base, and iii) the westerly polarized migration of the lithosphere and the plate boundaries, consistent with the geological asymmetries of subduction and

rift zones as a function of the geographic polarity. In this view, plate dynamics could be a combination of mantle convection and the shear induced by the tidal drag (Fig. 47 and 48).

Mantle wedge asymmetries and geochemical signatures along W- and E–NE-directed subduction zones

The triangular section of mantle in the hanging wall of subduction zones, schematized in Fig. 49, is usually defined mantle wedge. The wedge is a portion of the mantle with positive temperature anomalies up to 400–600 °C (Koper et al., 1999) with respect to average mantle, rich in fluids released by the downgoing slab (Billen and Gurnis, 2001; Abers, 2005; Grove et al., 2006; Panza et al., 2007a,b; Peccerillo et al., 2008) and marked by seismic velocities which are low with respect to those of the surrounding mantle (Conder and Wiens, 2006; Panza et al., 2003; Raykova and Panza, 2006; Gonzales et al., 2011). In the literature, the mantle wedge is mostly undifferentiated, with variations related to the thickness and composition of the upper and lower plates.

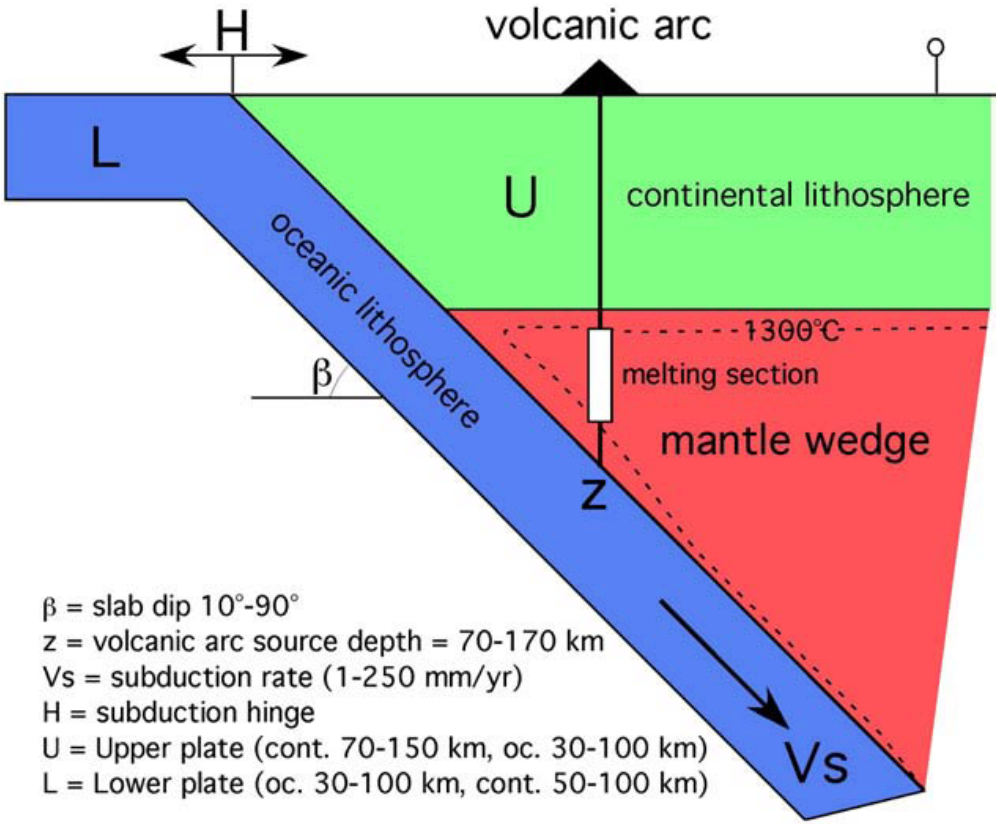

Fig. 49. The mantle wedge is the triangular section of mantle in the hanging wall of subduction zones. It is considered as the source for the magmatic arc, being percolated and metasomatized by the fluids delivered by the dehydration of the descending slab. Relative to the upper plate, the subduction hinge can diverge or converge. The kinematics of the hinge is a good indicator on the mantle wedge geometry. The legend in the figure indicates the range of values of the main parameters (Doglioni et al., 2009).

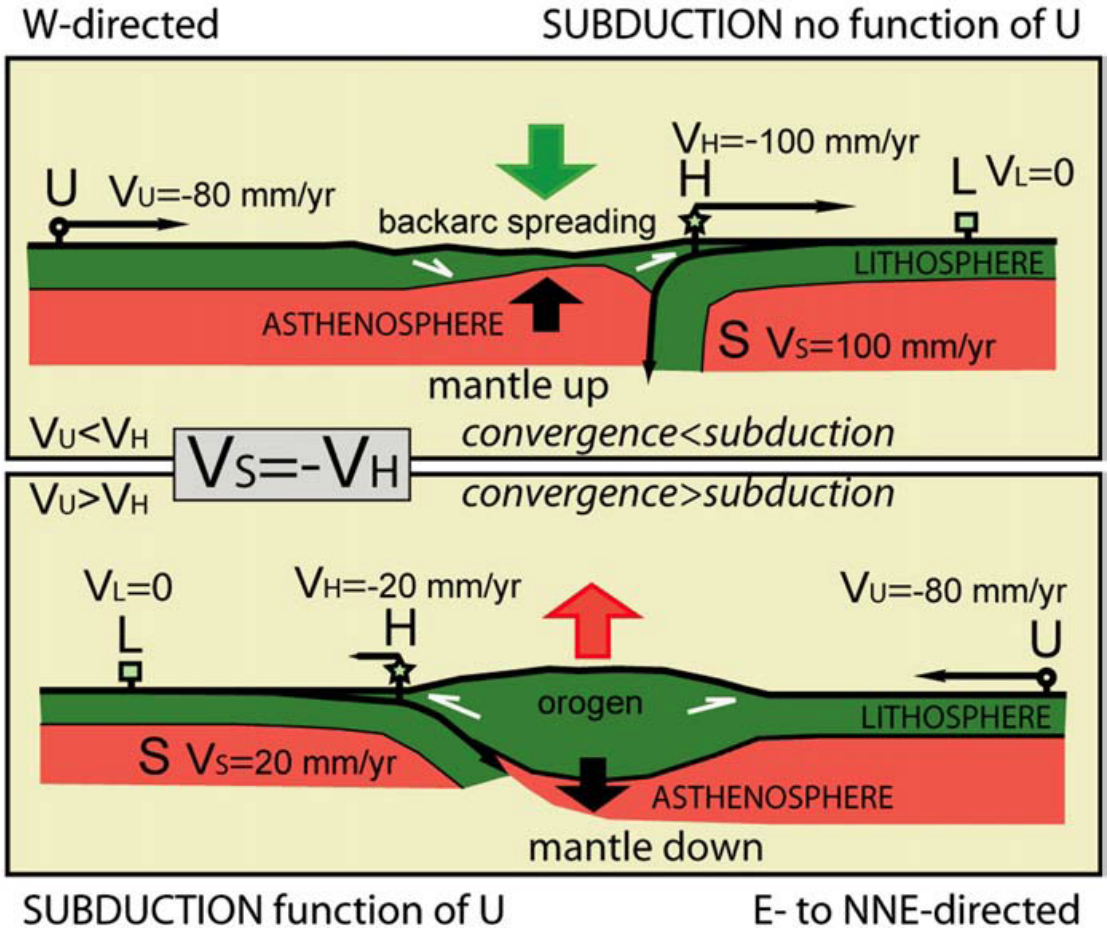

Fig. 50. Kinematics of subduction zones assuming fixed the lower plate L. The upper plate U converges at V_U=80 mm/year in both cases. If the transient location of the subduction hinge H moves at V_H=100 mm/year and V_H=20 mm/year, respectively, the resulting subduction S, given by V_S=−V_H, is 100 mm/year in the upper panel and 20 mm/year in the lower panel. The shortening in the orogen (lower panel) is V_U−V_H. S increases when H diverges relative to the upper plate (upper panel), whereas S decreases if H converges relative to the lower plate (lower panel). The case in the upper panel is characterized by backarc spreading and mantle upwelling, a low prism, and it is typical of W- (or SW-) directed subduction zones. The case in the lower panel is characterized by lowering of the mantle, double verging and elevated orogen and it forms along E- (or NE-) directed subduction zones. The velocity of the hinge equals the velocity of the subduction in both cases. In the upper panel the subduction is independent from the upper plate velocity while in the lower panel it is a function of it. These opposite kinematic settings indicate different dynamic origin of the subduction (1) slab/mantle interaction (upper panel) and (2) upper/lower plates interaction (lower panel) and support two end members of the mantle wedge, very thick (upper panel) and very thin (lower panel).

Independent of the westward drift, there are at least two basic reasons why in the E- (or NE-) directed subduction zones (e.g., central America, Andes, Alps, Dinarides, Zagros, Himalayas, Indonesia) the mantle wedge is thinner when compared with that of the W- (or SW-) directed ones: (1) as a rule, the continental upper plate of the E- (or NE-) directed subductions is thick (e.g., Panza, 1980; Panza et al., 1982; Artemieva and Mooney, 2001; Panza et al., 2003; Manea et al., 2004) and (2) the slab is on average less inclined than in W- (or SW-) directed subductions (Cruciani et al., 2005; Riguzzi et al. 2010).

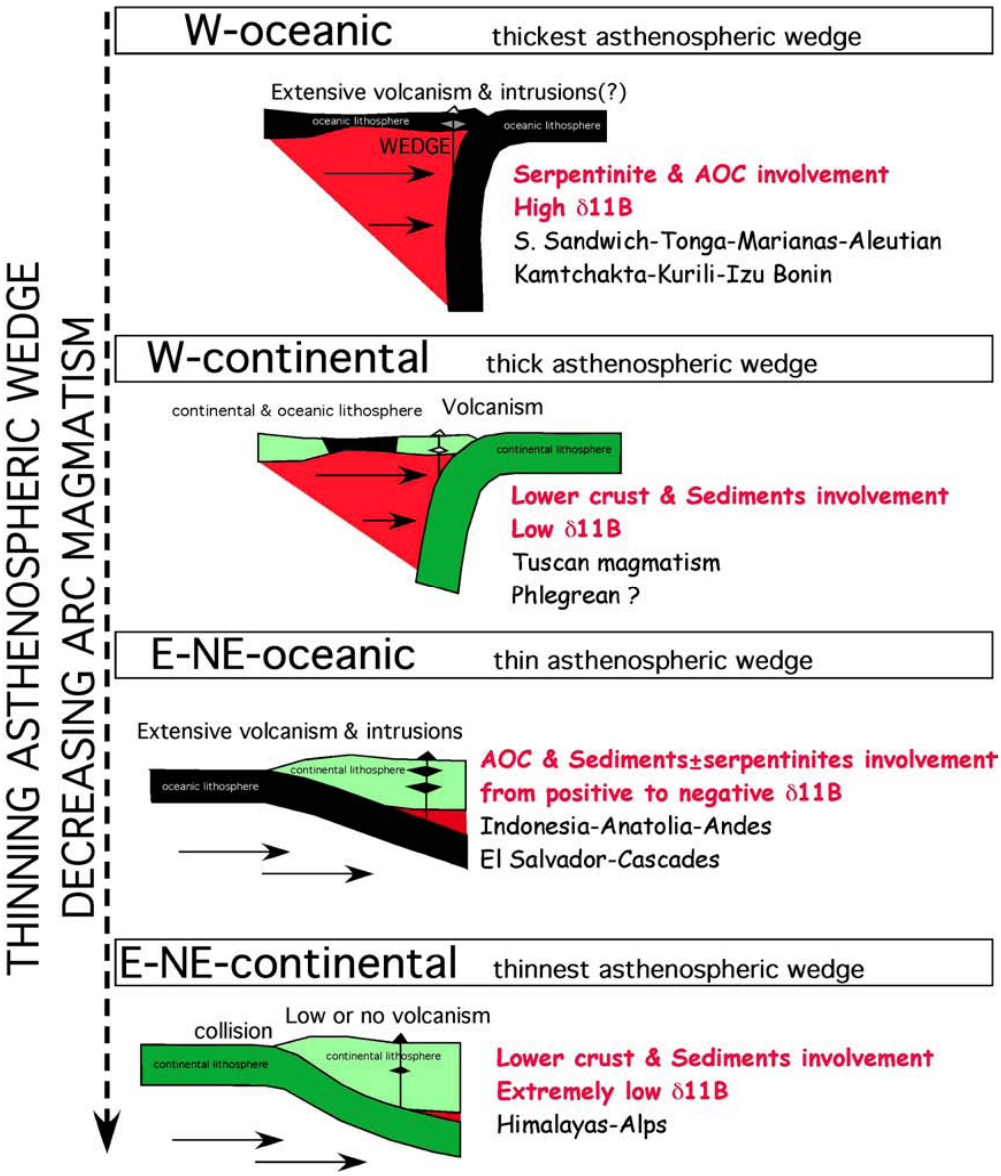

Fig. 51. The four cases represent the possible settings of W- (or SW-) directed and E- (or NE-) directed subduction zones as a function of the composition of the lower plate (oceanic or continental). The magmatism volume should be controlled by the slab dehydration, the asthenospheric wedge thickness and the subduction rate. The asthenospheric wedge thickness increases with the slab dip and decreases with the upper plate thickness. The thickest mantle wedge of asthenosphere is along the W- (or SW-) directed oceanic case, where the slab is steeper and the upper plate is young oceanic lithosphere. A slightly thinner asthenospheric wedge occurs in W- (or SW-) directed continental lithosphere, where it is expected a shallower melting of the lower plate. The steep slab along the W- directed cases is controlled by the negative buoyancy (if any) and the advancing mantle flow. Along the E- (or NE-) directed oceanic cases, widespread volcanism forms; the upper plate along the E-oceanic can also be oceanic (usually older than the lower plate). The thinnest asthenosphere should occur along the E- or NE-continental example, where in fact there is the lowest amount of volcanism. The shallow slab dip of the E-cases is controlled by low negative buoyancy (if any), and the sustaining mantle flow. AOC, altered oceanic crust.

Subduction zone kinematics predict that, assuming a fixed lower plate, the velocity of the subduction (V_S) equals the velocity of the subduction hinge ($V_S=-V_H$). In all subduction zones the subduction hinge

migrates toward the lower plate (Fig. 50). However, two main types of subduction zones can be distinguished: (1) those, mostly W- (or SW-) directed, where the upper plate converges towards the lower plate at a slower rate than the subduction hinge and (2) those, generally E- (or NE-) directed, in which the upper plate converges faster than the subduction hinge. Along the first type, as a rule, there is an upward flow of the asthenosphere in the hanging wall of the slab (e.g. Panza at al., 2007b), whereas along the second type, the mantle is pushed down due to the thickening (doubling) of the lithosphere (see Fig. 43 and 44).

The kinematics of W- (or SW-) directed subduction zones predicts a much thicker asthenospheric mantle wedge (Fig. 49), larger volumes and faster rates of subduction with respect to the slabs E- (or NE-) directed. The larger volumes of lithospheric recycling, the thicker column of fluids-rich, hotter mantle wedge, all should favour greater volumes of magmatism per unit time. The E– (or NE-) directed subduction zones show a thinner, if any, asthenospheric mantle wedge due to a thicker upper plate and shallower slab. Along these settings, the mantle wedge, where the percolation of slab-delivered fluids generates melting, mostly involves the cooler lithospheric mantle. Mantle wedge thickness, composition and temperature are all affected by the asymmetries imposed by the westward drift of the lithosphere (Fig. 31) and the consequent differences among subduction zones (Fig. 51). Therefore, regardless the mantle (hotspot) reference framework, the subduction systems are a function of the geographic polarity (Fig. 50) and the subducting slabs have a passive behaviour, rather than being the primary force in driving plate tectonics. The B and Nd isotopes confirm the asymmetry of subduction zones (Doglioni et al., 2009). Hotter and thicker asthenosphere in the hanging wall of W- (or SW-) directed subduction zones is generally accompanied by positive and higher $\delta^{11}B$ and $^{143}Nd/^{144}Nd$, except where there is a significant crustal contribution (e.g., Apennines). The flow due to the westward drift of the lithosphere can be interpreted as the first order flow between lithosphere and mantle, whereas the subduction and rift zones are secondary turbulences (Fig. 52). This first order circuitation may exist and takes place because of the presence of the global circuit of partially molten, low velocity material detected below the TE-pert (see Fig. 26 and 53) detected by Panza et al. (2010). Accordingly with Doglioni et al. (2009) the corner flow induced in the host mantle by subduction zones (e.g. Turcotte and Schubert, 2002) is not a general mechanism but it occurs dominantly along W- (or SW-) directed subduction systems. Along the E- (or NE-) directed subduction zones (Fig. 52), where plates move W-ward or SW-ward relative to the mantle, in a direction opposite to that of the subduction (Cuffaro and Doglioni, 2007), the dominant process is upduction, described in section

"Subduction, obduction and upduction (exumation)": the motion of the slab generates an upward flow of the mantle beneath the subduction zone, sucking up the mantle and depressurising it (Fig. 52). The upward suction (upduction) of the mantle inferred at depth along E– (or NE-) directed subduction zones (Fig. 43) provides a mechanism for syn-subduction alkaline magmatism in the upper plate, with or without contemporaneous rifting in the backarc. Unless large amounts of crustal rocks are subducted, as along the W-directed Apennines subduction zone, positive $\delta^{11}B$ and high $^{143}Nd/^{144}Nd$ characterize W- (or SW-) directed subduction zones where a thick and hot mantle wedge is present in the hanging wall of the slab. At a global scale the mantle would be flowing eastward relatively to the lithosphere, generating a first order flow. Subduction and rift zones are then a second order turbulence disturbing the main flow.

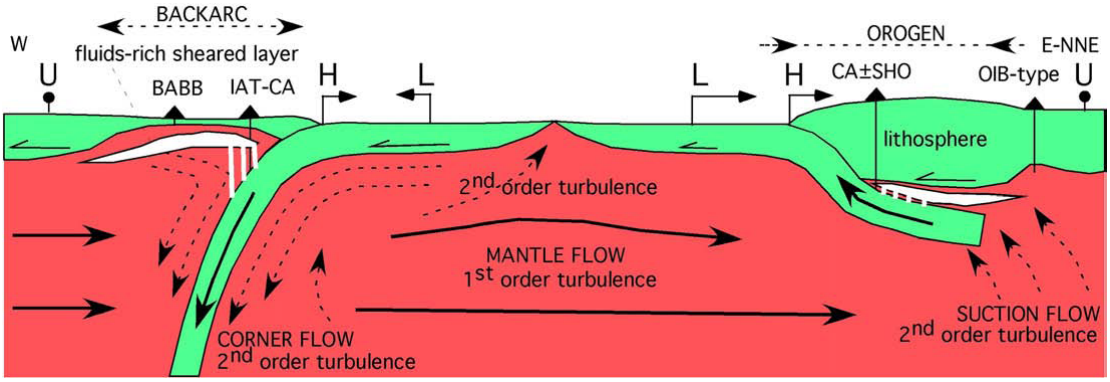

Fig. 52. The subduction zones disturb or deviate the general "eastward" flow of the mantle relative to the lithosphere. W- (or SW-) directed slabs produce a corner flow, whereas the opposite slab should rather generate an upward suction flow (upduction) from the underlying mantle. Such suction could trigger "fertile" mantle from below, and its decompression may locally generate OIB-type magmatism (e.g. Patagonia back-arc basalts, Bruni et al., 2008). The fluids released by both W- (or SW-) and E- (or NE-) directed slabs (e.g., the white lenses in the hanging wall of the subduction) decrease the viscosity at the top of the asthenosphere, speeding up the upper plate. The fluids are sheared by the lithospheric decoupling and determine a migration away from the lower plate along W- (or SW-) directed subduction zones, facilitating the backarc spreading. It triggers an opposite behaviour along the E- (or NE-) directed subduction zones where the westward increase of the upper plate velocity rather favours the convergence between the upper and lower plates, i.e., determining a double verging Andean-Alpine type orogen. BABB: back-arc basin basalts; IAT: island-arc tholeiites; CA, SHO: calc-alkaline and shoshonitic series; OIB-type: basalts with ocean island or intraplate affinity. H, subduction hinge; L, lower plate; U, upper plate. The arrows of L and H refer to fixed U, not to the mantle (see also Fig. 48).

Along W- (or SW-) directed subduction zones, slab retreat is compensated by the asthenosphere in the backarc, but it determines a down going corner flow in the host mantle. Conversely, along E- (or NE-) directed subduction zones, in general, there is no void to fill in the backarc setting. However, the slab is "remounting" relative to the mantle, and a suction flow from below is expected (Fig. 52). In fact, relative to the mantle, the lower plate is moving westward out of the mantle, in the direction opposed to the dip of the slab (upduction). The subduction

occurs because the upper plate is moving westward faster than the lower plate. A number of subduction zones are characterized by alkaline magmatism in the foreland of the retrobelt or within the orogen itself (e.g., Mineralnie Vodi in the northern Caucasus; Euganei Hills, in the Southern Alps; Patagonia; Aegean Sea, etc.). This magmatism may be related to an upward suction (upduction) of the mantle due to the opposite slab motion, as illustrated in Fig. 52. In this model, the high velocity body recorded by tomography along E- (or NE-) directed subduction zones, like the Andean "slab" (Heit, 2005) and the Dinarides sketch shown in Fig. 43 and 44, could be interpreted not as subducted lithosphere (in fact it is mostly aseismic), but as deeper mantle upraised by the suction mechanism. The deeper, more viscous and rigid mantle has a more compacted crystallographic structure and higher seismic velocities. The fluids released from the slab into the overlying mantle should trigger a decrease of viscosity in the hangingwall of the subduction, at the bottom of the upper plate. The top of the asthenosphere is the main decollement surface of the lithosphere, and the decrease of the viscosity can increase the decoupling. Therefore the upper plate increases its velocity moving away from the lower plate along the W- (or SW-) directed subduction zones. This facilitates the formation of the backarc spreading (Fig. 52). Along the E- (or NE-) directed subduction zones, the upper plate is converging faster with respect to the lower plate and this facilitates the generation of double verging orogens such as the Andes or Himalayas. This mechanism upraises the mantle from deeper levels, which have faster seismic velocities with respect to the shallower mantle. This could explain the ghost of a slab of tomographic origin, beneath E– (or NE-) directed subduction zones, where the presence of a real slab is questioned by the absence of continuous seismicity (see Fig. 38, 43 and 44). This could in turn facilitate partial melting and alkaline magmatism in "backarc" settings, with or without extensional tectonics, along the retrobelt of orogens associated with E- (or NE-) directed subduction zones. Release of fluids from the slab to the asthenosphere increases the decoupling at the base of the upper plate. However, this generates opposite tectonic consequences in the relationship between upper and lower plates along subduction zones. In fact, due to the W-ward drift of the lithosphere, it facilitates the widening between the upper and the lower plates along W- (or SW-) directed subduction zones, whereas it promotes the convergence along the E- (or NE-) directed subduction systems (Fig. 52).

Some concluding remarks

In plate tectonics it is assumed that the inertia and acceleration of the individual plates are nonexistent or negligible, and thus the plates

are in dynamic equilibrium (Forsyth and Uyeda, 1975). At present, the solid Earth can be considered in energetic equilibrium: the energy sources that keep running its dynamical processes and the most significant phenomena consumers of terrestrial energy resources are equivalent in magnitude (see the Appendix of Riguzzi et al. 2010). Thus it is natural to assume that the balance is in quasi equilibrium, i.e. there is no statistically meaningful difference between the total of income and expenditure energy rates. This circumstance allows for relatively small energy sources to influence global tectonic processes and therefore the tidal despinning can contribute to plate tectonics through the westward lithospheric drift (Bostrom, 1971; Knopoff and Leeds, 1972). Small perturbations in the velocity of rotation trigger the release of a large amount of energy and seismicity (Press and Briggs, 1975). The energy rate necessary to move the Earth's shields, i.e. to move the thicker lithosphere relative to the underlying poorly developed low velocity channel (as in the Baltic area), has been estimated at about $4 \cdot 10^{18}$ J/yr (Knopoff, 1972). Similar value is found by considering the energy of formation of tectonic dislocations that can be estimated as the consumption of energy rate $\dot{E}$ necessary for lateral displacement of the lithosphere plates relative to the viscous mantle. For a mantle viscosity of 10^{21} Pa▪s one gets $\dot{E}=6.5 \cdot 10^{19}$ J/yr (Riguzzi et al., 2010). Recent papers suggest viscosity values of 10^{17} Pa▪s (Aoudia et al., 2007; Melini et al., 2008), consequently, the power needed to move the lithosphere could be significantly lowered, possibly to $\dot{E}=6.5 \cdot 10^{15}$ J/yr. The tidal friction in the Earth–Moon system can be estimated as $\dot{E}=12 \cdot 10^{19}$ J/yr (Riguzzi et al., 2010) and most of this dissipation occurs in the oceans and shallow seas and only a limited part in the mantle. According to Ray (2001) the tidal dissipation in the mantle amounts to a maximum $0.42 \cdot 10^{19}$ J/yr, whereas the total oceanic and shallow seas dissipation is about $7.5 \cdot 10^{19}$ J/yr (Egbert and Ray, 2000). Therefore the residual available power, about $4 \cdot 10^{19}$ J/yr is larger than the one required to move the lithosphere with respect to the mantle, and the Earth's rotation plays a significant role in the generation of the relative shear.

The lithosphere and the underlying mantle represent a selforganized system in a critical state - SOC system (Stern, 2002) - open to external perturbations; plate tectonics is an example of a selforganizing complex system of hierarchical blocks in a critical state (Prigogine and Stengers, 1984). The Gutenberg–Richter law shows that large magnitude earthquakes are very rare events (Stein and Wysession, 2003), thus the energy released by one big earthquake seems to deplete temporally the energy budget of plate tectonics, i.e. a slab interacting with the surrounding mantle is not an isolated system, but it participates to a global expenditure of the stored energy.

Plate tectonics is an Earth's scale phenomenology, and the

energy source for its activation is not concentrated in limited zones (e.g., subduction zones), but it acts contemporaneously all over the whole Earth's lithosphere, like the Earth's rotation. Romashkova (2009) has recently shown how the planet seismicity indicates that the Earth's lithosphere can be considered as a single whole. Only the global seismicity follows the Gutenberg–Richter law, while this simple SOC relation does not hold when considering smaller portions of the Earth (Molchan et al., 1997). All these evidences and models are in favor, even if not conclusive, of a significant contribution to plate tectonics by the Earth's rotation.

The classic mantle convection, widely assumed as the main cause of plate tectonics, is complemented and polarized by the steady-state torque provided by the tidal bulge misalignment. The horizontal component of the Earth's tide pumps the system; the vertical component of the tides excites gravity oscillations, which locally load and unload the tectonic features (Fig. 11). Low solid tide (larger gravity) favors extensional tectonics, whereas high solid tide (lower gravity) triggers compressional tectonics. Tidal force on the early lithosphere of Mars by former satellites in retrograde orbits may have pulled the lithosphere in an east–west direction over hot mantle plumes (Kobayashi and Sprenke, 2010).

The differential velocity among plates would be controlled by the viscosity-related variable decoupling at the base of the lithosphere, combined with other forcing mechanisms of mantle convection such as mantle drag and slab pull. Numerical and analogue modeling should further test this model.

In 1678 Athanasius Kircher, depicts the most advanced thinking of his day about the internal structure of our planet. The Earth is supposed to contain a giant, fiery inferno, nicely coincident with the molten Earth’s core. The fires, through a complex network of channels and fissures and subsidiary bodies distributed through the interior, feed heat to the surface water, seeped in from the ocean, and give rise to hot springs (upper part of Fig. 53). Low velocity channels in the asthenosphere, where partially molten material is present, are indeed seen in shear wave velocity sections along the tectonic equator (TE) and a global circuit of partially molten material is seen along the perturbed path (TE-pert) (lower part of Fig. 53). Where tongues of fire (molten material) come close to Earth's surface, they start volcanoes, reflecting a pioneering awareness of volcanoes as a global phenomenon produced by a global process, rather than the purely localized product of wind action upon deposits of combustible materials. Kircher’s work played an important part in the dissemination of this notion.

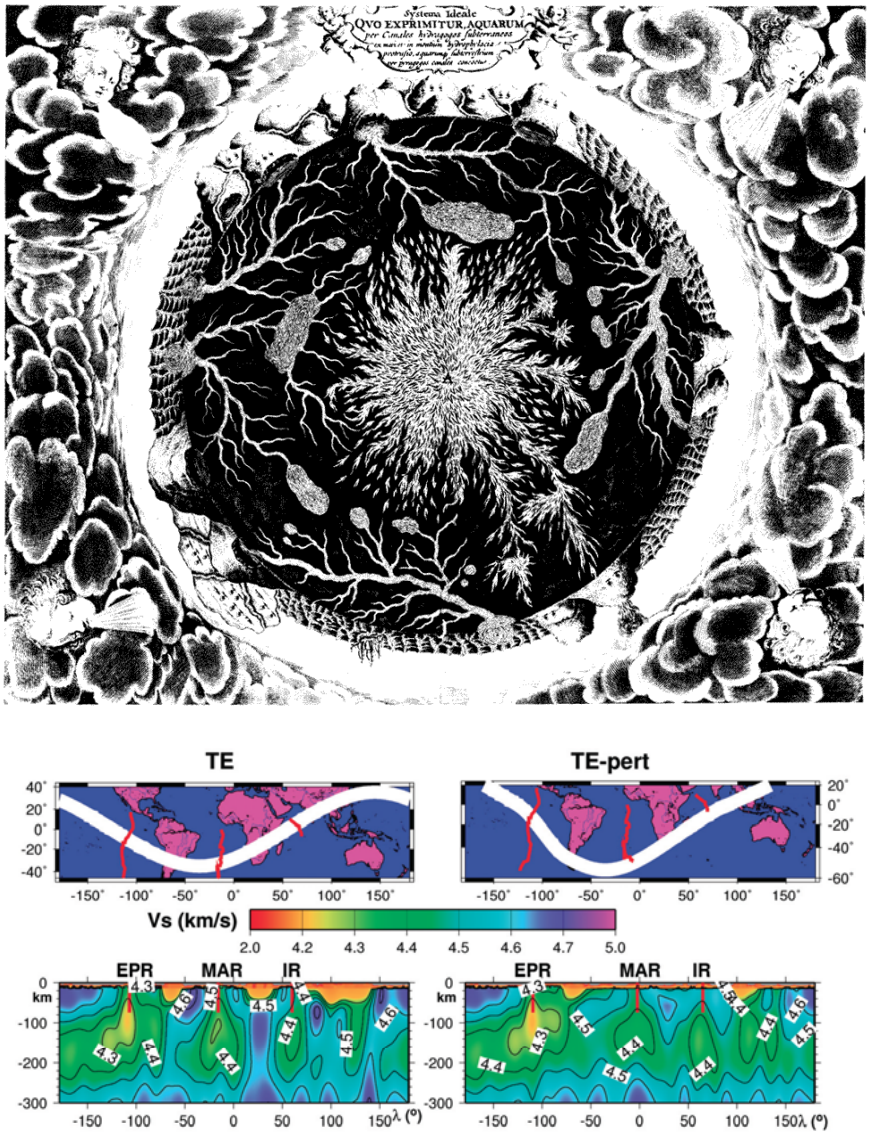

Fig. 53. The representation by Athanasius Kircher of the most advanced thinking of his day about the internal structure of our planet (upper part), and the shear wave velocity sections along the tectonic equator (TE) and a global circuit of partially molten material along the perturbed path (TE-pert), indicating the presence of partially molten material (lower part).

BOX 1: On the efficiency of the slab pull

The negative buoyancy of slabs should determine the pull of plates, but it has been shown that the dip of the subduction zones is not correlated with the age and the thermal state of the down going plates (Cruciani et al., 2005). Moreover relative convergence rates at subduction zones do not correlate with age of oceanic lithosphere at the trench (Fig. 39). One argument used to corroborate the slab pull is the trench length with respect to the plate velocity (Forsyth and Uyeda, 1975). On the basis of a similar observation it could be argued that fast spreading ridges generate fast plate motions. However these relations may be a circular reasoning, e.g., longer subduction zones and faster ridges form when plates move faster (Doglioni et al., 2006b). The relationship between trench length and plate velocity is also questionable for other reasons; for example the absolute plate velocity can be recomputed either in the deep hotspot (Fig. B1, part A) or in the shallow hotspot reference framework (Fig. B1, part B), and the different results do not support a correlation between slab length percentage (length of the trench with respect to the length of the boundary surrounding the plate) and plate velocity.

The relationship between the area of plates (Schettino, 1999) and the angular velocity of plates in the deep hotspot reference framework (HS3-NUVEL1A, Gripp and Gordon, 2002) shows no correlation (Fig. B1, part C), as already observed by Forsyth and Uyeda (1975). However, when plotting the area vs. the absolute angular velocities of plates in the shallow hotspot reference framework, a correlation seems to be present, being bigger plates generally faster (Fig. B1, part D). When comparing similar size of plates, the oceanic or continental plus oceanic, oceanic plates travel faster than purely continental.

Both analyses do not support a significant correlation casting more doubts on the importance of the slab pull, which has a number of further counterarguments. For example, the assumption that the slab is heavier than the country mantle remains debatable, particularly because there are not constraints on the composition of both slab and mantle at variable depth (e.g., the amount of Fe in the lower asthenosphere and the lower upper mantle). Is the slab pull the energetic source for plate motions? Is it large enough? Is it correctly calculated? Are the assumptions reliable? Most of the literature indicates that the slab pull is about $3.3 \cdot 10^{13} N \cdot m^{-1}$ (e.g., Turcotte and Schubert, 2002). This is a force per unit length parallel to the trench. However this value is very small when compared to other energetic sources for the Earth, such the energy dissipated by tidal friction, heat flow emission, and Earth's rotation (e.g., Denis et al., 2002). Moreover the slab pull would be even smaller if chemical and mineralogical stratification are introduced in the

upper mantle. Most of the Earth's volcanism is sourced from above 200 km: the subduction zones release magmatism at about 100 - 150 km of depth (Tatsumi and Eggins, 1995); mid-oceanic ridges are sourced by even shallower asthenosphere melting (100 - 30 km, e.g., Bonatti et al., 2003); hotspots are also debated as potentially very shallow, and sourced by the asthenosphere (Bonatti, 1990; Smith and Lewis, 1999; Doglioni et al., 2005; Foulger et al., 2005). Since even xenoliths in general and kimberlite chimneys originated at depth not deeper than the asthenosphere, there is no direct sampling of the composition of the standard lower part of the upper mantle. Therefore we cannot exclude for example a more Fe-rich fayalitic composition of the olivine, heavier and more compacted than the Mg-rich olivine (forsterite), which is presently assumed as the more abundant mineral of the upper mantle. In case more iron is present in the upper mantle olivine, the density of the ambient mantle would be slightly higher, making the slab pull smaller, if any. The slab pull concept is based on the hypothesis of a homogeneous composition of the upper mantle, with the lithosphere sinking only because it is cooler (e.g., Turcotte and Schubert, 2002). However, the oceanic lithosphere is frozen shallow asthenosphere, previously depleted beneath a mid-oceanic ridge. Depleted asthenosphere is lighter than the "normal" deeper undepleted asthenosphere (see Oxburgh and Parmentier, 1977; Doglioni et al., 2003, 2005 for a discussion). Therefore the assumption that the lithosphere is heavier only because it is cooler might not be entirely true, and the slab pull could be overestimated. Phase transitions within the subducting lithospheric mantle would enhance the slab pull in the transition zone (300 - 400 km of depth) (Stern, 2002; Poli and Schmidt, 2002), but again, the occurrence of higher density country rocks due to chemical and not only phase transitions could make the effect of the slab pull smaller and smaller. Moreover, the occurrence of metastable olivine wedges in fast subducting oceanic lithosphere is considered to create positive density anomalies that should counteract the effects of slab pull (Bina, 1996). A further density anomaly that is suggested to drive slab pull is expected to come from the eclogitization of the subducting oceanic crust. This process involves only a thin layer (5–8 km thick) and not the entire downgoing lithosphere (70–90 km thick). Nevertheless, this type of metamorphic transition is often assumed to be able to determine the slab pull. The eclogites reach densities of about 3440–3460 $kg \cdot m^{-3}$ only at depths of about 100 km (Hacker et al., 2003; Pertermann and Hirschmann, 2003). The density of the country mantle at comparable depths according to the PREM model is 3370 $kg \cdot m^{-3}$ (Anderson, 2007), i.e., only slightly lighter than the eclogitized oceanic crust. Both eclogite and mantle densities are quite speculative. The small density contrast between subducting crust and country mantle casts

doubts on the potential effect of the negative buoyancy of oceanic crust. Therefore we do not have hard constraints on the depth at which the slab pull should turn on and at what depth it should turn off since the mineralogy of the slab and the hosting mantle is still largely unknown. Why then a slab should maintain its shape and coherence down to the 670 km discontinuity? The easiest explanation would be its higher stiffness. Since seismic wave velocity is inversely proportional to density, the high velocity of the slab detected by tomography could be related not to its higher density, but to its higher rigidity. Certainly the slab becomes heavier during sinking for phase transformations, but is it a priori denser, or does it become heavier on the way down? Is it continuously reaching density equilibrium while moving down (Doglioni et al., 2006b)?

Trampert et al. (2004) have recently demonstrated that low velocity volumes of the mantle detected by tomography can be due to lateral variations in composition rather than in temperature, i.e., they can be even higher density areas rather than hotter lighter buoyant material, as so far interpreted. In fact, considering the main low velocity zones in the mantle such as the asthenosphere or the liquid core, their decrease in speed of the P waves is related to their lower rigidity (e.g., Secco, 1995) either generated by CO_2 content in the asthenosphere, or higher density — low viscosity iron alloys in the liquid core. As extreme examples, gold or lead have high density but low seismic velocity. Therefore the interpretation of tomographic images of the mantle where the red (lower velocity) areas are assumed as lighter and hotter rocks can simply be wrong, i.e., they may even be cooler and denser (Van der Hilst, 2004). With the same reasoning, blue (higher velocity) areas, which are assumed as denser and cooler rocks may even be warmer and lighter.

Trampert et al. (2004) also suggest that the low velocity in the lower mantle could for example be due to higher concentrations in iron. Minerals containing more iron are more conductive, and at that depth the coefficient of thermal expansion must be very low. Both factors decrease the Rayleigh number, making the convection very sluggish (e.g., Anderson, 2002). The onion structure of the Earth with shells compositionally homogeneous (e.g., the PREM, see Anderson, 2007) is a misleading oversimplification, since the occurrence of lateral heterogeneities in the whole Earth layers has been widely demonstrated.

The main geometric, kinematic and mechanical counterarguments on the slab pull as the primary mechanism for moving plates and for triggering subduction are listed:

1) The dip of the slab is independent from the age of the oceanic lithosphere (Cruciani et al., 2005). Therefore, the supposed larger negative buoyancy determined by the cooler oceanic lithosphere does not control the slab dip.

2) There are no stringent constraints of the real composition of the upper mantle: there could be more fayalite, making the upper mantle more dense and the slab negative buoyancy smaller.

3) Subduction processes involve also continental lithosphere descending to depths deeper than 100–150 km (Ampferer, 1906; Dal Piaz et al., 1972; Trümpy, 1975; Panza and Mueller, 1978; Ranalli et al., 2000; van Hinsbergen et al., 2005), although subducted average continental crust is most probably buoyant with respect to mantle rocks (Hermann, 2002).

4) The oceanic lithosphere is frozen shallow (30–100 km deep) asthenosphere, previously depleted below ridges. Therefore the oceanic lithosphere is the differentiated lighter upper part of the mantle. Then why should it be a priori heavier than the undepleted deeper (100–300 km) asthenosphere? A pyrolite density of 3400 $kg \cdot m^{-3}$ in the asthenosphere lying beneath the old oceanic lithosphere has been inferred (Jordan, 1988; Kelly et al., 2003). Moreover, hydrothermal activity generates serpentinization of the mantle along the ridge that decreases even more the density.

5) If oceanic lithosphere is heavier than the underlying mantle, why are there no blobs of lithospheric mantle (LID) falling in the upper mantle below the western older side of the Pacific plate?

6) Within a slab, eclogitization is assumed to make the lithosphere denser. However, eclogitization is concentrated in the 6–8 km thick oceanic crust, whereas the remaining 60–80 km thick lithospheric mantle does not undergo the same transformation. Therefore only 1/10 of the slab is apparently increasing density, but the main mass of the slab (90%) does not change significantly.

7) The density increase due to eclogitization is in contrast with the exhumation of the eclogitic prism that is usually detached with respect to the “lighter” lithospheric mantle.

8) Why the lithosphere should start to subduct? This crucial point arises particularly when considering an oceanic hydrated and serpentinized lithosphere that has not yet been metamorphosed by the subduction process, and consequently it is still less dense. In general the lid, once serpentinized, as it very often occurs along ridges and transform faults (e.g. Panza et al., 2007a), is lighter than the asthenospheric mantle, thus how can plates be pulled?

9) Down-dip compression affects most of the slabs, all below 300 km (Isacks and Molnar, 1971), most of them even at shallower depth (e.g., Frepoli et al., 1996), pointing out for a slab forced to sink rather than actively sinking.

10) The 700 km long W-Pacific slab, where only the upper 300 km show some potential down-dip extension seismicity (but it could be

generated also by horizontal shear in the mantle, Giardini and Woodhouse, 1986) should pull and carry the 10,000 km wide Pacific plate, 33 times bigger, winning the shear resistance at the plate base, and the opposing basal drag induced by the relative eastward mantle flow inferred from the hotspots migration (Doglioni et al., 2006b).

11) Kinematically, subduction rollback implies that the volumes left in the hanging wall of the slab have to be replaced by horizontal mantle flow, whether this is a consequence or the cause of the retreat (Doglioni et al., 1999b). However, in order to allow for the slab to move back, the slab retreat needs that also the mantle in the footwall of the slab moves away in the direction of the slab retreat. This is true regardless this motion is generated by the slab pull or it is an independent mantle horizontal flow. But the energy required to push forward the mantle is much greater than the slab pull can afford. Where there is no convergence or rather divergence occurs between upper and lower plates, the slab pull has been postulated as the only possible driving mechanism. However the slab pull has not the energy to push back eastward the whole section of mantle located east of the slab, in order to allow the slab rollback. A relative eastward motion of the mantle would be much more efficient in terms of scale of the process and mass involved, to generate the eastward slab hinge retreat, determining active subduction without plates convergence (e.g., Apennines, Barbados).

12) Are plates surrounded by long slabs and trenches faster? It might be a circular reasoning because long subduction zones might be a consequence of fast movements of plates. Moreover plates are considered fast in the no-net-rotation (NNR) reference framework (Conrad and Lithgow-Bertelloni, 2003). For example, measuring plate motions in the hotspot reference framework, i.e., relative to the mantle, Nazca is very slow relative to mantle, so the relation between plate velocity, slab age and length of a subduction zone is not that simple nor straightforward.

13) Some plates in the hotspot reference framework move without any slab pulling them, e.g., the westward movements of North America, Africa and South America (Gripp and Gordon, 2002). Trench suction has been proposed to explain these movements, but beneath both North and South America the mantle is relatively moving eastward, opposite to the kinematics required by the trench suction model.

14) Plate velocities in the hotspot reference framework seem to be inversely proportional to the viscosity of the asthenosphere rather than to the length of the subduction zones and the age of the downgoing lithosphere. In fact the Pacific, which is the fastest westerly moving plate (Gripp and Gordon, 2002), has the lowest viscosity (Pollitz et al., 1998).

15) The horizontal velocity of plates is 10–100 times faster than the vertical velocity (subduction related uplift or subsidence along

plate boundaries) and this fact suggests that vertical motions are rather passive movements. Moreover, the kinematic analysis (see Fig. 40) shows that subduction rates appear controlled by rather than controlling horizontal plate motions. For example, along E- (or NE-) directed slabs, the subduction is slower than the convergence rate and therefore it cannot be the energetic source to speed up plate motion.

16) The energy for shortening an orogen is probably larger than the one supposed for the slab pull.

17) When describing the plate motions relative to the mantle, e.g. in the hotspots reference framework, along E- (or NE-) directed subduction zones the slab might move out of the mantle, e.g., in the opposite direction of the subduction (upduction). It is sinking because the faster upper plate overrides it.

18) There are rift zones formed between plates not surrounded by oceanic subduction to which the pull for moving the lithosphere can be attributed (e.g., the Red Sea).

19) Although the knowledge of the rheological behavior of subducted lithosphere is very poor, it can be conjectured that the downgoing slab, being progressively heated, could potentially lose strength, diminishing the possibility to mechanically transfer the pull (Mantovani et al., 2002).

20) The folding and unfolding of the lithosphere at the subduction hinge makes the slab even weaker for supporting the slab pull.

21) Slab pull has been calculated to be potentially efficient only at a certain depth (e.g. 180 km, McKenzie, 1977); and at shallower depth how does subduction initiate?

22) At the Earth's surface, oceanic lithosphere has low strength under extension (e.g., $8 \cdot 10^{12}$ N$\cdot$m^{-1}, Liu et al., 2004) and it is able to resist a force smaller than that requested by slab pull ($3.3 \cdot 10^{13}$ N$\cdot$m^{-1}, Turcotte and Schubert, 2002). If the slab pull is the cause for the motion of the Pacific plate, this observation argues for a stretching of the Pacific lithosphere before slab pull being able to move the plate. In other words, the plate cannot sustain the tensional stresses eventually due to slab pull. The low lithospheric strength problem could be, however, partly counterbalanced by the mantle flow and viscous tractions acting on the plates induced by slab sinking (e.g., Lithgow-Bertelloni and Richards, 1998). Due to low temperature and high pressure, the strength of the subducted oceanic lithosphere rises to some $2 \cdot 10^{13}$-$6 \cdot 10^{13}$N$\cdot$m^{-1} (Wong A Ton and Wortel, 1997) and would make sustainable the eventual pull induced by density anomalies related to phase changes at depth. In summary the subducted slab is probably able to sustain the load induced by slab pull but probably this load cannot be transmitted to the unsubducted portion of the plate without breaking it apart.

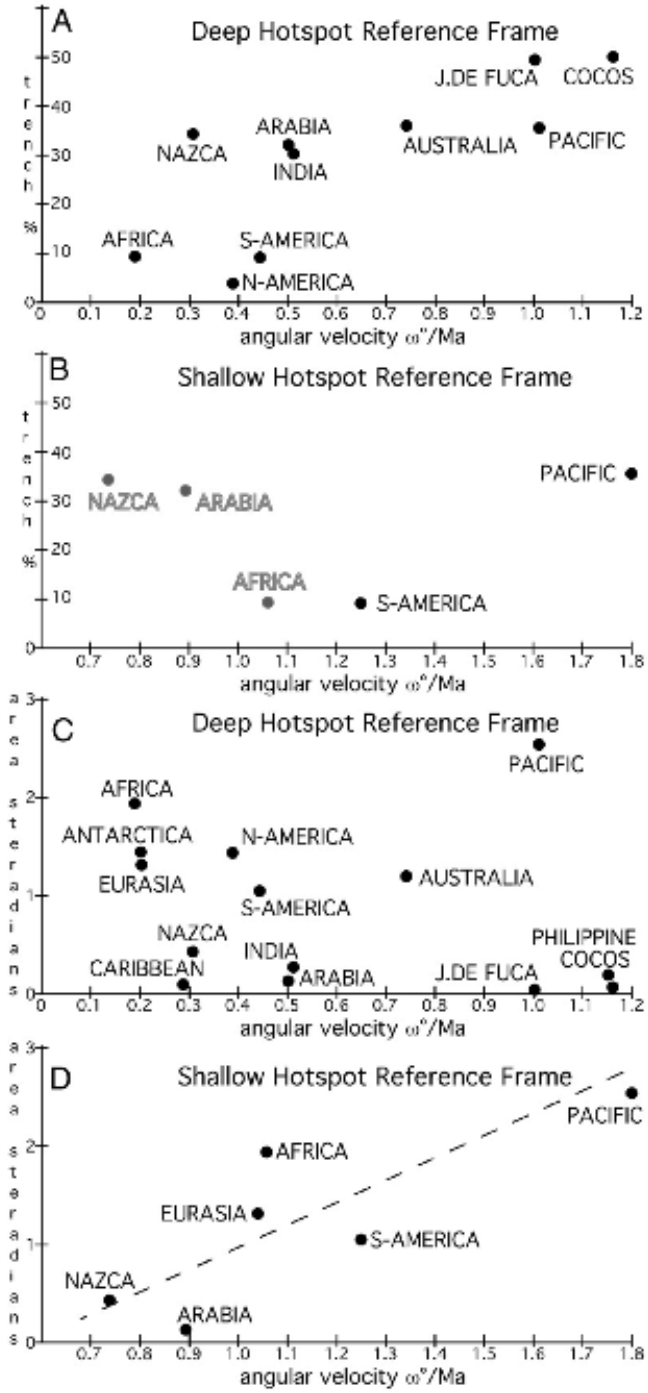

Fig. B1. A) Relationship between absolute plate motions angular velocity vs. trench percent in the deep hotspot reference framework. There is not evident correlation between the two values. For example, the Nazca and Pacific plates have about the same percentage of trench length with respect to the plate circumference, but the Pacific is much faster. Angular velocities after Gripp and Gordon (2002). B) Relationship between absolute plate motions angular velocity vs. trench percent in the shallow hotspot reference framework. The absence of correlation between the two values is even more evident, but the gray points on the left show a negative motion of the plates, i.e., away from the trench. Therefore, in this reference framework, plates cannot be moved by the slab pull. Angular velocities after Crespi et al. (2007). C) Plot of plate areas and absolute angular velocities in the deep hotspot reference framework. Areas of plates after Schettino (1999). As already shown by Forsyth and Uyeda (1975), no relation is observable. D) Plot of plate areas and absolute angular velocities in the shallow hotspot reference framework. Angular velocities after Crespi et al. (2007). Unlike the previous figure, a correlation seems to exist, i.e., larger plates move faster, even if oceanic plates still move relatively faster than continental plates for comparable areas.

This long list of geometric, kinematic and mechanical arguments against the relevant role of slab pull for moving plates and for triggering subduction casts doubts on the possibility that the slab pull can actually trigger subduction, slab rollback, and drive plate motions.

Density anomalies due to phase changes occurring at depth within the slab could enhance the sinking of the slab. However, the slab pull alone, even if efficient at some depths, it is unable to explain the initiation of the subduction, and the mechanism perpetuating plate motions in general. The slab detachment model is conceived as a consequence of the negative buoyancy of the slab and it has been invoked many times to explain the supposed rupture of the slab in tomographic images (e.g., Wortel and Spakman, 2000) and to fit the geochemistry of magmatism (e.g., Lustrino, 2005). However, tomographic images are based on velocity models that often overestimate the velocity of the asthenosphere where usually the detachment is modeled (e.g. see Fig. 45). Therefore the detachment disappears when using slower velocity for the asthenosphere in the reference velocity model or when considering regional tomographic images (e.g., Piromallo and Morelli, 2003). Recently, Rychert et al. (2005) have shown how the base of the lithosphere — top of the asthenosphere (LVZ, e.g., Panza, 1980) is characterized by unexpected, few km thick, extremely low velocities beneath northwestern North America, far from subduction zones. This implies a revision, particularly in areas characterized by strong lateral variations in composition of the subducting lithosphere (e.g., continental vs. oceanic) where the use of 1D reference velocity model is meaningless, of the velocity models resulting from mantle tomography. The revision should also consider the limitations of the theoretical framework employed in tomography; ray theory does not handle diffraction and frequency dependence, whereas normal mode perturbation theory requires weak and smooth lateral variations of structure (Waldhauser et al., 2002; Romanowicz, 2003; Anderson, 2007a,b; Panza et al., 2007b; Boschi et al., 2007; Boyadzhiev et al., 2008).

Additional references box specific

Ampferer, O., 1906. Uber das Bewegungbild von Faltengebirge, Austria. Geol. Bundesanst. Jahrb. 56, 539–622.

Anderson, D.L., 2002. The case for irreversible chemical stratification of the mantle. Int. Geol. Rev. 44, 97–116.

Anderson, D.L., 2007. New Theory of the Earth.Cambridge Univ. Press, 405pp, ISBN 0-521-84959-4 (hardback).

Bina, C.R., 1996. Phase transition buoyancy contributions to stresses in subducting lithosphere. Geophys. Res Lett., 23, 3563–3566.

Bonatti, E., Ligi, M., Brunelli, D., Cipriani, A., Fabretti, P., Ferrante, V., Ottolini, L., 2003. Mantle thermal pulses below the Mid Atlantic Ridge and temporal variations in the oceanic lithosphere. Nature, 423, 499–505.

Dal Piaz, G.V., Hunziker, J.C., Martinotti, G., 1972. La Zona Sesia-Lanzo e l'evoluzione tettonico-metamorfica delle Alpi nordoccidentali interne. Mem. Soc. Geol. Ital., 11, 433–466.

Foulger, G.R., Natland, J.H., Presnall, D.C., Anderson, D.L., 2005. Plates, plumes, and paradigms. Geol. Soc. Am., Spec. Pap. 388.

Giardini, D., Woodhouse, J.H., 1986. Horizontal shear flow in the mantle beneath the Tonga arc. Nature, 319, 551–555.

Hacker, B.R., Abers, G.A., Peacock, S.M., 2003. Subduction factory 1: theoretical mineralogy, densities, seismic wave speeds and H_2O contents. J. Geophys. Res. 108 (B1), 2029, doi:10.1029/2001JB001127

Hermann, J., 2002. Experimental constraints on phase relations in subducted continental crust. Contrib. Mineral. Petrol. 143, 219–235.

Jordan, T.H., 1988. Structure and formation of the continental tectosphere. J. Petrol. (Special Lithosphere Issue), 11–37.

Kelly, R.K., Kelemen, P.B., Jull, M., 2003. Buoyancy of the continental upper mantle. Geochem. Geophys. Geosyst., 4, 1017, doi:10.1029/2002GC000399.

Lustrino, M., 2005. How the delamination and detachment of lower crust can influence basaltic magmatism. Earth-Sci. Rev. 72, 21–38.

Mantovani, E., Viti, M., Albarello, D., Babbucci, D., Tamburelli, C., Cenni, N., 2002. Generation of backarc basins in the Mediterranean region: driving mechanisms and quantitative modelling. Boll. Soc. Geol. Ital., Vol. Spec. 1, 99–111.

McKenzie, D.P., 1977. The initiation of trenches: a finite amplitude instability. In: Talwani, M. and Pitman III, (Eds.), Island Arcs, Deep Sea Trenches and Back-Arc Basins. Maurice Ewing Ser., vol. 1, 57–61,

Am. Geophys. Un., Washington, D.C.

Oxburgh, E.R., Parmentier, E.M., 1977. Compositional and density stratification in oceanic lithosphere; causes and consequences. J. Geol. Soc. (Lond.), 133 , 343–355.

Pertermann, M., Hirschmann, M.M., 2003. Anhydrous partial melting experiments on MORB-like eclogite: phase relations, phase compositions and mineral-melt partitioning of major elements at 2–3 Gpa. J. Petrol., 44, 2173–2201

Poli, S., Schmidt, M.W., 2002. Petrology of subducted slabs. Annu. Rev. Eart Planet. Sci., 20, 207–235.

Ranalli, G., Pellegrini, R., D'Offizi, S., 2000. Time dependence of negative buoyancy and the subduction of continental lithosphere. J. Geodyn., 30, 539–555.

Schettino, A., 1999. Computational methods for calculating geometrical parameters of tectonic plates. Comput. Geosci., 25, 897–9907.

Secco, R.A., 1995. Viscosity of the outer core. Mineral Physics and Crystallography. A Handbook of Physical Constants. AGU Reference Shelf, vol. 2, 218–226.

Trampert, J., Deschamps, F., Resovsky, J., Yuen, D., 2004. Probabilistic tomography maps chemical heterogeneities throughout the lower mantle. Science, 306, 853–856.

Trümpy, R., 1975. On crustal subduction in the Alps. In: Mahel, M. (Ed.), Tectonic Problems in the Alpine system, Bratislava. Slovak Academy of Sciences, pp. 121–130.

Tatsumi, Y., Eggins, S., 1995. Subduction zone magmatism. Frontiers in Earth Sciences. Blackwell Science, 211 pp.

Van der Hilst, R., 2004. Changing views on Earth's deep mantle. Science, 306, 817–818.

van Hinsbergen, D.J., Hafkenscheid, E., Spakman,W.,Meulenkamp, J.E., Wortel, R., 2005. Nappe stacking resulting fromsubduction of oceanic and continental lithosphere below Greece. Geology, 33, 325–328.

BOX 2: Mantle convection

It is obvious that convection occurs in the mantle, not only from modeling, but also from the kinematics of plate boundaries, where mantle upraises along ridges and lithosphere sinks along subduction zones. It is also evident that oceanic lithosphere circulates in the mantle much more easily than the continental lithosphere, since only relatively young (180–0 Ma) oceans cover the Earth's surface, comparing to the much older cratons (>3000Ma), being the thick continental lithosphere buoyant over the mantle. Convection is required to cool the Earth. But convection models are necessarily oversimplified and possibly overrated. The mantle is considered compositionally quite homogeneous, but it is not, and has both vertical and lateral significant heterogeneities. The whole Earth is intensely stratified both in physical and chemical properties from the topmost atmosphere down to the core. The supposed convection cells should be made of an uprising warmer buoyant mantle, laterally accompanied by downwelling cooler currents. In the view of convection modelers, the surface expression of cells should be the plates. But the Atlantic, E-Africa and Indian rifts have no intervening subductions; there are also several cases of paired subduction zones without rifts in between: this shows the inapplicability of the convection cells to the simple superficial plate tectonics kinematics.

In most of the convection models, uprising and down welling mantle currents are stationary, but it is well known that all plate margins rather migrate. Convection styles frequently generate polygonal shapes for the cells, but plate margins can be very linear e.g., the Atlantic ridge, in contrast with the typical mushroom shape of mantle plumes. The fastest W-ward moving plate relative to the mantle (the Pacific plate) has the lowest asthenosphere viscosity value (Pollitz et al., 1998), and it is the most decoupled plate, while mantle convection requires that faster moving plates are more coupled (higher viscosity) with the mantle than slower ones. The Hawaii hotspot volcanic chain indicates that the underlying mantle is moving E–SE-ward. Beneath the East Pacific Rise, an eastward migrating mantle has been modeled by Doglioni et al. (2003) and Hammond and Toomey (2003). An eastward migrating mantle has been suggested also beneath the Nazca plate by Russo and Silver (1994) through shear wave splitting analysis. An eastward relative mantle flow beneath the South America plate is required by the hotspot reference framework (Van Hunen et al., 2002). A relatively moving eastward mantle flow has been proposed also beneath North America (Silver and Holt, 2002) and beneath the Caribbean plate (Negredo et al., 2004). Beneath the Tyrrhenian Sea a similar west to east flow of the mantle can be inferred from mantle anisotropy (Margheriti et al., 2003) and geometry (Panza et al., 2007b). A global reconstruction of the anisotropy

in the asthenosphere (Debayle et al., 2005) fits quite well the sinusoidal flow of plate motions (e.g., Doglioni et al., 1999a), apart along subduction zones where the shear wave splitting anisotropy shows orthogonal trend compatible with the re-orientation of a flow encroaching an obstacle.

Additional references box specific

Hammond, W.C., Toomey, D.R., 2003. Seismic velocity anisotropy and heterogeneity beneath the Mantle Electromagnetic and Tomography Experiment (MELT) region of the East Pacific Rise from analysis of P and S body waves. J. Geophys. Res., 108, 2176, doi:10.1029/2002JB001789.

Margheriti, L., Lucente, F.P., Pondrelli, S., 2003. SKS splitting measurements in the Apenninic–Tyrrhenian domain (Italy) and their relation with lithospheric subduction and mantle convection. J. Geophys. Res., 108, 2218, doi:10.1029/2002JB001793.

Negredo, A.M., Jiménez-Munt, I., Villasenor, A., 2004. Evidence for eastward mantle flow beneath the Caribbean plate from neotectonic modeling. Geophys. Res. Lett., 31, L06615, doi:10.1029/2003GL019315.

Van Hunen, J., van den Berg, A.P., Vlaar, N.J., 2002. The impact of the South-American plate motion and the Nazca Ridge subduction on the flat subduction below South Peru. Geophys. Res. Lett., 29, 14 (10.1029/2001GL014004).

Abers, G.A., 2005. Seismic low-velocity layer at the top of subducting slabs beneath volcanic arcs: observations, predictions, and systematics. Phys. Earth Planet. Int., 149, 7–29, doi:10.1016/j.pepi.2004.10.002.

Abers, G.A., van Keken, P.E., Kneller, E.A., Ferris, A. and Stachnik, J.C., 2006. The thermal structure of subduction zones constrained by seismic imaging: implications for slab dehydration and wedge flow. Earth Planet. Sci. Lett., 241, 387–397.

Altamimi, Z., Sillard, P. and Boucher, C., 2002. ITRF2000: A new release of the international terrestrial reference frame for earth sciences applications. J. Geophys. Res., 107 (B10), 2214, doi: 10.1029/2001JB000561.

Ammon, C.J., Kanamori, H. and Lay, T., 2008. A great earthquake doublet and seismic stress transfer cycle in the central Kuril islands. Nature, 451, 7178, 561-565, doi:10.1038/nature06521

Anderson, D. L., 1999. A theory of the Earth: Hutton and Humpty-Dumpty and Holmes, In: Craig, G. Y. and Hull, J. H. (Eds.), James Hutton: Present and Future, Geol. Soc. Spec. Publ., 150, 13 – 35.

Anderson, D.L., 2000. Thermal state of the upper mantle; no role for mantle plumes. Geophys. Res. Lett., 27, 3623–3626, doi: 10.1029/2000GL011533.

Anderson, D.L., 2001. Topside tectonics. Science, 293, 2016–2018.

Anderson, D. L., 2007a. The New Theory of the Earth. Cambridge University Press, 384 pp.

Anderson, D. L., 2007b. Slabs on command - Is there convincing tomographic evidence for whole mantle convection? http://www.mantleplumes.org/TomographyProblems.html

Aoudia, A., Ismail-Zadeh, A.T. and Romanelli, F., 2007. Buoyancy-driven deformation and contemporary tectonic stress in the lithosphere beneath Central Italy. Terra Nova, 19, 490–495.

Argus, D.F. and Gross, R.S., 2004. An estimate of motion between the spin axis and the hotspots over the past century. Geophys. Res. Lett., 31 (6), L006614, doi: 10.1029/2004GL019657.

Artemieva, I.M. and Mooney, W.D., 2001. Thermal structure and evolution of Precambrian lithosphere: a global study. J. Geophys. Res., 106, 16,387–16,414.

Asimow, P.D. and Langmuir, C.H., 2003. The importance of water to oceanic mantle melting regimes. Nature, 421, 815–820, doi: 10.1038/nature01429.

Baranzangi, M. and Isacks, B.L., 1979. Subduction of the Nazca plate beneath Peru: evidence from spatial distribution of earthquakes. Geophys. J.R. Astron. Soc. 57, 537–555.

Barklage, M., Wiens, D.A., Nyblad, A. and Anandakrishnan, S., 2009. Upper mantle seismic anisotropy of South Victoria Land and the Ross Sea coast, Antarctica from SKS and SKKS splitting analysis. Geophys. J. Int., 178, 729-741, doi: 10.1111/j.1365-246X.2009.04158.x

Bercovici, D., 1998. Generation of plate tectonics from lithospheremantle flow and void-volatile self-lubrication. Earth Planet. Sci. Lett., 154, 139–151.

Bevis, M., 1988. Seismic slip and down-dip strain rates inWadati–Benioff Zones. Science, 240, 1317–1319.

Biagi, L., Pierantonio, G. and Riguzzi, F., 2006. Tidal errors and deformations in regional GPS networks. In: Sansò, F. and Gil, A.J. (Eds.), Geodetic Deformation Monitoring: From Geophysical to Engineering Roles. IAG symp.,131, 73-82, Berlin, Springer, ISBN/ISSN: 0939-9585.

Billen, M.I. and Gurnis, M., 2001. A low viscosity wedge in subduction zones. Earth Planet. Sci. Lett., 193, 227–236.

Billen, M.I., Gurnis, M. and Simons, M., 2003. Multiscale dynamic models of the Tonga–Kermadec subduction zone. Geophys. J. Int., 153, 359–388.

Billen, M.I. and Hirth, G., 2007. Rheologic controls on slab dynamics. Geochem. Geophys. Geosyst., 8, Q08012, doi:10.1029/2007GC001597.

Boccaletti, D. and Pucacco, G., 2002, Theory of orbits: Perturbative and geometrical methods, Volume 2 , 278–286, Berlin, Springer Verlag.

Bohannon, R.G., Naeser, C.W., Schmidt, D.L. and Zimmermann, R. A.,

1989. The timing of uplift, volcanism and rifting peripheral to the Red Sea: A case for Passive Rifting?. J. Geophys. Res., 94 (B2), 10, 1683-1701.

Bokelmann, G.H.R., 2002. Which forces drive North America? Geology, 30, 1027–1030, doi:10.1130/0091-7613.

Bonatti, E., 1990. Not so hot "hot spots" in the Oceanic mantle. Science, 250, 107–111.

Boschi, L., Ampueroa, J.-P., Peter, D., Maia, P.M., Soldati, G. and Giardini, D., 2007. Petascale computing and resolution in global seismic tomography, Phys. Earth Planet. Int., 163, 245–250.

Bostrom, C., 1971. Westward dosplacement of the lithosphere. Nature, 234, 536-538.

Boyadzhiev, G., Brandmayr, E., Pinat, T. and Panza, G.F., 2008. Optimization for non-linear inverse problems. Rendiconti Lincei, 19, 17-43.

Brandmayr, E., Raykova, R., Zuri, M., Romanelli, F., Doglioni, C., and Panza, G., 2010. The lithosphere in Italy: structure and seismicity. In: Beltrando, M., Peccerillo, A., Mattei, M., Conticelli, S. and Doglioni, C. (Eds.), Journal of the Virtual Explorer, volume 36, paper 1, doi: 10.3809/jvirtex.2009.00224

Bruni, S., D'Orazio, M., Haller, J.M., Innocenti, F., Manetti, P., Pécskay, Z. and Tonarini, S., 2008. Time-evolution of magma sources in a continental back-arc setting: the Cenozoic basalts from Sierra de san Bernardo (Patagonia, Chubut, Argentina). Geological Magazine, 145, 714–732. doi:10.1071/S0016756808004949.

Cahill, T., Isacks, B.L., 1992. Seismicity and shape of the subducted Nazca plate. J. Geophys. Res., 97, 17,503–17,529, doi:10.1029/92JB00493

Caputo, M., Panza, G.F. and Postpischl, D., 1970. Deep structure of the Mediterranean basin. J. Geophys. Res., 75, 4919-4923.

Caputo, M., Panza, G.F. and Postpischl, D., 1972. New evidences about the deep structure of the Lipari Arc. Tectonophysics, 15, 219-231.

Carlson, R.L., Hilde, T.W.C. and Uyeda, S., 1983. The driving

mechanism of plate tectonics: relation to age of the lithosphere at trenches. Geophys. Res. Lett., 10, 297–300.

Castle, J.C. and Creager, K.C., 1998. NW Pacific slab rheology, the seismicity cutoff, and the olivine to spinel phase change. Earth Planets Space, 50, 977–985.

Cathles, L.M., 1975. The viscosity of the Earth's mantle. Princeton University Press, 386 pp.

Cernobori, L., Hirn, A., McBride, J.H., Nicolich, R., Petronio, L., Romanelli, M., and STREAMERS/PROFILES Working Groups, 1996, Crustal image of the Ionian basin and its Calabrian margin, Tectonophysics, 264,175-189.

Chen, P.-F., Bina, C.R. and Okal, E.A., 2001. Variations in slab dip along the subducting Nazca Plate, as related to stress patterns and moment release of intermediate-depth seismicity and to surface volcanism. Geochem. Geophys. Geosyst., 2, doi:10.1029/2001GC000153.

Chiarabba, C., De Gori, P. and Speranza, F., 2008. The southern Tyrrhenian subduction zone: deep geometry, magmatism and Plio-Pleistocene evolution. Earth Planet. Sci. Lett., 268, 408–423.

Christova, C. and Nikolova, S.B., 1993. The Aegean region: deep structures and seismological properties. Geophys. J. Int., 115, 635–653.

Conder, J.A. and Wiens, D.A., 2006. Seismic structure beneath the Tonga arc and Lau backarc basin determined from joint Vp, Vp/Vs tomography. Geochem. Geophys. Geosyst., 7, Q03018.

Conrad, C.P. and Lithgow-Bertelloni, C., 2003. How mantle slabs drive plate tectonics. Science, 298, 207–209.

Craig C.H. and McKenzie D. 1986. The existence of a thin low-viscosity layer beneath the lithosphere. Earth Planet. Sci. Lett., 78, 420-426, doi:10.1016/0012-821X(86)90008-7.

Crespi, M., Cuffaro, M., Doglioni, C., Giannone, F. and Riguzzi, F., 2007. Space geodesy validation of the global lithospheric flow, Geophys. J. Int., 168, 491–506, doi: 10.1111/j.1365-246X.2006.03226.x

Cross, T.A. and Pilger, R.H., 1982. Controls of subduction geometry,

location of magmatic arcs, and tectonics of arc and back-arc regions, Geol. Soc. Amer. Bull., 93, 545–562.

Cruciani, C., Carminati, E. and Doglioni, C., 2005. Slab dip vs. lithosphere age: No direct function. Earth and Planet. Sci. Lett., 238, 298– 310.

Cuffaro, M., Carminati, E. and Doglioni, C., 2006. Horizontal versus vertical plate motions. Earth Discuss., 1, 1–18.

Cuffaro, M., and Doglioni, C., 2007. Global kinematics in deep versus shallow hotspot reference frames, In: Foulger, G.R., and Jurdy, D.M. (Eds.), Plates, plumes, and planetary processes: Geological Society of America Special Paper 430, 359–374, doi: 10.1130/2007.2430(18).

Das, S., 2004. Seismicity gaps and the shape of the seismic zone in the Band Sea region from relocated hypocenters. J. Geophys. Res., 109, B12303, doi:10.1029/2004JB003192.

Debayle, E., Kennett, B., and Priestley, K., 2005. Global azimuthal seismic anisotropy and the unique plate-motion deformation of Australia. Nature, 433, 509–512, doi: 10.1038/nature03247.

DeMets, C., Gordon, R.G., Argus, D.F., and Stein, S., 1990. Current plate motions. Geophys. J. Int., 101, 425–478.

DeMets, C., Gordon, R.G., Argus, D.F. and Stein, S., 1994. Effect of recent revisions to the geomagnetic reversal time scale on estimates of current plate motions. Geophys. Res. Lett., 21, 2191–2194, doi: 10.1029/ 94GL02118.

Denis, C., Schreider, A.A., Varga, P. and Zavoti, J., 2002. Despinning of the Earth rotation in the geological past and geomagnetic paleointensities. Journal of Geodynamics, 34, 667–685, doi: 10.1016/S0264-3707(02)00049-2.

de Voogd, B., Truffert, C., Chamot-Rooke, N., Huchon, P., Lallemant, S. and Le Pichon, X., 1992. Two-ship deep seismic soundings in the basins of the eastern Mediterranean sea (Pasiphae cruise). Geophys. J. Int., 109, 536–552.

Dickinson, W.R., 1978. Plate tectonic evolution of North Pacific rim. J. Phys. Earth, 26, 51–519 (Suppl.).

Doglioni, C., 1990. The global tectonic pattern, J. Geodyn., 12, 21-38.

Doglioni, C., 1992. Main differences between thrust belts, Terra Nova, 4, 152-164.

Doglioni, C., 1993a. Geological evidence for a global tectonic Polarity, Journal of the Geological Society of London, 150, 991–1002.

Doglioni, C., 1993b. Some remarks on the origin of foredeeps, Tectonophysics, 228, 1-20.

Doglioni, C., 1994. Foredeeps versus subduction zones. Geology, 22, 271–274.

Doglioni, C., 1995. Geological remarks on the relationships between extension and convergent geodynamic settings. Tectonophysics, 252, 253–268.

Doglioni, C., Carminati, E. and Bonatti, E., 2003. Rift asymmetry and continental uplift. Tectonics, 22, 1024-1037, doi:10.1029/2002TC001459

Doglioni, C., Carminati, E., and Cuffaro, M., 2006a. Simple kinematics of subduction zones: International Geological Review, 48, 479–493.

Doglioni, C., Cuffaro, M., and Carminati, E., 2006b. What moves slabs? Bollettino Geofisica Teorica e Applicata, 47, 224–247.

Doglioni, C., Carminati, E., Cuffaro, M. and Scrocca, D., 2007. Subduction kinematics and dynamic constraints. Earth-Science Reviews, 83, 125–175.

Doglioni, C., Green, D.H. and Mongelli, F., 2005. On the shallow origin of hotspots and the westward drift of the lithosphere. In: Foulger, G.R., Natland, J.H., Presnall, D.C., and Anderson, D.L. (Eds.), Plates, plumes, and paradigms: Geological Society of America Special Paper 388, 735–749, doi: 10.1130/2005.2388(42).

Doglioni, C., Gueguen, E. Harabaglia, P. and Mongelli, F., 1999a. On the origin of W-directed subduction zones and applications to the western Mediterranean. In: Durand, B. et al. (Eds.), The Mediterranean Basins: Tertiary Extensions Within the Alpine Orogen, Geol. Soc. Spec. Publ., 156, 541 – 561.

Doglioni, C., Harabaglia, P., Merlini, S., Mongelli, F., Peccerillo, A. and Piromallo, C., 1999b. Orogens and slabs vs their direction of subduction. Earth-Science Reviews, 45, 167–208.

Doglioni, C., Tonarini, S. and Innocenti, F., 2009. Mantle wedge asymmetries and geochemical signatures along W- and E–NE-directed subduction zones. Lithos, 113, 179–189.

Drewes, H., and Meisel, B., 2003. An actual plate motion and deformation model as a kinematic terrestrial reference system. Geotechnologien Science Report, 3, 40–43.

Egbert, G.D. and Ray, R.D., 2000. Significant dissipation of tidal energy in the deep ocean inferred from satellite altimeter data. Nature, 405, 775–778.

Elsasser, W. M., 1969. Convection and stress propagation in the upper mantle. In: Runcorn, S. K. (Ed.), The Application of Modern Physics to the Earth and Planetary Interiors, 223-246, John Wiley & Sons, New York.

Engdahl, E.R., van der Hilst, R.D., Buland, R., 1998. Global teleseismic earthquake relocation with improved travel times and procedures for depth determination. Bull. Seismol. Soc. Am., 88, 722–743.

Engdahl, E.R. and Villaseñor, A., 2002. Global Seismicity: 1900–1999. In: Lee, W.H.K., Kanamori, H., Jennings, P.C., Kisslinger, C. (Eds.), International Handbook of Earthquake and Engineering Seismology, 41, 665–690, Academic Press.

Espurt, N., Funiciello, F., Martinod, J., Guillaume, B., Regard, V., Faccenna and C., Brusset, S., 2008. Flat subduction dynamics and deformation of the South American plate: insights from analog modeling. Tectonics 27, TC3011, doi:10.1029/2007TC002175.

Faccenna, C. and Becker, T.W., 2010. Shaping mobile belts by small-scale convection. Nature, 465, 602-605, doi:10.1038/nature09064.

Fischer, K.M., Fouch, M.J., Wiens, D.A. and Boettcher, M.S., 1998. Anisotropy and Flow in Pacific Subduction Zone Back-arcs. Pure appl. geophys., 151, 463–475.

Forsyth, D. and Uyeda, S., 1975. On the relative importance of driving forces of plate motion. Geophys. J. R. Astron. Soc., 43, 163-200.

Forte, A. A. and Peltier, W. R., 1987. Plate tectonics and aspherical Earth strucuture: the importance of poloidal-Toroidal coupling. J. Geophys. Res., 92 (B5), 3654-3679.

Fowler, C.M.R., 1990. The Solid Earth. Cambridge Univ. Press, 472 pp.

Frepoli, A., Selvaggi, G., Chiarabba, C., Amato, A., 1996. State of stress in the Southern Tyrrhenian subduction zone from fault-plane solutions. Geophys. J. Int., 125, 879–891.

Frezzotti, M.L., Peccerillo, A. and Panza, G.F., 2009. Carbonate metasomatism and CO2 lithosphere-asthenosphere degassing beneath the Western Mediterranean: An integrated model arising from petrological and geophysical data. Chemical Geology, 262, 108-120.

Garfunkel, Z., Anderson, C.A. and Schubert, G., 1986. Mantle circulation and the lateral migration of subducted slabs. J. Geophys. Res. 91 (B7), 7205–7223.

Garzanti, E., Vezzoli, G. and Andò, S., 2002. Modern sand from obducted ophiolite belts (Sultanate of Oman and United Arab Emirates). J. Geol., 110, 371–391.

Gonzales, O., Alvarez, L., Moreno, B. and Panza, G.F., 2011. S-waves's velocities of the lithopshere-asthenosphere system in the Caribean region. ICTP preprint IC/2010/032, available at: http://publications.ictp.it, submitted to Pure Appl. Geophys.

Gordon R. G. and Jurdy, D.M., 1986. Cenozoic Global Plate Motion. J. Geophys. Res., 91(B12), 12,389-12,406.

Green, D.H., 2003. "Hot-spots" and other intraplate settings: Constraints on mantle potential temperatures. http://www.mantleplumes.org/.

Gripp, A.E. and Gordon, R.G., 2002. Young tracks of hotspots and current plate velocities. Geophys. J. Int., 150, 321–361.

Grove, T.L., Chatterjee, N., Parman, S.W. and Médard, E., 2006. The influence of H_2O on mantle wedge melting. Earth Planet. Sci. Lett., 249, 74–89, doi:10.1016/j.epsl.2006.06.043

Gudmundsson, O. and Sambridge, M., 1998. A regionalized upper mantle (RUM) seismic model. J. Geophys. Res. 103 (B4), 7121–7136.

Gutscher, M.-A., Malavieille, J., Lallemand, S. and Collot, J.Y., 1999. Tectonic segmentation of the North Andean margin: impact of the Carnegie Ridge collision. Earth Planet. Sci. Lett., 168, 255–270, doi:10.1016/S0012-821X(99)00060-6.

Gutscher, M.-A., Malod, J., Rehault, J.-P., Contrucci, I., Klinghoefer, F., Mendes-Victor L. and Spakman, W., 2002. Evidence for active subduction beneath Gibraltar. Geology, 30, 1071–1074.

Hager, B.H. and O'Connell, R.J., 1978. Subduction zone dip angles and flow driven by plate motion. Tectonophysics, 50, 111– 133.

Harabaglia, P. and Doglioni, C., 1998. Topography and gravity across subduction zones. Geophys. Res. Lett., 25, 703–706.

Harpp, K. S., Wirth, K. R. and Korich, D. J., 2002. Northern Galapagos Province: Hotspot-induced, near ridge volcanism at Genovesa Island. Geology, 30, 399 –402.

Heflin, M., et al., 2007, GPS time series, global velocities, http://sideshow.jpl.nasa.gov/mbh/series.html.

Heit, B. 2005. Teleseismic tomographic images of the Central Andes at 21°S and 25.5°S. FU Berlin, Digitale Dissertation, http://www.diss.fu-berlin.de/2005/319/.

Herak, M., Panza, G.F. and Costa, G., (2001). Theoretical and observed depth correction for Ms. Pure appl. geophys., 158, 1517-1530.

Hirth, G. and Kohlstedt, D.L., 1996. Water in the oceanic upper mantle: implications for rheology, melt extraction and the evolution of the lithosphere. Earth planet. Sci. Lett., 144, 93–108.

Hirth, G. and Kohlstedt, D., 2003. Rheology of the upper mantle and the mantle wedge: a view from the experimentalists. In: Eiler, J. (Ed.), Inside the Subduction Factory, Geophys. Monogr. Ser., 138, 83–105, AGU, Washington, D.C.

Holtzman, B.K., Groebner, N.J., Zimmerman, M.E., Ginsberg, S.B. and

Kohlstedt, D.L., 2003. Stress-driven melt segregation in partially molten rocks. G3, 4, 8607, doi:10.1029/2001GC000258.

Isacks, B.L. and Barazangi, M., 1977. Geometry of Benioff zones: lateral segmentation and downward bending of the subducted lithosphere. In: Talwani, M., Pitman, W.M. III (Eds.), Island Arcs, Deep Sea Trenches and Back-arc Basins. Maurice Ewing Series 1, 99–114, AGU, Washington, D. C.

Isacks, B. and Molnar, P., 1971. Distribution of stresses in the descending lithosphere from a global survey of focal-mechanism solutions of mantle earthquakes. Rev. Geophys., 9, 103– 174.

Ismail-Zadeh, A., Aoudia, A. and Panza, G.F., 2010. Three-dimensional numerical modeling of contemporary mantle flow and tectonic stress beneath the Central Mediterranean. Tectonophysics, 482, 226-236.

Ismail-Zadeh, A. and Tackley, P., 2010. Computational Methods for Geodynamics. Cambridge: Cambridge University Press, 336 pp.

Jarrard, R.D., 1986. Relations among subduction parameters. Rev. Geophys., 24, 217–284.

Jeffreys, H., 1976. The Earth, Sixth Edition. Cambridge, Cambridge University Press, 574 pp.

Jin, Z.-M., Green, H.G. and Zhou, Y., 1994. Melt topology in partially molten mantle peridotite during ductile deformation. Nature, 372, 164-167.

Jordan, T.H., 1974. Some comments on tidal drag as a mechanism for driving plate motions. J. Geophys. Res., 79 (14), 2141–2142.

Jurdy, D.M., 1990. Reference frames for plate tectonics and uncertainties: Tectonophysics, 182, 373–382, doi: 10.1016/0040-1951(90)90173-6.

Jurdy, D.M. and Stefanik, M., 1988. Plate-Driving forces over the Cenozoic Era. J. Geophys. Res., 93 (B10), 11,833-11,844.

Karato, S., Jung, H., Katayama, I. and Skemer P., 2008. Geodynamic Significance of Seismic Anisotropy of the Upper Mantle: New Insights from Laboratory Studies. Annu. Rev. Earth Planet. Sci., 36, 59-95.

Karato, S., Riedel, M.R. and Yuen, D.A., 2001. Rheological structure and deformation of subducted slabs in the mantle transition zone: implications for mantle circulation and deep earthquakes. Phys. Earth Planet. Inter., 127, 83–108.

Karig, D.E., Caldwell, J.G. and Parmentier, E.M., 1976. Effects of accretion on the geometry of the descending lithosphere. J. Geophys. Res., 81, 6281– 6291.

King, S.C., 2001. Subduction zones: observations and geodynamic models, Phys. Earth Planet Inter., 127, 9– 24.

Kircher, A., 1678. Mundus Subterraneus in XII libros digestus. Editio tertia, Amsterdam, 1687. Reprint: G.B. Vai (Ed.), Arnaldo Forni Publisher, Sala Bolognese, 2004, 942 pp.

Knopoff, L., 1972. Observations and inversion of surface-wave dispersion. Tectonophysics, 13, 497–519.

Knopoff, L. and Leeds, A., 1972. Lithospheric momenta and the deceleration of the Earth. Nature, 237, 93–95.

Kobayashi, D. and Sprenke, K.F. Lithospheric drift on early Mars: Evidence in the magnetic field. Icarus (2010), doi:10.1016/j.icarus.2010.06.015

Koper, K.D., Wiens, D.A., Dorman, L., Hildebrand, J. and Webb, S., 1999. Constraints on the origin of slab and mantle wedge anomalies in Tonga from the ratio of S to P velocities. J. Geophys. Res., 104, 15,089–15,104.

Korenaga, J. and Karato, S., 2008. A new analysis of experimental data on olivine rheology. J. Geophys. Res., 113, B02403, doi:10.1029/2007JB005100.

Krasinsky, G.A., 1999. Tidal effects in the Earth-Moon system and the Earth's rotation. Celestial mechanics and dynamical astronomy, 75, 39-66, doi: 10.1023/A:1008381000993.

Lallemand, S., Heuret, A. and Boutelier, D., 2005. On the relationships between slab dip, back-arc stress, upper plate absolute motion and crustal nature in subduction zones. Geochem. Geophys. Geosyst., 6, Q09006, doi:10.1029/2005GC000917.

Lallemand, S.E., Schnurle, P. and Manoussis, S., 1992. Reconstruction of subduction zone paleogeometries and quantification of upper plate material losses caused by tectonic erosion. J. Geophys. Res., 97, 217–239.

Lambeck, K., 1980. The Earth's variable rotation. In: Batchelor, G.K., and Miles, J.W. (Eds.), Geophysical causes and consequences: Cambridge, Cambridge University Press, 449 pp.

Laubscher, H.P., 1988. The arcs of the Western Alps and the Northern Apennines: an updated view. Tectonophysics, 146, 67–78.

Lenci, F. and Doglioni, C., 2007. On some geometric prismasymmetries. In: Lacombe, O., Lavé, J., Roure and F., Verges, J. (Eds.), Thrust belts and Foreland Basins: From Fold Kinematics to Hydrocarbon Systems. Frontiers in Earth Sciences, 24, 41–60, Springer.

Le Pichon, X., 1968. Sea-floor spreading and continental drift. J. Geophys. Res., 73: 12, 3661-3697.

Lithgow-Bertelloni, C. and Richards, M.A., 1998. The dynamics of Cenozoic and Mesozoic plate motions. Rev. Geophys., 36, 27–78.

Lippitsch, R., E. Kissling, and J. Ansorge, 2003. Upper mantle structure beneath the Alpine orogen from high-resolution teleseismic tomography. J. Geophys. Res., 108(B8), 2376, doi:10.1029/2002JB002016.

Liu, S., Wang, L., Li, C., Li, H., Han, Y., Jia, C. and Wei, G., 2004. Thermal-rheological structure of lithosphere beneath the northern flank of Tarim Basin, western China: implications for geodynamics. Sci. China, Ser. D: Earth Sci. 47 (7), 659–672.

Liu, M., Yang, Y., Stein, S., Zhu, Y. and Engeln, J., 2000. Crustal shortening in the Andes: why do GPS rates differ from geological rates? Geophys. Res. Lett., 27, 3005–3008.

Luyendyk, B.P., 1970. Dips of downgoing lithospheric plates beneath island arcs. Geol. Soc. Amer. Bull., 81, 3411 – 3416.

Manea, V.C., Manea, M., Kostoglodov, V., Currie, C.A. and Sewell, G., 2004. Thermal structure, coupling and metamorphism in the Mexican subduction zone beneath Guerrero. Geophysical Journal International

158, 775–784.
McGeary, S., Nur, A. and Ben-Avraham, Z., 1985. Special gaps in arc volcanism: the effect of collision or subduction of oceanic plateaus. Tectonophysics, 119, 195–221, doi:10.1016/0040-1951(85)90039-3.

Mei, S., Bai, W., Hiraga, T., and Kohlstedt, D.L., 2002. Influence of melt on the creep behavior of olivine basalt aggregates under hydrous conditions. Earth Planet. Sci. Lett, 201, 491–507, doi: 10.1016/S0012-821X(02)00745-8.

McCarthy, D.D. and Petit, G., 2004. IERS Conventions (2003), IERS Technical Note No. 32, Verlag des Bundesamts für Kartographie uns Geodäsie, Frankfurt am Main.

Melini, D., Cannelli, V., Piersanti, A. and Spada, G., 2008. Post-seismic rebound of a spherical Earth: new insights from the application of the Post-Widder inversion formula. Geophys. J. Int., 174, 672–695.

Milsom, J., 2005. The Vrancea seismic zone and its analogue in the Banda Arc, eastern Indonesia. Tectonophysics, 410, 325–336.

Molchan, G., Kronrod, T., Panza, G.F., 1997. Multi-scale seismicity model for seismic risk. Bull. Seism. Soc. Am., 87, 1220–1229.

Montagner, J.-P., 2002. Upper mantle low anisotropy channels below the Pacific Plate. Earth Planet. Sci. Lett., 202, 263–274.

Moore, G.W., 1973. Westward tidal lag as the driving force of plate tectonics. Geology, 1, 99–100.

Moretti, I. and Chènet, P. Y., 1987. The evolution of the Suez rift: a combination of stretching and secondary convection. Tectonophysics, 133, 229-234.

Morgan, W.J., 1971, Convection plumes in the lower mantle. Nature, 230, 42–43.

Mueller, S. and Panza, G.F., 1986. Evidence of a deep-reaching lithospheric root under the Alpine Arc. In: Wezel, F.C. (Ed.), The Origin of Arcs, 21, 93-113, Elsevier.

Mueller, R.D., Roest, W.R., Royer, J.Y., Gahagan, L.M. and Sclater, J.G., 1997. Digital isochrons of the world's ocean floor. J. Geophys. Res., 102,

3211–3214.

Nicolas, A., Boudier, B., Ildefonse, B. and Ball, E., 2000. Accretion of Oman and United Arab Emirates ophiolite: discussion of a new structural map, with three structural maps, scale 1:500,000. In: Boudier, F. and Juteau, T. (Eds.), The Ophiolite of Oman and United Arab Emirates. Mar. Geophys. Res., 21, 147–179.

Nicolich, R., Laigle, M., Hirn, A., Cernobori, L. and Gallart, J., 2000. Crustal structure of the Ionian margin of Sicily: Etna volcano in the frame of regional evolution. Tectonophysics, 329, 121-139.

O'Connell, R., Gable, C.G. and Hager, B., 1991. Toroidal–poloidal partitioning of lithospheric plate motions. In: Sabadini, R., et al. (Eds.), Glacial Isostasy, Sea-Level and Mantle Rheology, 334, 535–551, Kluwer Academic Publisher.

Oncescu, M.C. and Trifu, C.-I., 1987. Depth variation of moment tensor principal axes in Vrancea (Romania) seismic region. Ann. Geophys., 5B, 149–154.

Panza, G., 1980. Evolution of the Earth's lithosphere, In: Davies, P.A. and Runcorn, S.K. (Eds.) Mechanisms of Continental Drift and Plate Tectonics., 75–87, Academic Press.

Panza, G.F., Calcagnile, G., Scandone, P. and Mueller, S., 1982. Die Geologische Tiefenstruktur des Mittelmeerraumes. Spektrum Wissen., 1, 18-28.

Panza, G.F., Doglioni, C. and Levshin, A., 2010. Asymmetric ocean basins. Geology, 38, 1, 59-62.

Panza, G.F. and Mueller, S., 1978. The plate boundary between Eurasia and Africa in the Alpine Area. Mem. Sc. Geol., 33, 43-50.

Panza, G.F., Peccerillo, A., Aoudia, A. and Farina, B., 2007a. Geophysical and petrological modeling of the structure and composition of the crust and upper mantle in complex geodynamic settings: The Tyrrhenian Sea and surroundings. Earth-Science Reviews, 80, 1-46.

Panza, G.F., Pontevivo, A., Chimera, G., Raykova, R. and Aoudia, A., 2003. The Lithosphere–Asthenosphere: Italy and surroundings. Episodes, 26, 169–174.

Panza, G. F., Raykova, R.B., Carminati, E. and Doglioni, C., 2007b. Upper mantle flow in the western Mediterranean. Earth Planet. Sci. Lett., 257, 200-214.

Panza, G.F. and Suhadolc, P., 1990. The Mediterranean area: a challenge for plate tectonics. In: Beloussov, V. et al. (Eds.), Critical aspects of the Plate tectonics theory, volume 1, 339-363, Theophrastus Publications, S.A., Athens.

Papazachos, B. C. and Comninakis, P. E., 1978. Geotectonic significance of the deep seismic zones in the Aegean area. Thera and the Aegean world. Second International Scientific Congress, Santorini, Greece, August 1978, 121-129.

Papazachos, B.C., Dimitriadis, S.T., Panagiotopoulos, D.G., Papazachos, C.B. and Papadimitriou, E.E., 2005. Deep structure and active tectonics of the southern Aegean volcanic arc. In: Fytikas, M., and Vougioukalakis, G.E. (Eds.), The South Aegean Active Volcanic Arc. Developments in Volcanology, 7, 47–64, Elsevier.

Pardo, M., Comte, D. and Monfret, T., 2002. Seismotectonic and stress distribution in the central Chile subduction zone. J. South Am. Earth Sci. 15, 11–22, doi:10.1016/S08959811(02)00003-2.

Peccerillo, A., Panza, G.F., Aoudia, A. and Frezzotti, M.L., 2008. Relationships between magmatism and lithosphere–asthenosphere structure in the western Mediterranean and implication for geodynamics. Rendiconti Lincei, 19, 291–309. doi:10.1007/ s12210-008-0020-x.

Pérez-Campos, X., Kim, Y., Husker, A., Davis, P.M., Clayton, R.W., Iglesias, A., Pacheco, J.F., Singh, S.K., Manea, V.C. and Gurnis, M., 2008. Horizontal subduction and truncation of the Cocos Plate beneath central Mexico. Geophys. Res. Lett., 35, L18303, doi:10.1029/2008GL035127

Pfiffner, O. A., Lehner, P., Heitzmann, P., Müller St. and Steck, A., 1997. Deep Structure of the Swiss Alps, Results of NRP 20, Birkhauser Verlag, Basel, 380 pp.

Pilger, R.H., 1981. Plate reconstructions, aseismic ridges, and low-angle subduction beneath the Andes. Geol. Soc. Am. Bull., 92, 448–456, doi:10.1130/0016-7606(1981) 92-448.

Piromallo, C. and Morelli, A., 1997. Imaging the Mediterranean upper mantle by P-wave travel time tomography. Ann. Geofis., 40, 963–979.

Pollitz, F.F., Bürgmann, R., and Romanowicz, B., 1998, Viscosity of oceanic asthenosphere inferred from remote triggering of earthquakes. Science, 280, 1245–1249, doi: 10.1126/science.280.5367.1245.

Pontevivo, A. and Panza, G.F., (2006). The Lithosphere-Asthenosphere System in the Calabrian Arc and Surrounding Seas - Southern Italy. Pure appl. geophys., 163, 1617-1659.

Press, F., Briggs, P., 1975. Chandler Wobble, earthquakes, rotation and geomagnetic changes. Nature, 256, 270–273.

Prigogine, I., Stengers, I., 1984. Order Out of Chaos. Bantam, New York, 349 pp.

Ranalli, G., 1995. Rheology of the Earth. Chapman and Hall, 413 pp.

Ray, R., 2001. Tidal friction in the Earth and Ocean. Journées Luxembourgeoises de Géodynamique´JLG 89th, Nov. 12–14, http://www.ecgs.lu/.

Raykova R. B. and Panza G. F., 2006. Surface waves tomography and non-linear inversion in the southeast Carpathians. Phys. Earth Planet. Int., 157, 164–180.

Reyners, M., Eberhart-Phillips, D., Stuart, G. and Nishimura, Y., 2006. Imaging subduction from the trench to 300 km depth beneath the central North Island, New Zealand, with Vp and Vp/Vs. Geophys. J. Int., 165, 565–583, doi:10.1111/j.1365-246X.2006.02897.x.

Ricard, Y., Doglioni, C. and Sabadini, R., 1991. Differential rotation between lithosphere and mantle: a consequence of lateral viscosity variations. J. Geophys. Res., 96, 8407–8415.

Ricard, Y., and Vigny, C., 1989. Mantle dynamics with induced Plate Tectonics, J. Geophys. Res., 94 (B12), 17,543-17,559.

Riguzzi, F., Panza, G., Varga P. and Doglioni, C., (2010). Can Earth's rotation and tidal despinning drive plate tectonics? Tectonophysics, 484, 60-73.

Rivera, L., Sieh, K., Helmberger, D. and Natawidjaja, D., 2002. A comparative study of the Sumatran subduction-zone earthquakes of 1935 and 1984. Bull. Seism. Soc. Am., 92, 1721–1736.

Romanowicz, B., 2003. Global mantle tomography: Progress status in the Past 10 Years. Annu. Rev. Earth Planet. Sci., 31, 303–328, doi: 10.1146/annurev.earth.31.091602.113555.

Romashkova, L.L., 2009. Global-scale analysis of seismic activity prior to 2004 Sumatra-Andaman mega-earthquake. Tectonophysics, 470, 329–344, doi:10.1016/j.tecto.2009.02.011.

Royden, L.H., 1993. The tectonic expression slab pull at continental convergent boundaries. Tectonics, 12, 303–325.

Russo, R.M. and Silver, P.G., 1994. Trench-parallel flow beneath the Nazca plate from seismic anisotropy. Science 263, 1105–1111.

Rychert, C.A., Fischer, C.M. and Rondenay, S., 2005. A sharp lithosphere–asthenosphere boundary imaged beneath eastern North America. Nature, 436, 542–545.

Sacks, I.S. and Okada, H., 1974. A comparison of the anelasticity structure beneath western South America and Japan. Phys. Earth Planet. Inter. 9, 211–219, doi:10.1016/0031-9201(74)90139-3.

Savage, M.K., 1999. Seismic anisotropy and mantle deformation: What have we learned from shear wave splitting? Rev. Geophys., 37, 65–106.

Scalera, G., 2005. A new interpretation of the Mediterranean arcs: Mantle wedge intrusion instead of subduction, Boll. Soc. Geol. It., Volume Speciale n. 5, 129-147.

Scalera, G., 2008a. Is large scale subduction made unlikely by the Mediterranean deep seismicity? New Concepts in Global Tectonics Newsletter, 47, 24-29.

Scalera, G., 2008b. Great and old earthquakes against great and old paradigms-paradoxes, historical roots, alternative answers. Adv. Geosci., 14, 41–57.

Scholz, C.H. and Campos, J., 1995. On the mechanism of seismic decoupling and back arc spreading at subduction zones. J. Geophys. Res.,

100 (B11), 22,103–22,115.

Schubert, G., Turcotte, D.L. and Olson, P., 2001. Mantle convection in the Earth and planets. Cambridge University Press, Cambridge, UK, 940 pp.

Scoppola, B., Boccaletti, D., Bevis, M., Carminati, E. and Doglioni, C., 2006. The westward drift of the lithosphere: a rotational drag? Bull. Geol. Soc. Am., 118, 199–209, doi:10.1029/2004TC001634.

Sella, G.F., Dixon, T.H., and Mao, A., 2002, REVEL: A model for recent plate velocity from space geodesy: J. Geophys. Res., 107, 2081, doi: 10.1029/2000JB000033.

Selvaggi, G., Chiarabba, C., 1995. Seismicity and P-wave velocity image of the southern Tyrrhenian subduction zone. Geophys. J. Int. 121, 818–826.

Shaw, H.R., and Jackson, E.D., 1973, Linear island chains in the Pacific, result of thermal plumes or gravitational anchors?: J. Geophys. Res., 78, 8634–8652.

Silver, P.G. and Holt,W.E., 2002. The mantle flow field beneath western North America. Science, 295, 1054–1057.

Smith, A.D., 1993, The continental mantle as a source for hotspot volcanism. Terra Nova, 5, 452–460.

Smith, A. D. and C. Lewis, 1999. The planet beyond the plume hypothesis, Earth-Science Reviews, 48, 135 – 182.

Spakman, W., Wortel, M. J. R. and Vlaar, N. J., 1988. The Hellenic Subduction Zone: A tomographic image and its geodynamic implications, Geophys. Res. Lett., 15, 60-63.

Stampfli, G.M. and Borel, G.D., 2002. A plate tectonic model for the Paleozoic and Mesozoic constrained by dynamic plate boundaries and restored synthetic oceanic isochrons. Earth Planet. Sci. Lett., 196, 17–33.

Stern, R.J., 2002. Subduction zones. Rev. Geophys., 40, 1012.

Stevenson, D.J., 1994. Weakening under stress. Nature, 372, 129-130.

Stein, S. and Wysession, M., 2003. An Introduction to Seismology, Earthquakes, and Earth Structure. Blackwell Science, Oxford, 498 pp.

Suhadolc, P., Panza, G.F. and Mueller, St., 1988. Lateral variations of the lithosphere-asthenosphere system and plate boundaries in Europe. In: Baldi, P. and Zerbini, S. (Eds.), Proc. Third Int. Conf. WEGENER/MEDLAS PROJECT, 53-60, Esculapio, Bologna.

Syracuse, E.M., Abers, G.A., 2006. Global compilation of variations in slab depth beneath arc volcanoes and implications. Geochem. Geophys. Geosyst. 7, Q05017, doi:10.1029/2005GC001045

Tackley, P., 2008. Modelling compressible mantle convection with large viscosity contrasts in a three-dimensional spherical shell using the yin-yang grid. Phys. Earth Planet. Int., 171, 7–18.

Tovish, A. and Schubert, G, 1978. Island arc curvature, velocity of convergence and angle of subduction. Geophys. Res. Lett., 5, 329–332.

Turcotte, D. L. and Schubert, G., 1982. Geodynamics, Wiley, New York, 450 pp.

Turcotte, D.L. and Schubert, G., 2002. Geodynamics. Cambridge University Press. 456 pp.

Uyeda, S. and Kanamori, H., 1979. Back-arc opening and the mode of subduction. J. Geophys. Res., 84 (B3), 1049–1061.

van Hunen, J., van den Berg, A.P. and Vlaar, N.J. (2001). Latent heat effects of the major mantle phase transitions on low-angle subduction, Earth Planet. Sci. Lett., 190, 125– 135.

Varga, P., Denis, C., and Varga, T., 1998, Tidal friction and its consequences in paleogeodesy, in the gravity field variations and in tectonics. J. Geodyn., 25, 61–84, doi: 10.1016/S0264-3707(97)00007-0.

Varga, P., Krumm, F., Riguzzi, F., Doglioni C., Süle B., Wang K. and Panza G. F., 2011. Earthquake energy release along the Earth surface and radius, in preparation.

Vassiliou, M.S., Hager, B.H., Raefsky, A.,1984. The distribution of earthquakes with depth and stress in subducting slabs. J. Geodyn., 1, 11–

Venisti, N., Calcagnile, G., Pontevivo, A. and Panza, G.F., 2005. Tomographic Study of the Adriatic Plate. Pure appl. Geophys., 162, 311-329.

Vinnik, L., Singh, A., Kiselev, S., Ravi Kumar, M., 2007. Upper mantle beneath foothills of the western Himalaya: subducted lithospheric slab or a keel of the Indian shield? Geophys. J. Int., 171, 1162–1171, doi:10.1111/j.1365-246X.2007.03577.x.

Waldhauser, F., Lippitsch, R., Kissling, E. and Ansorge, J., 2002. High-resolution teleseismic tomography of upper-mantle structure using an a priori three-dimensional crustal model. Geophys. J. Int., 150, 403–414.

Waschbusch, P. and Beaumont, C., 1996. Effect of slab retreat on crustal deformation in simple regions of plate convergence. J. Geophys. Res., 101 (B12), 28133–28148.

Wong A Ton, S.Y.M., Wortel, M.J.R., 1997. Slab detachment in continental zones: an analysis of controlling parameters. Geophys. Res. Lett., 24, 2095–2098.

Wortel, M.J.R. and Spakman,W., 2000. Subduction and slab detachment in the Mediterranean–Carpathian region. Science, 290, 1910–1917.

Zandt, G., Gilbert, H., Owens, T.J., Ducea, M., Saleeby, J., and Jones, C.H., 2004. Active foundering of a continental arc root beneath the southern Sierra Nevada in California. Nature, 431, 41–46, doi: 10.1038/nature02847.